TUMOR-STROMA INTERACTION MEDIATED BY TISSUE TRANSGLUTAMINASE IN PANCREATIC CANCER

Jiyoon Lee

Submitted to the faculty of the University Graduate School
in partial fulfillment of the requirements
for the degree
Doctor of Philosophy
in the Department of Biochemistry and Molecular Biology,
Indiana University

August, 2015

Accepted by the Graduate Faculty, Indiana University, in partial fulfillment of the requirements for the degree of Doctor of Philosophy.

_____

Daniela Matei, M.D., Chair

_____

Maureen Harrington, Ph.D.

Doctoral Committee

_____

Brittney-Shea Herbert, Ph.D.

July 08, 2015

_____

Jingwu Xie, Ph.D.

DEDICATION

To my parents,

whom I love and respect beyond expression.

Thank you for raising me up with endless love to be who I am today.

To my fiancé,

the best and forever companion in my life.

Thank you for caring and loving me the way no one can.

I would never have reached this point without your love, support,

encouragement, and trust.

Thank you.

Love you.

ACKNOWLEGEMENTS

First and foremost, I would like to express my deepest and sincere gratitude to my mentor, Dr. Daniela Matei, for her support, guidance, and encouragement throughout my graduate studies. I would not have made it this far without her help. She had a great deal of influence over my scientific life by teaching me how to be a diligent, passionate, and critically thinking scientist. Thank you for your patience and wise advices. I will always remember your mentorship.

I am indebted to my committee members, Dr. Maureen Harrington, Dr. Brittney-Shea Herbert, and Dr. Jingwu Xie for their insightful and invaluable advices and suggestions to help me move forward. I will always remember your advices and guidance. Thank you.

I am grateful to current and former members in Matei's laboratory. My big thanks to Bakh, whom I called as father, and Salvatore, as uncle in the lab. They were the best friends and positive spirits who were always there, helping and encouraging me with thoughtful discussions both on science and life. I would never forget our friendship. I would like to thank Andrea for her tremendous support on the animal work. She taught me from touching the mice to giving orthotopic surgery. I would never forget your training. I also would like to thank Horacio for his guidance on critical and scientific thinking. He was always opened to discussions and led me to be fulfilled with inspirations. I would never forget your help. I also would like to acknowledge Edyta, our boss in the lab, for

keeping everything clean, neat, and in order, which made our life easier to do experiments. Also, she was a nice storyteller with various topics, which led our lab to a brighter atmosphere. I would like to thank Qing, who used a small office together, for sharing his experiences and opinions both on science and life. He helped me to re-establish my dreams and future goals. I will always keep your advices in my mind. Lastly, I would like to acknowledge Bhadrani, a former lab member who was my early morning labmate, for her technical support and for her warm words and encouragements. I will always remember your kindness.

I would like to thank all my classmates and friends for their supports, encouragements, and wonderful memories. I deeply wish the best for everyone. I also would like to give a special thanks to Dr. Misook Oh for inviting and feeding all Korean friends with homemade Korean foods, whenever it was someone's birthday, Korean holidays, or American holidays. Thanks to her, I could overcome homesickness during my graduate studies and have a happier life in the United States. Also, to all other friends whom I could not mention all, thank you and wish you the best in your life.

Moreover, my big thanks to the IBMG program and the Department of Biochemistry and Molecular Biology for the wonderful graduate education.

My best regards and blessings to all of those who made this achievement possible. Thank you.

Jiyoon Lee

TUMOR-STROMA INTERACTION MEDIATED BY TISSUE TRANSGLUTAMINASE IN PANCREATIC CANCER

Pancreatic ductal adenocarcinoma (PDA) is a deadly disease due to early metastasis and resistance to chemotherapy. PDA is commonly associated with a dense desmoplastic stroma, which forms a protective niche for cancer cells. Tissue transglutaminase (TG2), a Ca^{2+}-dependent enzyme, is abundantly expressed in pancreatic cancer cells and crosslinks proteins through acyl-transfer transamidation between glutamine and lysine residues. The objective of the study was to determine the functions of TG2 in the pancreatic stroma. Orthotopic pancreatic xenografts and co-culture systems tested the mechanisms by which the enzyme modulates tumor-stroma interactions. We showed that TG2 secreted by cancer cells is enzymatically active and renders the stroma denser by crosslinking collagen, which in turn activates fibroblasts and stimulates their proliferation. Yes-associated protein (YAP) and transcriptional co-activator with PDZ-binding motif (TAZ) are transcription factors involved in mechanotransduction. The TG2-mediated fibrosis-rich, stiff microenvironment conveys mechanical cues to cancer cells leading to activation of YAP and TAZ, promoting cell proliferation and tumor growth. Stable knockdown of TG2 in pancreatic cancer cells led to decreased size of pancreatic xenografts and increased sensitivity of xenografts to gemcitabine. Taken together, our results demonstrate that TG2 secreted in the tumor microenvironment orchestrates the crosstalk between cancer cells and the stroma, fundamentally impacting tumor

growth and response to chemotherapy. Our study supports TG2 inhibition in the pancreatic stroma as a novel strategy to block pancreatic cancer progression.

Daniela Matei, M.D., Chair

TABLE OF CONTENTS

CHAPTER 2. MATERIALS AND METHODS

CHAPTER 3. RESULTS

LIST OF TABLES

LIST OF FIGURES

LIST OF ABBREVIATIONS

5-BP (BPA)	5-(Biotinamido) pentylamine
Ab	Antibody
α-SMA	Alpha-smooth muscle actin
BrdU	Bromodeoxyuridine
CCK-8	Cell counting kit-8
CDKN2A	Cyclin-dependent kinase inhibitor 2A (p16)
COX-2	Cyclooxygenase-2
CE	Cornified envelope
CM	Conditioned media
CTGF	Connective tissue growth factor
DAG	Diacylglycerol
dCTP	Deoxycytidine triphosphate
dFdCTP	Difluorodeoxycytidine triphosphate
dFdU	2',2'-difluorodeoxyuridine
DOPC	1,2-dioleoyl-sn-glycero-3-phosphatidylcholine
DS	Desmoplastic stroma
DTT	Dithiothreitol
ECM	Extracellular matrix
EGF	Epidermal growth factor
EFGR	Epidermal growth factor receptor
EMT	Epithelial-to-mesenchymal transition
ER	Endoplasmic reticulum

ERK	Extracellular signal-regulated kinases
FAK	Focal adhesion kinase
FBS	Fetal bovine serum
FN	Fibronectin
GDP	Guanosine diphosphate
Gem	Gemcitabine
GFP-HNDFs	Green fluorescence protein expressing human neonatal dermal fibroblasts
GPCR	G-protein coupled receptor
GTP	Guanosine 5'-triphosphate
Hh	Hedgehog
hpFibroblasts	Human pancreatic cancer associated fibroblasts
HPNE	Human pancreatic normal epithelial
hTERT	Human telomerase reverse transcriptase
IF	Immunofluorescence
IGFBP-3	Insulin-like growth factor-binding protein-3
IHC	Immunohistochemistry
IL	Interleukin
ILD	Interstitial lung disease
IP_3	Inositol triphosphate
IUSCC	Indiana university simon cancer center
KRAS	Kirsten rat sarcoma viral oncogene homolog
LC3	Light chain 3

MMP	Matrix metalloproteinase
MVD	Microvessel density
NHF544	Normal human dermal fibroblasts
NF-κB	Nuclear factor -kappaB
NRP-1	Neuropilin-1
OC	Ovarian cancer
PDA	Pancreatic ductal adenocarcinoma
PanIN	Pancreatic intraepithelial neoplasia
PDGF	Platelet-derived growth factor
PDI	Protein disulphide isomerase
PI3K	Phosphatidylinositol 3-kinase
PIP_2	Phosphatidylinositol diphosphate
PIP_3	Phosphatidylinositol (3,4,5)-triphosphate
PKA	Protein kinase A
PKCδ	Protein kinase Cδ
PLC	Phospholipase C
PSCs	Pancreatic stellate cells
PSR	Picrosirius red
PTEN	Phosphatase and tensin homologue
PVDF	Polyvinylidene difluoride
Rb	Retinoblastoma protein
RFU	Relative fluorescence unit
SDS-PAGE	Sodium dodecyl sulfate polyacrylamide gel electrophoresis

SE	Standard error
SHH	Sonic hedgehog
shRNA	Short hairpin ribonucleic acid
siRNA	Small interfering ribonucleic acid
SPARC	Secreted protein acidic and rich in cysteine
TG2	Tissue transglutaminase
TGF-β	Transforming growth factor-beta
TGase	Transglutaminase
THU	Tetrahydrouridine
TMA	Tissue microarray
TME	Tumor microenvironment
TRAP	Telomerase repeat amplification protocol
Trx	Thioredoxin
YAP	Yes-associated protein
TAZ	Transcriptional co-activator with PDZ-binding motif
VEGF	Vascular endothelial growth factor
WB	Western blot

CHAPTER 1. INTRODUCTION

1.1. Pancreatic ductal adenocarcinoma

Pancreatic ductal adenocarcinoma (PDA), originating in the pancreatic ductal epithelium, is the fourth leading cause of cancer mortality in the world with a 5-year survival rate of less than 7% (R. L. Siegel, Miller, & Jemal, 2015). Most PDA patients are diagnosed at an advanced stage with only 10-15% patients being candidates for curative surgical resection (Sultana, Cox, Ghaneh, & Neoptolemos, 2012). This late diagnosis is due to the rapid tumor growth and metastatic propensity, lack of sensitive early screening biomarkers, and resistance to chemotherapy and radiation (Feig et al., 2012; Willett, Czito, Bendell, & Ryan, 2005). Currently approved drugs including gemcitabine and erlotinib induce a modest increase in patient survival, but do not cure the disease (Burris et al., 1997; Moore et al., 2007).

The cause of PDA is multifactorial including smoking, family history of chronic pancreatitis, diabetes, obesity, blood type, advanced age, and male sex (Klein et al., 2004; Raimondi, Maisonneuve, & Lowenfels, 2009; Wolpin et al., 2009). Among these risk factors, smoking (~20%) and family history (~10%) are the most influential causes (Blackford et al., 2009; Petersen et al., 2006). In addition, PDA tumors from smokers contain more genetic mutations than those from non-smokers (Blackford et al., 2009).

The exact cell type that gives rise to PDA is not yet known. In recent years, however, PDA is thought to arise from non-invasive precursor lesions and

progress to invasive adenocarcinomas through a series of hyperplastic and dysplastic ductal lesions termed pancreatic intraepithelial neoplasia (PanIN; **Figure 1**) (Hezel, Kimmelman, Stanger, Bardeesy, & Depinho, 2006; Ralph H. Hruban, Wilentz, & Kern, 2000; Vincent, Herman, Schulick, Hruban, & Goggins, 2011). The PanIN progresses through three different stages, PanIN-1 (PanIN-1A and PanIN-1B), PanIN-2, and PanIN-3, in an order of increasing cytological atypia with genetic aberrations. Early stage of PanIN (PanIN-1) often harbors *KRAS* oncogene mutations; *KRAS* and *CDKN2A*/*p16* tumor suppressor mutations are present in the intermediate stage (PanIN-2); and nuclear atypia and mitotic phenotype with *p53* tumor suppressor mutations are present (PanIN-3) as PanIN progresses to pancreatic carcinoma (Feig et al., 2012; R. H. Hruban et al., 2006; Li, Xie, Wolff, & Abbruzzese, 2004).

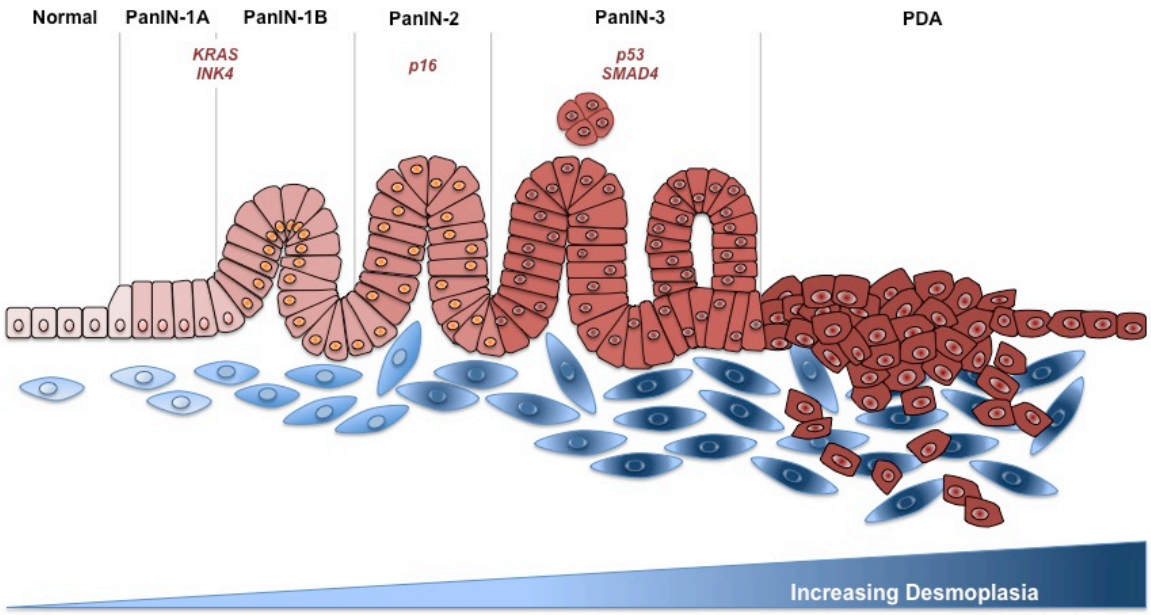

Figure 1. Progression model for PDA. PDA is appreciated to develop through a series of hyperplastic and dysplastic lesions termed pancreatic intraepithelial neoplasia (PanIN). Mutations of the oncogene (*KRAS*) and tumor suppressors (*INK4*, *p16*, *p53*, *SMAD4*) take place in the progression from normal to malignant epithelium. *Figure is modified from "Progression model for pancreatic cancer" by R. Hruban, M. Goggins, J. Parsons, and S. Kern, 2000, Clinical Cancer Research, 6, p. 2969-72 © 2000 American Association for Cancer Research*.

KRAS is a GTPase, which regulates growth factor signaling and activates multiple downstream signaling cascades involved in cellular proliferation, survival, and differentiation (Campbell, Khosravi-Far, Rossman, Clark, & Der, 1998). Mutation of *KRAS* is the most common genetic alteration observed in PDA cases (≥ 90%) and represents a gain-of-function mutation of glycine 12 to aspartate at codon (G12D) (Nakanishi & Toi, 2005). Several studies have reported that *KRAS* mutations are also a marker of poor prognosis in PDA patients (Ghosh, May, & Kopp, 1998; Witkiewicz et al., 2015). Most PDA tumors, which have mutational activation of *KRAS*, overexpress growth factors and cytokines and have lost activation of tumor suppressor genes including

CDKN2A/p16 and *p53* (Kanda et al., 2012). Combination of these abnormalities activates downstream signaling pathways of *KRAS,* such as Src, nuclear factor-kB (NF-kB), and Stat pathways resulting in cancer cell proliferation, tumor growth, and metastasis.

A recent analysis of the genetic diversity of PDA used a whole-exome sequencing approach in 109 PDA specimens (Witkiewicz et al., 2015). Tumors with higher chromosomal instability harbored mutations in DNA break repair genes and were associated with poor prognosis. Overexpression of *MYC* was observed in the adenosquamous subtype of PDA and in PanIN-2, suggesting its role in initiation and progression of PDA. *RBM10*, a regulator of alternative splicing (Inoue et al., 2014), was found to be mutated in the aggressive PDA. On the other hand, mutation in *ARID1A*, a chromatin remodeling gene (Helming et al., 2014), was related with poor survival. In addition, even though mutation of *KRAS*, mostly on codon 12, is an indicator of poor prognosis, mutation on codon 61 was identified to lead to lesser activation of ERK and to be associated with improved survival, suggesting diverse consequences of *KRAS* mutations in PDA (Biankin et al., 2012; Ihle et al., 2012; Jones et al., 2008). *BRAF* V600E mutation was found to be mutually exclusive with *KRAS* mutations, and led to sensitivity to BRAF inhibitors, such as vemurafenib, in PDA models. In addition, alterations in the TGF-β, Wnt/β-catenin, NOTCH, Hedgehog, and RB pathways, chromatin remodeling, and DNA repair have been identified (Witkiewicz et al., 2015). These recent data provide a more detailed molecular landscape of pancreatic tumors.

1.2. PDA Stroma

A unique hallmark of PDA is the dense desmoplastic stroma (DS) (Feig et al., 2012; Korc, 2007). The activated DS is heterogenous and composed of fibroblasts, pancreatic stellate cells (PSCs), endothelial cells, immune cells, nerve cells, extracellular matrix (ECM), cytokines and growth factors, and other cellular components (Karin, Cao, Greten, & Li, 2002; Korc, 2007; Wang et al., 1999). The DS is dynamic, and its composition changes constantly during the progression from early stage PanIN to aggressive PDA (**Figure 2**) (Feig et al., 2012). Cytokines and growth factors secreted into the PDA tumor microenvironment (TME) include the transforming growth factor-beta (TGF-β), the platelet-derived growth factor (PDGF), the epidermal growth factor (EGF), the vascular endothelial growth factor (VEGF), and interleukin-1 and -6 (IL-1 and IL-6), all of which activate stromal cells (Maehama & Dixon, 1998; Tamura et al., 1998; J. Zhao & Guan, 2009).

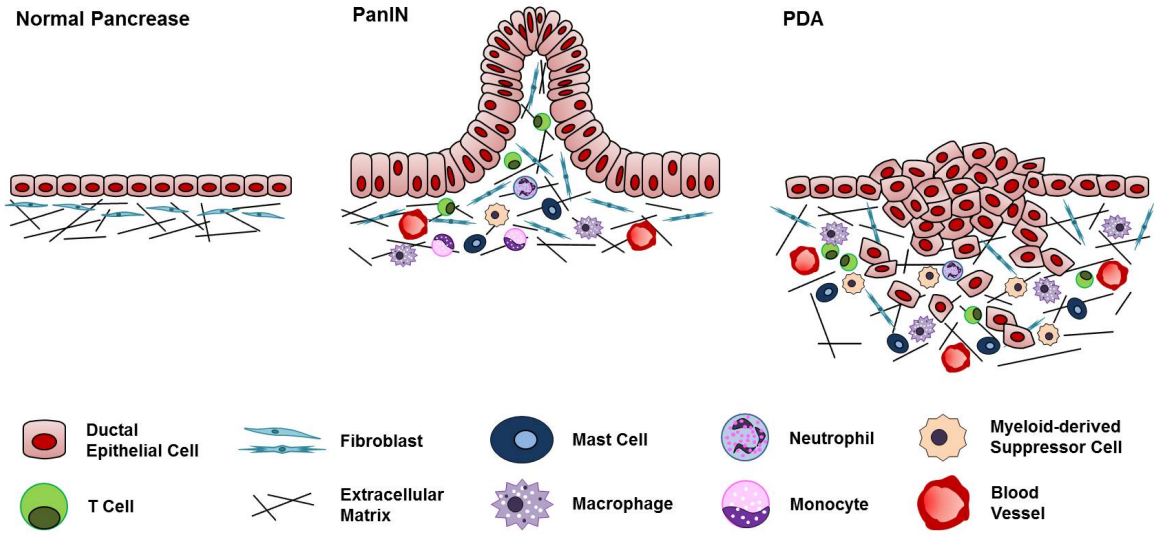

Figure 2. Changes of the PDA stroma composition during the progression from early stage PanIN to aggressive PDA. As tumorigenesis progresses, vasculature, collagen production, and immune cell recruitment increases in the tumor microenvironment, resulting in formation of the dense desmoplastic stroma. *Figure is modified from "The role of inflammatory cells in fostering pancreatic cancer cell growth and invasion" by A. Evans and E. Costello, 2012, Frontiers in physiology, 3, p. 270 © Evans and Costello.*

PSCs are the most prominent fibroblastic cells in the DS and are activated by stimulants secreted in the tumor milieu by PDA cells and proliferate rapidly (Karin et al., 2002; Maehama & Dixon, 1998). Activated myofibroblasts and PSCs produce and secrete ECM proteins including collagen I and III, fibronectin, matrix metalloproteinases (MMPs), and other matrix proteins into the TME (Mizushima, 2007; Rossin et al., 2014; J. Zhao & Guan, 2009). These proteins remodel the ECM and interact with PDA cells leading to increased tumorigenicity and metastatic potential (Willett et al., 2005). All the components in the PDA TME (cells and ECM components) interact with each other through autocrine and paracrine mechanisms to induce formation of the dense DS (Wang et al., 1999). This heterotypic interaction provides a supportive TME for survival and

progression of PDA, protecting cancer cells from environmental stress including chemo- and radiotherapy (D. Hanahan & Weinberg, 2011). In addition, PSCs expressing CD10 surface marker secrete elevated levels of MMP-3 and promote invasion and tumor growth (Ikenaga et al., 2010; Wilson, Pirola, & Apte, 2014).

The ECM of the pancreatic DS is prominently composed of collagens, non-collagen glycoproteins, growth factors, and modulators of the cell-matrix interaction (Feig et al., 2012; Karin et al., 2002). The alterations of ECM protein composition determine the invasion and migration ability of PDA cells (Grzesiak & Bouvet, 2006). Collagen I, III, and fibronectin are the major components of the pancreatic DS (Gress et al., 1995; Lunardi, Muschel, & Brunner, 2014; Wang et al., 1999). It has been reported that alterations of collagen deposition or degradation are involved in cell-survival and migration of PDA cells, and that adhesion of PDA cells to fibronectin, collagen I, IV, and laminin decreases their sensitivity to anticancer drugs (Ohlund, Franklin, Lundberg, Lundin, & Sund, 2013; Shields, Dangi-Garimella, Krantz, Bentrem, & Munshi, 2011; J. Zhao & Guan, 2009). Therefore, the increased expression of these ECM proteins may correlate with PDA resistance to chemotherapy.

Vasculature and angiogenesis are recognized hallmarks of tumorigenesis (Douglas Hanahan & Weinberg, 2000). However, in PDA, blood microvessel density (MVD) is lower than in normal pancreas and the vasculature is disorganized, so that the partial pressure of oxygen is low, leading to hypoxia (Erkan et al., 2012). The lack of vasculature in the pancreatic tumors is inversely correlated with elevated expression of angiogenic factors including VEGF,

cyclooxygenase-2 (COX-2), and neuropilin-1 (NRP-1) (Fukahi, Fukasawa, Neufeld, Itakura, & Korc, 2004; Haixia, Qikui, Liuping, & Li, 2005; Hlatky, Hahnfeldt, & Folkman, 2002). The vasculature of PDA tumors develops in coordination with inflammatory and stromal cell accumulation (Lunardi et al., 2014). For example, it has been reported that the activation of CXCR2, an IL-8 receptor that mediates neutrophil migration to inflammation sites, increases angiogenesis by promoting connective tissue growth factor (CTGF) secretion by stromal cells (Ijichi, 2012). On the other hand, overexpression of sonic hedgehog (SHH) by neoplastic cells in PDA during inflammation and neoplasia promotes desmoplasia while decreasing vasculature (Kenneth P Olive et al., 2009).

The hypo-vascular and hypoxic dense stroma is presumed to be less permeable to chemotherapy, protecting PDA cells from environmental stress (Miyamoto et al., 2004; K. P. Olive et al., 2009). Related to this perspective, a recent study using clinical PDA specimens demonstrated that the delivery of gemcitabine into human pancreatic tumors is highly heterogenous and strongly correlated with the existing stromal reaction (Koay, Baio, et al., 2014; Koay, Truty, et al., 2014). In addition, Olive *et al*. have proposed that the altered vascularity and vascular architecture of PDA tumors to impaired drug delivery and penetration (K. P. Olive et al., 2009). Improved delivery of gemcitabine can be achieved by inhibiting the hedgehog (Hh) pathway, resulting in the depletion of PDA stroma (K. P. Olive et al., 2009). KPC mice, which conditionally express mutated *KRAS* and *p53* alleles and form PDA tumors, were used for that investigation. The KPC mice were given IPI-926, a Smoothened (Smo; Hh

signaling mediator) inhibitor, daily. Treatment resulted in modification of the stroma; decreased collagen I content and reduced proliferation of α-smooth muscle actin $(\alpha\text{-SMA})^+$ myofibroblasts. Moreover, inhibition of Hh pathway increased angiogenesis and proliferation of endothelial ($CD31^+$) cells. KPC mice treated with IPI-926 had tumors with increased microvessel density (MVD) and displayed more effective delivery of gemcitabine into tumors, as evidenced by elevated gemcitabine metabolites and increased apoptotic tumor cells. KPC mice treated with the combination of IPI-926 and gemcitabine also showed extended median survival from 11 days to 25 days, decreased tumor burden, and reduced metastases (K. P. Olive et al., 2009).

In contrast to this study, two other recent reports have suggested the opposite concept, specifically, that the inhibition of some stroma components may enhance cancer cell invasion, tumor growth, and metastasis (Gore & Korc, 2014; Ozdemir et al., 2014; Rhim et al., 2014). Rhim *et al*. used conditional Shh knockout mice and IPI-926 administration to suppress stroma (Rhim et al., 2014). Attenuation of stroma formation by using a Shh knockout or by using IPI-926 treatment led to undifferentiated PDA, increased metastasis, and decreased survival. Özdemir *et al*. used a transgenic mouse model which lacks $\alpha\text{-SMA}^+$ myofibroblasts in the pancreas (Ozdemir et al., 2014). Depletion of $\alpha\text{-SMA}^+$ myofibroblasts led to undifferentiated, invasive PDA tumors with enhanced hypoxia, epithelial-to-mesenchymal transition (EMT), and increased number of cancer stem cells, which led to reduced survival of the mice. One important

difference between the previous and these two latter studies was the length of the observation period (weeks; 2009 study vs. months; 2014 studies).

Taken together, these studies suggest that the PDA stroma is composed of diverse components and affected by a complex interplay between the components. Therefore, targeting stroma can enable tumors to respond more efficiently to chemotherapy, but also can lead to enhanced proliferation of cancer cells enabling tumors to become more aggressive. Moreover, even though the experimental models, genetically engineered mouse models and orthotopic xenograft mouse models, mimic human tumors, the biological circumstances may vary. For example, the proportion of stroma and diversity of components in mouse-derived tumors is significantly less than that observed in human tumors. Therefore, further studies are necessary to more clearly delineate characteristics and functions of PDA stroma, using both *in vitro*, murine and human specimen based analyses.

1.3. Chemotherapy

1.3.1. Gemcitabine

Gemcitabine (difluorodeoxycytidine; dFdC) is a novel nucleoside analog, which has a wide range of antitumor activity and is a standard treatment for several cancers, including PDA (Burris et al., 1997; Hertel et al., 1990).

To become active, gemcitabine undergoes intracellular phosphorylation by deoxycytidine kinase, resulting in the accumulation of difluorodeoxycytidine triphosphate (dFdCTP) within cells. dFdCTP competes with deoxycytidine triphosphate (dCTP) for incorporation into DNA, which results in inhibition of DNA synthesis (Huang, Chubb, Hertel, Grindey, & Plunkett, 1991). Moreover, gemcitabine presumably inhibits ribonucleotide reductase, which reduces intracellular deoxynucleoside triphosphate pools, and deoxycytidine monophosphate (dCMP) deaminase, which is responsible for gemcitabine degradation (Gandhi & Plunkett, 1990).

Advanced pancreatic cancer patients who received gemcitabine showed improved symptoms compared to those who received 5-fluorouracil (5-FU), which was the most commonly used agent for PDA prior to the gemcitabine (Burris et al., 1997). Clinical benefit was determined by monitoring pain, performance status, and weight of the patients. Even though patients receiving gemcitabine experienced clinical benefit, there was no significant effect on survival. Thus, gemcitabine improves quality of life but does not cure the disease or prolong survival (Seufferlein, Bachet, Van Cutsem, Rougier, & Group, 2012).

Some studies have suggested that gemcitabine-based cytotoxic combinations have a significant benefit in patients with good performance status (Cunningham et al., 2009; Heinemann, Boeck, Hinke, Labianca, & Louvet, 2008; Locher et al., 2008). Recent studies, therefore, are focusing on combination therapy of gemcitabine with other cytotoxic or biologic agents including erlotinib and nab-paclitaxel (Moore et al., 2007; Von Hoff et al., 2011).

1.3.2. Erlotinib

Erlotinib is an approved oral human epidermal growth factor receptor type 1 (HER1/EGFR) tyrosine kinase inhibitor for non-small-cell lung cancer patients (Rich & Whittaker, 2005). Pancreatic tumors often overexpress HER1/EGFR, which is an indicator of poor prognosis and disease progression (Akar et al., 2007; Cheung et al., 2008; Iacobuzio-Donahue et al., 2003). It has been reported that inhibition of HER1/EGFR tyrosine kinase signaling decreases the growth and metastasis of human pancreatic tumor xenografts and improves the anticancer effects of gemcitabine (D.-S. Kim, Park, Nam, Kim, & Kim, 2006; Mann et al., 2006).

Randomly assigned patients who received combination therapy of gemcitabine and erlotinib showed improved overall survival by 2 weeks and improved progression-free survival compared to those who received only gemcitabine (Moore et al., 2007). However, the patients on the erlotinib and gemcitabine combination therapy experienced more toxicity including rash, diarrhea, infection, stomatitis, protocol-related death, and interstitial lung disease (ILD)-like syndrome. Interestingly, the occurrence of rash was associated with better outcome and longer survival.

1.3.3. Nab-paclitaxel

Nab-paclitaxel (Abraxane), an albumin-bound paclitaxel formulation, has antitumor activity as a single agent and synergistic activity in combination with gemcitabine in pancreatic cancer mouse models (Frese et al., 2012; Von Hoff et

al., 2011). It has been suggested that nab-paclitaxel binds to the secreted protein acidic and rich in cysteine (SPARC), overexpressed in the PDA stroma, and facilitates increased delivery of chemotherapeutic agents to tumors (R. H. Hruban & Klimstra, 2014; Infante et al., 2007; Von Hoff et al., 2013).

According to Von Hoff *et al.* (Von Hoff et al., 2013), PDA patients who received the combination of gemcitabine and nab-paclitaxel had significantly improved median overall survival from 6.7 months (gemcitabine alone) to 8.5 months (combination of gemcitabine and nab-paclitaxel), progression-free survival, and response rate compared to gemcitabine single treatment. However, the gemcitabine-nab-paclitaxel combination also increased the rates of peripheral neuropathy and myelosuppression. At present time, the combination of gemcitabine and nab-paclitaxel has become a new standard treatment for patients with advanced stage PDA (Hidalgo et al., 2015).

1.3.4. FOLFIRINOX

FOLFIRINOX is a combination chemotherapy regimen, composed of 5-FU, oxaliplatin, irinotecan, and leucovorin (Ychou, 2003). Oxaliplatin has clinical activity against pancreatic cancer only when combined with 5-FU (Ruiz, Del Valle, & Gomez, 2004). Irinotecan also has some clinical activity against advanced pancreatic cancer, and is synergistic when administered before 5-FU and leucovorin (Azrak et al., 2004; Pavillard et al., 1998). In addition, an *in vitro* experiment showed that oxaliplatin and irinotecan have synergistic activity (Zeghari-Squalli, Raymond, Cvitkovic, & Goldwasser, 1999).

Conroy *et al.* performed phase 2-3 studies comparing FOLFIRINOX and gemcitabine in patients with PDA (Conroy et al., 2011). The FOLFIRINOX treated group showed improved median overall survival by 4 months and improved progression-free survival and response rate compared to the gemcitabine group. However, adverse events, such as febrile neutropenia and deterioration of quality of life, occurred more frequently in the FOLFIRINOX group compared to the gemcitabine group. FOLFIRINOX provides survival advantage, but is more toxic than gemcitabine, thus its use may be limited to relatively younger patients with good performance status (Conroy et al., 2011; Hidalgo et al., 2015).

1.3.5. Summary of current treatments

At current time, 'gemcitabine and nab-paclitaxel' or 'FOLFIRINOX' are offered to patients with advanced PDA and good performance status. Single agent gemcitabine remains a reasonable option for more debilitated patients.

1.4. Transglutaminase

1.4.1. Transglutaminase family

The human transglutaminases (TGases) are a protein family that consists of protein 4.2, factor XIII-A (FXIII-A), and TG1-7 (Griffin, Casadio, & Bergamini, 2002) (**Table 1** and **Figure 3**). Protein 4.2 lacks catalytic activity and is restricted to erythrocytes (Lorand & Graham, 2003). FXIII-A and TG1-7, produced as

zymogens, are enzymes that catalyze Ca^{2+}-dependent post-translational modifications. FXIII-A is involved in wound healing where it stabilizes fibrin clots (Iismaa, Mearns, Lorand, & Graham, 2009). TG1 is a keratinocyte TGase that is involved in keratinocyte differentiation. TG2 is a tissue TGase, which will be discussed in detail in the next section. TG3 is an epidermal TGase involved in skin maturation, and TG4 is a prostatic secretory TGase, which is important for sperm maturation. TG5, also called TGx, is involved in cornified envelope assembly and keratinocyte differentiation. TG6 and TG7 are also named as TGy and TGz, respectively, but have not been well characterized to date (Griffin et al., 2002; Lorand & Graham, 2003).

Table 1. TGase family members; expressions, localizations, encoding genes, and related diseases.

Proteins	Tissue Expression	Localization	Gene	Related Biology
FXIIIA	Platelets, Astrocytes, Placenta, Plasma	Cytosol, Extracellular	*F13A1*	Blood coagulation
TG1	Keratinocytes, Brain	Cytosol, Membrane	*TGM1*	Keratinocyte differentiation
TG2	Ubiquitous	Cytosol, Nucleus, Membrane, Extracellular	*TGM2*	Multiple
TG3	Squamous epithelium, Brain	Cytosol	*TGM3*	Cornified envelope (CE) formation
TG4	Prostate	Unknown	*TGM4*	Semen coagulation
TG5	Ubiquitous	Unknown	*TGM5*	CE formation, Keratinocyte differentiation
TG6	Unknown	Unknown	*TGM6*	Unknown
TG7	Ubiquitous	Unknown	*TGM7*	Unknown
Band 4.2	Red blood cells, Bone marrow, Fetal liver and spleen	Membrane	*EBP42*	Erythrocyte membrane integration, Hereditary spherocytosis

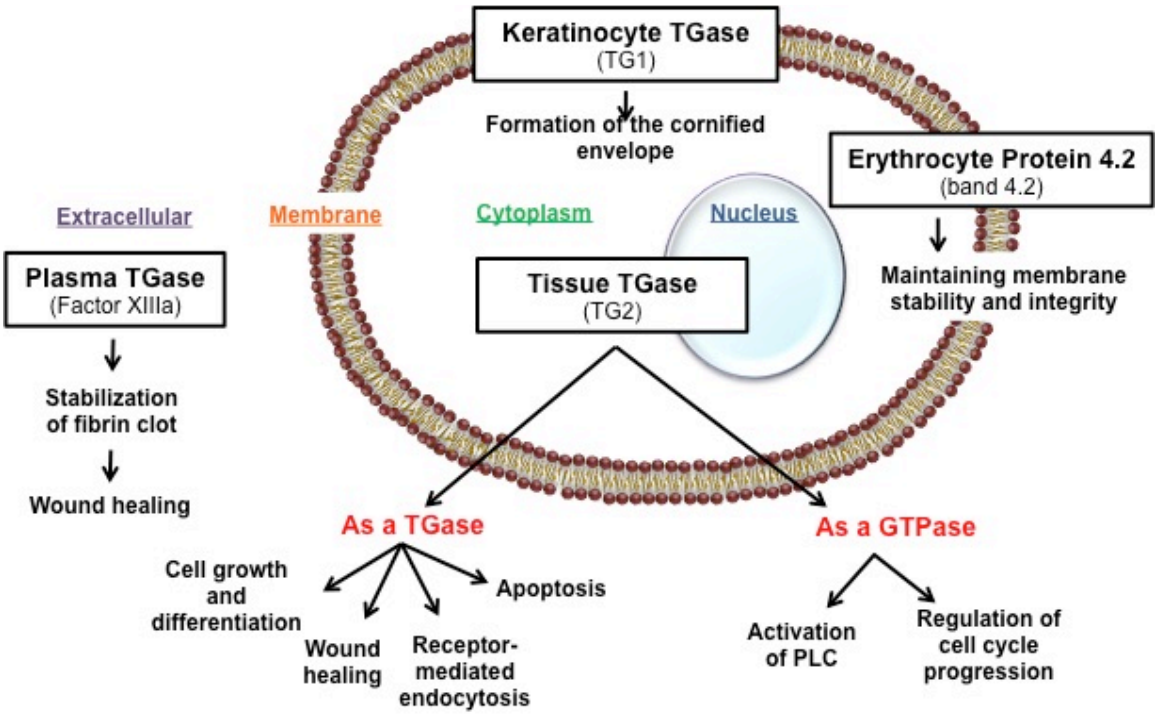

Figure 3. Cellular distribution and possible functions of TGases. TGases can localize on membrane (e.g. TG1), in cytoplasm and nucleus (e.g. TG2), and in extracellular compartment (Factor XIIIa). *Figure is modified from "Tissue transglutaminase: an enzyme with a split personality" by J.Chen and K. Mehta, 1999, The International Journal of Biochemistry and Cell Biology, 31, p. 817-36 © 1999 Elsevier Science Ltd.*

TGase family members have a conserved structure with four distinct domains: an N-terminal β-sandwich domain, a catalytic domain, and two C-terminal β-barrel domains (Mehta, Kumar, & Kim, 2010) (**Figure 4**). The catalytic core domain of TGases contains a catalytic triad (Cys^{277}, His^{335}, and Asp^{358}), essential residues for catalysis. Band 4.2 is catalytically inactive because it lacks the required cysteine residue in the catalytic triad (**Figure 4**).

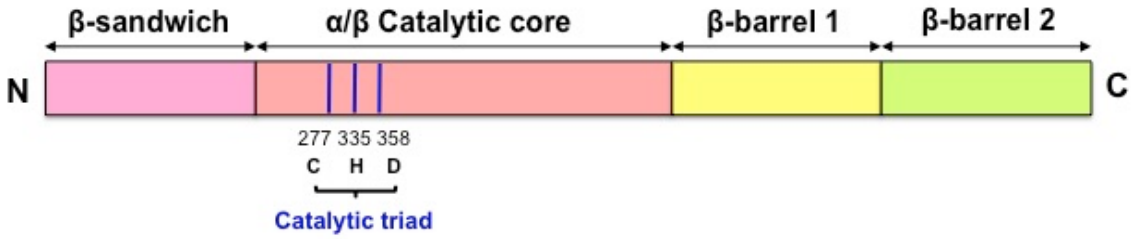

Figure 4. Schematic illustration of TGase domains. TGases are consisted of 4 distinct domains; a N-terminal β-sandwich domain, an α/β catalytic core domain containing Cys^{277}, His^{335}, and Asp^{358} catalytic triad, and 2 C-terminal β-barrel domains.

The post-translational reactions catalyzed by TGs can be separated into three reactions (**Figure 5**): transamidation (crosslinking, amine incorporation, and acylation), hydrolysis (deamination and isopeptide cleavage), and esterification. Transamidation causes (a) protein crosslinking by forming a ε-(γ-glutamyl)-lysine isopeptide bond between the lysine residue of one donor protein and the glutamine residue of another acceptor protein; (b) amine incorporation of an amine into the glutamine residue of the acceptor protein; and (c) acylation of a lysine side chain of the donor protein. Hydrolysis and esterification are caused via the direct attack of γ-amides of glutamine residues by water and alcohol each. The first TGase enzyme, TG2, was identified based on its ability to catalyze amine incorporation into proteins. Ca^{2+}-dependent amine incorporation remains the major modality of detecting TG2 activity (Griffin et al., 2002; Liu, Cerione, & Clardy, 2002; Mehta et al., 2010).

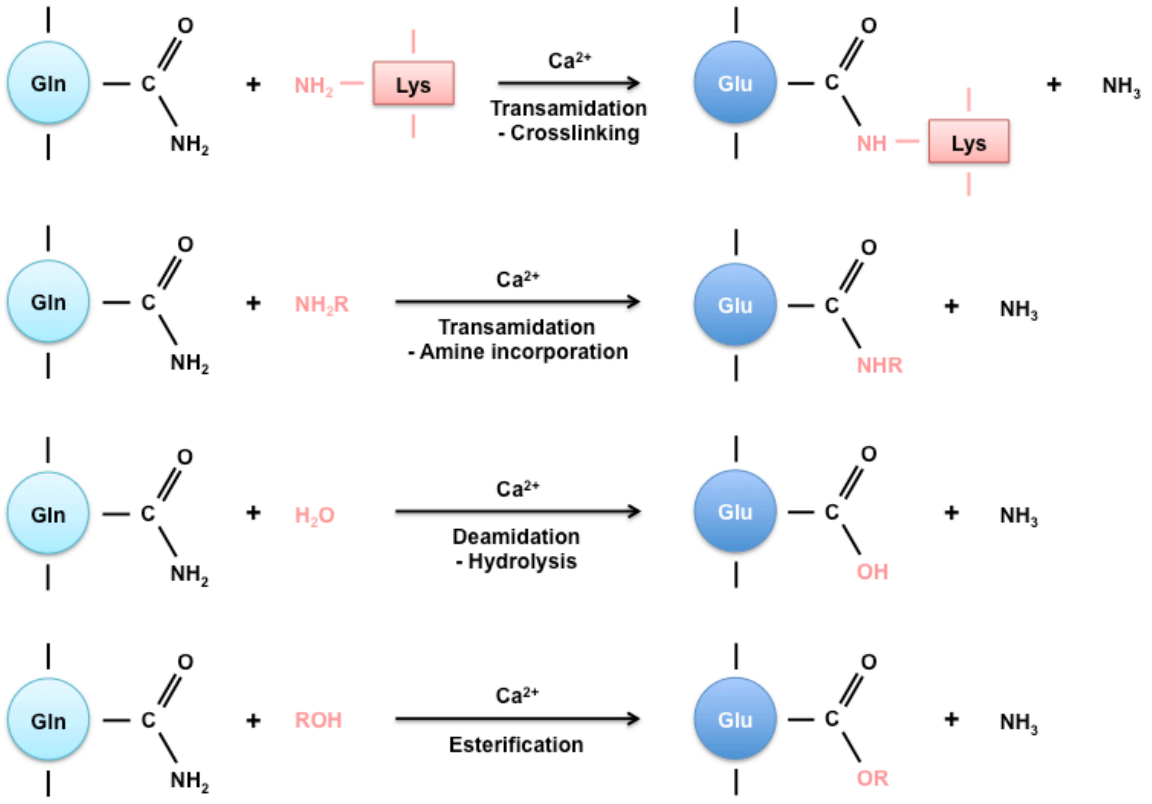

Figure 5. Catalytic activity of TGases. TGases catalyze Ca^{2+}-dependent reactions; transamidation, hydrolysis, and esterification. Glutamine-containing protein or peptide is the major substrate of TGases and reacts with 1) a lysine-containing protein or peptide to cause crosslinking of the 2 substrates, with 2) a polyamine to cause amine incorporation into the glutamine-containing protein or peptide, with 3) H_2O to cause deamidation, and with 4) alcohol to cause esterification. *Figure is modified after "Transglutaminases: Nature's biological glues" by M. Griffin, R. Casadio, and C. Bergamini, 2002, The Biochemical Journal, 368, p.377-396 © 2002 Biochemical Society.*

1.4.2. Tissue transglutaminase

TG2 is a multifunctional protein with a molecular weight of 78kDa. TG2 is encoded by *TGM2* on human chromosome 20q11-12 and is composed of 13 exons and 12 introns (Iismaa et al., 2009; Mehta et al., 2010). TG2 is distinguished from other TGs by its unique characteristics which include ubiquitous expression, multi-compartmental cellular localization, and binding to

and hydrolysis of guanine nucleotides (Lorand & Graham, 2003). Ubiquitous expression of TG2 is due to constitutive expression in endothelial cells, smooth muscle cells, and fibroblasts (Thomazy & Fesus, 1989). TG2 is localized predominantly in the cytoplasm (80%), partly in the plasma membrane and ECM (10~20%), and sparsely in the nucleus (5%) (Bruce & Peters, 1983). Since there is no leader peptide or transmembrane domain in TG2 (Gentile et al., 1991; Liu et al., 2002), the mechanism by which TG2 is secreted from the intracellular compartment onto the cell surface and into the ECM remains unclear.

However, the Belkin's laboratory proposed that TG2 is secreted via non-classical, ER/Golgi-independent pathway, which involves endosomal trafficking (Evgeny A Zemskov, Mikhailenko, Hsia, Zaritskaya, & Belkin, 2011). This endosome-mediated TG2 externalization is processed through phosphoinositide-dependent recruitment of cytoplasmic TG2 to the perinuclear recycling endosome, its delivery inside these vesicles, their anterograde trafficking, and their fusion with the plasma membrane, which in turn releases TG2 onto the cell surface. In addition, Belkin and co-workers reported that this non-classical externalization of TG2 is regulated by nitric oxide via protein trafficking inhibition (Santhanam, Berkowitz, & Belkin, 2011).

TG2 is structurally and functionally a multi-functional protein with both intracellular and extracellular functions (Mehta et al., 2010). TG2 is structured with four distinct domains: an N-terminal β-sandwich domain, a catalytic domain, and two C-terminal β-barrel domains (Mehta et al., 2010) (**Figure 6**). The N-terminal β-sandwich domain contains high affinity binding site for fibronectin,

which promotes attachment of cells to extracellular matrix (ECM) and enhance cell growth, survival, and motility. The catalytic core domain includes a catalytic triad (Cys^{277}, His^{335}, and Asp^{358}) and a Ca^{2+} binding site. Exposure to Ca^{2+} induces crosslinking of various cellular proteins and leads to apoptosis or inflammation. The C-terminus β-barrel 1 and 2 domains are arranged in antiparallel β-barrels and contain a GTP/GDP binding site. The C-terminal domains are important in regulating transamidation activity and GTPase activity which are related to the TG2 signaling pathways involved in cell survival, cell growth, and invasion. The C-terminus β-barrel 2 domain can interact with and activate phospholipase C and contribute to inflammation in GTP-bound state (Griffin et al., 2002; Mehta et al., 2010).

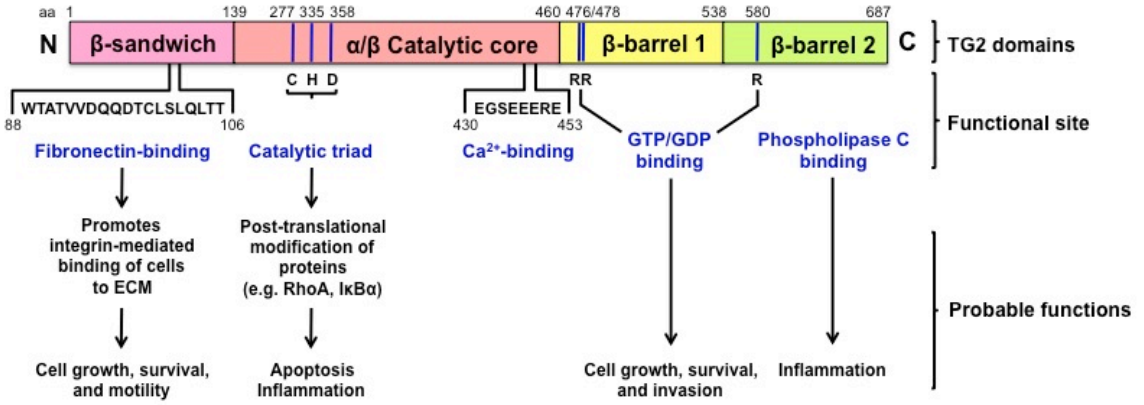

Figure 6. Schematic representation of the structural and functional domains of TG2. TG2 contains four distinct domains, and each domain has unique function. The N-terminal β-sandwich domain contains fibronectin-binding site and is responsible for cell adhesion to the ECM. The α/β catalytic core contains catalytic triad and Ca^{2+}-binding sites and is responsible for crosslinking reaction, contributing to cell death. The C-terminal β-barrels contain GTP/GDP binding sites that play an important role in cell survival signaling pathways. Phospholipase C also can bind to β-barrel 2, involving in inflammation. *This figure is modified after "Transglutaminase 2: A multi-tasking protein in the complex circuitry of inflammation and cancer" by K. Mehta, A. Kumar, and H. Kim, Biochemical Pharmacology, 80, p. 1921-1929 © 2010 Elsevier Inc.*

The functions of TG2 depend on its subcellular localization and interaction with its regulators (**Figure 7**). Calcium (Ca^{2+}) and GTP are the two crucial regulators, and the binding of Ca^{2+} and GTP inversely regulate TG2 activity through alteration of the TG2 protein conformation (Di Venere et al., 2000; Pinkas, Strop, Brunger, & Khosla, 2007; E. A. Zemskov, Janiak, Hang, Waghray, & Belkin, 2006). TG2 binding of Ca^{2+} causes an extended-form conformation exposing the active catalytic site and exerting enzymatic activity, but inhibits binding and hydrolysis of GTP. TG2 binding to GTP induces a compact conformation and inhibits the TG catalytic activity (Iismaa et al., 2009). In the cytoplasm where Ca^{2+} concentration is low, TG2 transamidating activity is inhibited, while the GTPase, the disulfide isomerase, and the protein kinase function may be activated (Fesus & Piacentini, 2002; Pinkas et al., 2007). Influx of extracellular Ca^{2+} by cellular stress or release of Ca^{2+} from intracellular storages, such as endoplasmic reticulum (ER), can activate TG2 catalytic activity.

In contrast, TG2 on the cell surface and in the ECM, where the Ca^{2+} concentration is high, promotes cell-matrix interactions by binding to integrins and fibronectin and by modifying extracellular proteins (Griffin et al., 2002). TG2 in the nuclear compartment associates with histones and has been implicated in phosphorylation of the histones at Ser (10), and histones 1 and 3 in chromatic preparations (Kuo, Tatsukawa, & Kojima, 2011).

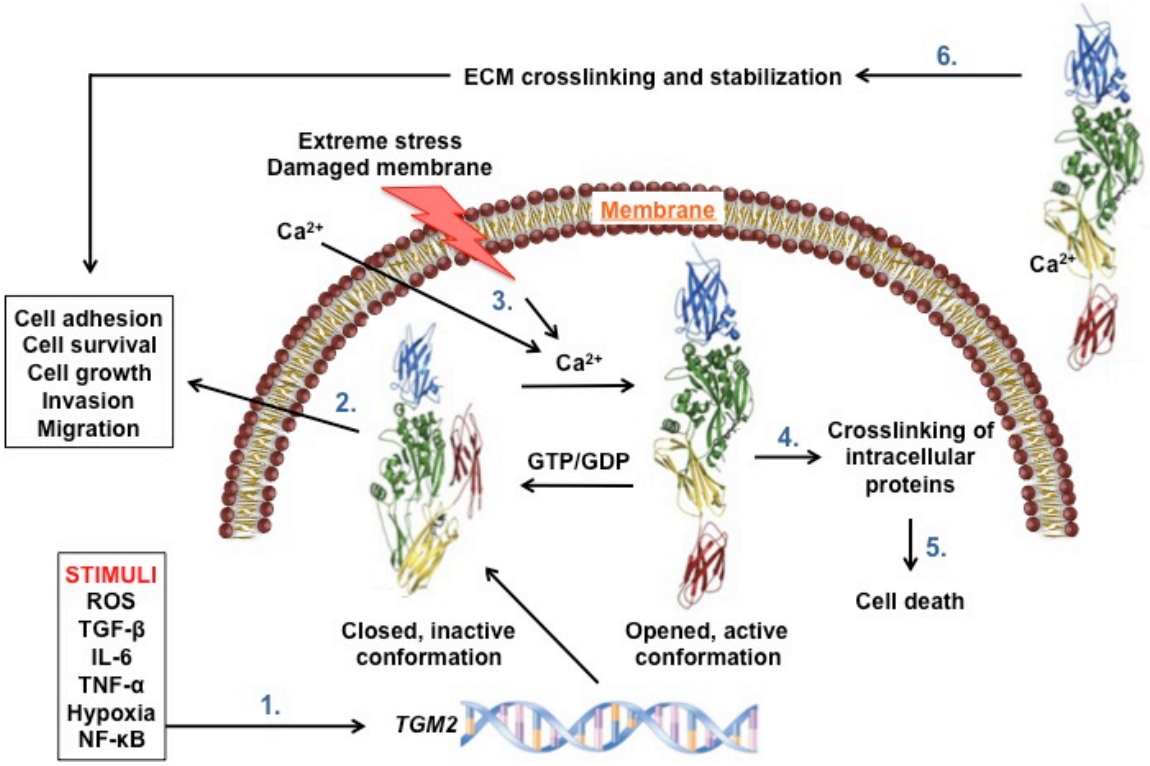

Figure 7. Corresponding functions of TG2 depending on its localization and conformation. 1) Various stimuli up-regulate TG2 expression. 2) Under normal conditions, Ca^{2+} concentration is low and GTP concentration is high, causing TG2 to adopt a closed conformation and be catalytically inactive. TG2 can promote cell adhesion, survival, growth and motility. 3) Influx of Ca^{2+} into the intracellular compartment due to stress leads TG2 to open and become enzymatically active. 4) Active TG2 crosslinks intracellular proteins and leads to 5) apoptosis. 6) Externalized TG2 is catalytically active by binding to Ca^{2+} and crosslinks and stabilizes ECM proteins, promoting cell adhesion and motility. *Figure is modified from "Transglutaminase 2: A multi-tasking protein in the complex circuitry of inflammation and cancer" by K. Mehta, A. Kumar, and H. Kim, 2010, Biochemical Pharmacology, 80, p. 1921-1929 © 2010 Elsevier Inc.*

1.4.2-a. Catalytic function of TG2

TG2, in a Ca^{2+}-dependent manner, crosslinks ECM proteins by catalyzing the formation of protease-resistant covalent ε-(γ-glutamyl)-lysine isopeptide bonds between donor lysine residue of one protein and acceptor glutamine residue of another protein (Griffin et al., 2002; Lorand & Graham, 2003; Mchta, 2005). This transamidating activity alters ECM deposition and promotes cell adhesion, migration, invasion, and ECM stabilization (Mehta, 2009). Enzymatic substrates of TGases, particularly TG2, include nuclear (Rb and histones), cytoplasmic (RhoA and eIF5A), cytoskeletal (β-tubuline, tau, troponin, actin, and myosin), membrane (C-CAM), and ECM (FN, fibrinogen, vitronectin, collagen, laminin, nidogen, osteopontin, ostesonectin, osteocalcin, and LTBP-1) target proteins (E. A. Zemskov et al., 2006) (Table 2). Type I collagen, one of the ECM proteins, is abundant in the human body and is known to be a substrate for TG2, which causes formation of ε-(γ-glutamyl)-lysine isopeptide bonds between molecules (Chau, Collighan, Verderio, Addy, & Griffin, 2005). TG2-mediated type I collagen crosslinking results in increased strength and stability of collagen fibers and resistance to proteolytic degradation (Chau et al., 2005; Orban et al., 2004).

Table 2. Known TG2 substrates

Intracellular proteins

• Cytosolic proteins	Aldolase A Glyceraldehyde-3-phosphoate dehydrogenase Phosphorylase kinase Crystallins Glutathione S-transferase
• Cytoskeletal proteins	Actin Myosin Troponin B-tubulin Tau Rho A
• Organelle proteins	Histone H2B A-Oxaloglutarate dehydrogenase Cytochromes Erythrocyte band III CD38 Acetylcholine esterase

Extracellular proteins

• Matrix-associated proteins	Collagen Fibronectin Fibrinogen Vitronectin Osteopontin Nidogen Laminin LTBP-1 Osteonectin Osteocalcin
• Signaling proteins and peptides	Substance P Phospholipase A2 Midkine

1.4.2-b. Non-catalytic functions of TG2

TG2 as a GTPase:

In addition to its Ca^{2+}-dependent enzymatic activity, TG2 functions as a GTPase (Mhaouty-Kodja, 2004; Nakaoka et al., 1994). Achyuthan *et al*. have found that guanosine 5'-triphosphate (GTP) and guanosine diphosphate (GDP) bind to guinea pig liver TGase and inhibit its transamidation activity, which can be reversed by Ca^{2+} (Achyuthan & Greenberg, 1987). In addition, Lee *et al*. have reported that TGase purified from guinea pig liver hydrolyzes GTP (Lee, Birckbichler, & Patterson, 1989). Following this report, Im *et al*. reported a 74-kD GTP binding protein (G-protein; Ga_h), which is involved in α_1-adrenergic receptor (α_1-adrenoceptor)-mediated activation of phospholipase C (PLC-δ1) (Im & Graham, 1990). The activated PLC hydrolyzes phosphatidylinositol diphosphate (PIP_2) to inositol triphosphate (IP_3), an inducer of Ca^{2+} release from intracellular organelles, and diacylglycerol (DAG), an activator of protein kinase C, which plays a role in various biological processes. Im *et al*. have also reported that Ga_h forms a complex with the 50-kD subunit Gb_h (Im, Riek, & Graham, 1990), an inhibitory regulator of Ga_h (Baek et al., 1996). Later, Nakaoka *et al*. reported that Ga_h was in fact TG2 possessing both TGase activity and G-protein coupled receptor (GPCR) signal transduction function (Nakaoka et al., 1994).

As reported by Im *et al*., binding of GTP/GDP on Ga_h (TG2) leads to a compact (closed), catalytically inactive conformation of Ga_h (TG2). Binding of an agonist to the α_1-adrenoceptor drives conformational change of GPCR, which in

turn activates the $G\alpha_h$ (TG2) by releasing GDP and binding GTP. Once GTP is bound, $G\alpha_h$ (TG2) dissociates from both the α_1-adrenoceptor and $G\beta_h$. The GTP-bound $G\alpha_h$ (TG2) interacts with the effector (PLC), which produces the second messenger (DAG) to amplify signals important in biological activities including sympathetic nervous system responses, platelet aggregation and secretion, vasoconstriction, and mitogenesis. Once GTP is hydrolyzed to GDP and Pi by the GTPase function of $G\alpha_h$ (TG2), GDP-bound $G\alpha_h$ (TG2) dissociates from the effector and re-associates with $G\beta_h$, completing an activation/deactivation cycle of GTPase (Im et al., 1990).

TG2 as a serine/threonine kinase:

Mishura and Murphy have reported that TG2 also has an intrinsic kinase activity. They identified TG2 in the kinase fraction associated with the insulin-like growth factor-binding protein-3 (IGFBP-3) in T47D breast cancer cells (S. Mishra & Murphy, 2004). They found that TG2 is able to phosphorylate IGFBP-3 and IGFP-5 at multiple serine and threonine residues, and that this kinase activity can be inhibited by Ca^{2+}, in a concentration-dependent manner. The authors also identified p53 (Suresh Mishra & Liam J Murphy, 2006), H1, H2A, H2B, H3, H4 histones (Suresh Mishra, Saleh, Espino, Davie, & Murphy, 2006), and retinoblastoma protein (Rb) (Suresh Mishra, Melino, & Murphy, 2007) as other substrates of TG2 kinase activity. TG2-mediated phosphorylated p53 blocks the interaction between p53 and Mdm2, and TG2-mediated phosphorylated Rb disrupts the Rb/E2F1 complex, which has an important role in the regulation of the cell cycle (Suresh Mishra et al., 2007; S. Mishra & L. J. Murphy, 2006). In

addition, they have discovered that TG2 is also phosphorylated by the protein kinase A (PKA), which in turn abolishes the protein's transamidating activity and enhances its kinase function (Suresh Mishra et al., 2007). These findings suggested that activation of PKA leads to phosphorylation of TG2, which phosphorylates Rb.

***TG2 interaction with fibronectin*:**

TG2 forms ternary complex with fibronectin (FN) and integrin on the cell surface where all three proteins can interact with each other, facilitating cell adhesion and migration (Turner & Lorand, 1989). TG2 contains a FN binding domain on the β-sandwich domain located at the TG2 N-terminus spanning amino acids 88 to 106 (Hang, Zemskov, Lorand, & Belkin, 2005). A 42 kDa sub-domain of FN consisting of $I_6\,II_{1,2}\,I_{7\text{-}9}$ modules binds to the FN binding domain on TG2 with a high affinity, facilitating cell adhesion to the ECM through β-integrins (Akimov & Belkin, 2001; Radek, Jeong, Murthy, Ingham, & Lorand, 1993). Formation of FN-TG2-β-integrin ternary complex activates cell survival and triggers motility-associated signaling pathways including the focal adhesion kinase (FAK), Raf-1, and GTP-binding protein, Rho (Hang et al., 2005; Janiak, Zemskov, & Belkin, 2006). These interactions do not require Ca^{2+} and are independent of the transamidation and GTPase activity of TG2. Since most integrin ligands in the ECM are substrates for TG2, the extracellular TG2 is involved in the assembly, remodeling, and stabilization of ECM in various tissues (Aeschlimann & Thomazy, 2000).

***TG2 as a protein disulphide isomerase*:**

Hasegawa *et al*. have described a novel function of TG2 as a protein disulphide isomerase (PDI) (Hasegawa et al., 2003). PDIs are members of the thioredoxin superfamily, which resides in the lumen of the endoplasmic reticulum (ER), supporting conformational changes of proteins by forming disulphide bridges within polypeptides (Ferrari & Soling, 1999; Freedman, Hirst, & Tuite, 1994; Noiva & Lennarz, 1992). The authors have shown that TG2 converts reduced/denatured inactive RNase A molecule to the native active enzyme, and this PDI function could be inhibited by bacitracin, a typical PDI inhibitor, and reduced BSA, but not by Ca^{2+} or GTP (Hasegawa et al., 2003).

1.4.3. TG2 and diseases

Up-regulation of TG2 has been evidenced in various human pathological conditions (**Figure 8**) such as degenerative neurological diseases (Junn, Ronchetti, Quezado, Kim, & Mouradian, 2003), autoimmune diseases (Sollid, Molberg, McAdam, & Lundin, 1997), fibrosis and atherosclerosis (Grenard et al., 2001; T. S. Johnson et al., 1999; S.-Y. Kim, Jeitner, & Steinert, 2002), chronic inflammatory diseases (Elisabetta AM Verderio, Johnson, & Griffin, 2005), neoplastic disease (Barnes, Bungay, Elliott, Walton, & Griffin, 1985), and cancers. Especially, TG2 expression is increased in ovarian cancer (L Cao et al., 2012; Satpathy et al., 2007), breast carcinoma (Herman, Mangala, & Mehta, 2006), malignant melanoma (Fok, Ekmekcioglu, & Mehta, 2006), lung carcinoma

(Park et al., 2010), and pancreatic cancer (Verma et al., 2006) as shown in several studies.

TG2 expression in cancer is directly related to cancer progression, chemoresistance (Kotsakis & Griffin, 2007), pro- or anti-apoptotic effects (Fesus & Szondy, 2005), and invasiveness (Mehta et al., 2010). Because of these observations, TG2 expression is usually associated with poor survival. TG2 expression can be induced by various cytokines and growth factors, such as TGF-β (Quan, Choi, Lee, & Lee, 2005) and IL-6 (Suto, Ikura, & Sasaki, 1993). TG2 is up-regulated in ovarian cancer (OC) cells compared to normal ovarian epithelial cells by TGF-β (L. Cao et al., 2012; Matei et al., 2002), and induces intraperitoneal dissemination by enhancing cancer cell adhesion to the ECM and interaction with integrins (Satpathy et al., 2007). Down-regulation of TG2 in OC cells decreased adhesion and migration *in vitro* and intraperitoneal dissemination *in vivo*.

In the context of apoptosis, TG2 acts either as an inducer or as an inhibitor via cellular specific mechanisms. Under physiological conditions, intracellular TG2 is enzymatically inactive due to low Ca^{2+} concentrations and high GTP concentrations. When Ca^{2+} influx occurs during the late phases of apoptosis, TG2 crosslinks cytosolic proteins and finalizes the cell death process (Lorand & Graham, 2003). On the other hand, TG2 plays an anti-apoptotic role in malignant cells by promoting cell survival (e.g. NF-κB) and activating anti-apoptotic (e.g. FAK, PI3K/Akt) signaling pathways, which will be described in detail in next section.

Overall, these studies suggest TG2 involvement in the process of chemotherapy resistance and support developing TG2 inhibitors as anticancer therapy (Yuan et al., 2005).

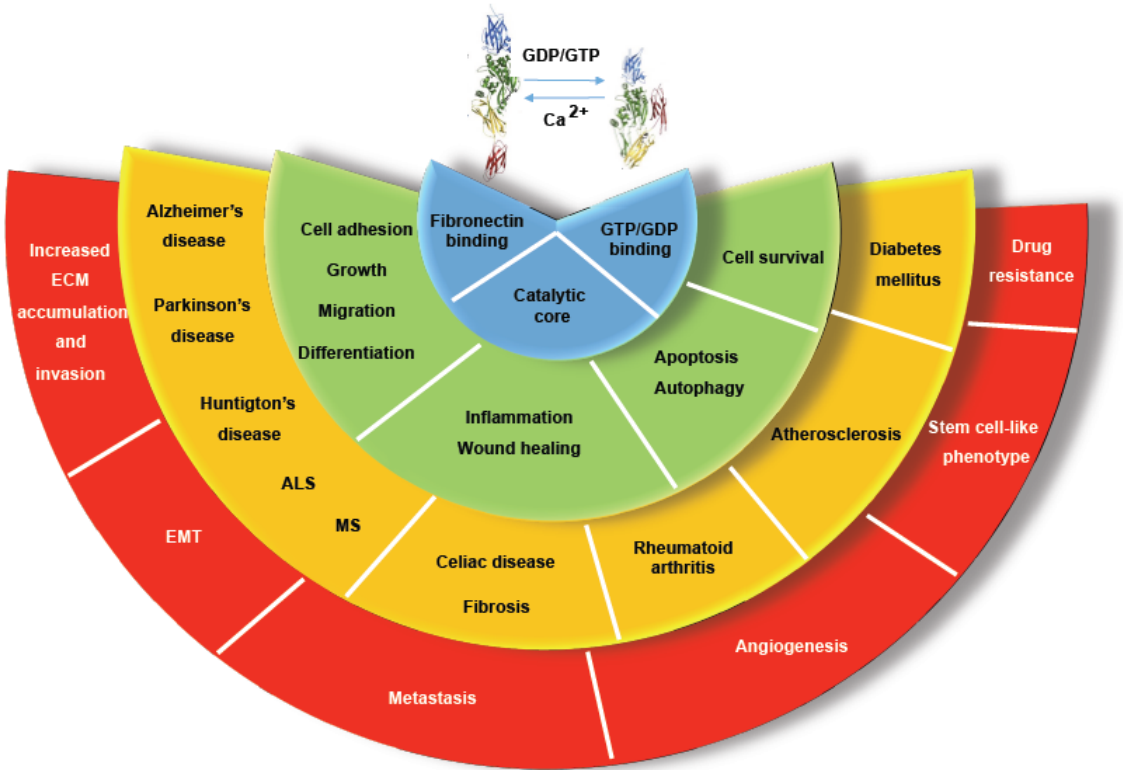

Figure 8. TG2 involvement in human diseases. Conformational changes of TG2 induced by Ca^{2+} concentrations regulate the TG2 functions that are associated with different pathological and physiological conditions.

1.4.3-a. TG2 in Pancreatic Cancer

TG2 is a highly expressed protein in pancreatic tumors (Cheung et al., 2008; Iacobuzio-Donahue et al., 2003; Verma et al., 2006). Elevated TG2 expression in PDA cells was linked to development of drug resistance, metastatic phenotype, and poor patient prognosis (Iacobuzio-Donahue et al., 2003; Verma,

Guha, Diagaradjane, et al., 2008). Mehta and colleagues reported elevated TG2 expression in the majority of drug resistant and metastatic PDA tumors and cell lines (Verma et al., 2006). TG2 expression level was high in 42 out of 75 (56%) PDA tumor samples compared to normal pancreatic ducts and in all of 12 PDA cell lines analyzed. They reported a trend of increasing TG2 expression with increasing tumor stage (T1, 3 out of 5 (60%); T2, 32 out of 44 (73%); T3, 13 out of 16 (81%)).

In these studies, the elevated TG2 expression in PDA was associated with constitutive activation of the nuclear factor κB (NF-κB) and of the focal adhesion kinase (FAK)/phosphatidylinositol 3-kinase (PI3K)/AKT signaling pathway leading to chemo-resistance and invasive phenotypes (Mann et al., 2006; Verma, Guha, Diagaradjane, et al., 2008; Verma, Guha, Wang, et al., 2008). In addition, TG2 expression was promoted by the activation of protein kinase Cδ (PKCδ), resulting in inhibition of autophagy in PDA cells (Akar et al., 2007).

NF-κB is a transcription factor that contains a highly conserved DNA-binding domain called the Rel homology domain (Ghosh et al., 1998), and in cancer, it plays an important role in regulation of cell growth, metastasis, and apoptosis (D.-S. Kim et al., 2006; Mann et al., 2006; Mehta, Fok, Miller, Koul, & Sahin, 2004; Verma et al., 2006). Under normal conditions, NF-κB is present in an inactive form in cells by interacting with IκBα, a cytosolic protein that functions to inhibit NF-κB through non-covalent association with the DNA-binding domain of NF-κB. Under various stimuli including oxidative stress, cytokines, growth factors, or in the presence of bacterial or viral antigens, NF-κB is activated by

dissociation from IκBα and translocates to the nucleus leading to increased expression of target genes. Such genes are involved in cell growth, adhesion, migration, and apoptosis inhibition (Karin et al., 2002; Nakanishi & Toi, 2005). Generally, cellular response to various stimuli is well controlled by transient activation of NF-κB. However, in PDA, NF-κB is constitutively activated due to unregulated binding of IκBα to the DNA-binding domain of NF-κB (Bours, Dejardin, Goujon-Letawe, Merville, & Castronovo, 1994; Wang et al., 1999).

Mann *et al*. have shown that TG2 forms a complex with IκBα and directly crosslinks IκBα (Mann et al., 2006). The crosslinked IκBα dissociates from the Rel homology domain of NF-κB and is processed for proteasomal degradation, resulting in nuclear localization and constitutive activation of NF-κB. Overexpression of TG2 or direct activation of TG2 by treatment with Ca^{2+} ionophore resulted in activation of NF-κB in PDA cells. In addition, down-regulation of TG2 expression level by transfecting TG2-specific small interfering RNA (siRNA) and inhibition of TG2 enzymatic activity by using TG2-specific inhibitors, monodansylcadaverine and 5-(Biotinamido)pentylamine (BPA), in PDA cells expressing abundant TG2 resulted in reduced activation of NF-κB by increased formation of IκBα and NF-κB complex. These observations support that elevated TG2 expression is a key player in the constitutive activation of NF-κB in PDA.

FAK is a cytosolic protein tyrosine kinase that is involved in cell adhesion, migration, and survival via its downstream phosphatidylinositol 3-kinase (PI3K)/AKT signaling pathway (Verma et al., 2006). In the presence of stimuli,

such as growth factors and integrin engagement, FAK is phosphorylated and activated, which leads to activation of PI3K/AKT signaling pathway (J. Zhao & Guan, 2009). The activation of FAK/PI3K/AKT signaling pathway is negatively regulated by the tumor suppressor, PTEN (phosphatase and tensin homologue) (Maehama & Dixon, 1998; Tamura et al., 1998). PTEN directly interacts with FAK and inactivates it by dephosphorylation, and also dephosphorylates PIP_3 (phosphatidylinositol (3,4,5)-trisphosphate), resulting in the inhibition of the FAK/PI3K/AKT signaling pathway.

Verma *et al*. have shown that elevated expression of TG2 in PDA contributed to drug resistant and metastasis via activation of FAK (Verma et al., 2006). Resistance to gemcitabine treatment and invasiveness as measured through matrigel-transwell assay were correlated with higher expression level of either TG2 or of its mutant, $C_{277}S$, in PDA cells. In addition, overexpression of TG2 in low TG2-expressing PDA cells increased FAK activation leading to AKT activation, while down regulation of TG2 with siRNA in PDA cells diminished FAK activation, suggesting that the elevated TG2 expression induces constitutive activation of FAK and may contribute to the drug resistance and invasion in PDA, independent of its enzymatic activity.

In addition, they showed that TG2 directly interacts with PTEN, inhibits its phosphorylation at Ser^{380}, and promotes ubiquitination of PTEN, leading to proteasomal degradation in PDA cells (Verma, Guha, Wang, et al., 2008). An inverse correlation between TG2 expression levels and PTEN was demonstrated in high TG2-expressing PDA cell lines. Overexpression of TG2 in low TG2-

expressing PDA cell lines decreased PTEN expression. On the other hand, down-regulation of TG2 in high TG2-expresssing cell lines by transfecting TG2-specific shRNA or siRNA increased total PTEN expression and phosphorylation. Overexpression of mutated, catalytically inactive TG2 ($C_{277}S$) in low TG2-expressing PDA cells inhibited PTEN expression and phosphorylation, suggesting that TG2-mediated regulation of PTEN expression is independent of its enzymatic activity. Moreover, treatment of TG2 overexpressing PDA cells with cycloheximide, a protein biosynthesis inhibitor, in the presence of MG132, a proteasome inhibitor, resulted in the accumulation of ubiquitinated PTEN without alteration in PTEN expression, suggesting that TG2 inhibits PTEN phosphorylation and promotes its ubiquitination, which results in proteasomal degradation. In addition, 51 specimens of stage II human PDA on a tissue microarray (TMA) was analyzed and reported that 11 out of 32 (34%) TG2-expressing specimens showed weak PTEN expression, while 13 out of 19 (68%) TG2-negative specimens expressed strong PTEN (Verma, Guha, Wang, et al., 2008).

Overall, these results supported that overexpression of TG2 in PDA activates FAK/PI3K/AKT cell survival signaling pathway by inhibiting expression and phosphorylation of the tumor suppressor protein PTEN and promoting its proteasomal degradation.

Autophagy is a process involved in the degradation of protein aggregates and dysfunctional organelles through the autophagosome-lysosome system (Rossin et al., 2014). Cellular waste is captured in autophagosome, and the

autophagosomes merge with lysosomes where digestion event of organelles occurs (Mizushima, 2007).

Akar *et al*. have shown that PKCδ, an enzyme involved in cell growth, differentiation, and apoptosis, promotes the expression of TG2, which in turn inhibits autophagy in PDA cells (Akar et al., 2007). Inhibition of PKCδ by a PKCδ-specific inhibitor, rottlerin, or by siRNA down regulated the expression of TG2 in PDA cells and resulted in inhibition of cell growth. Additionally, treatment with rottlerin or TG2 knockdown (siRNA) in PDA cells led to accumulation of microtubule-associated protein 1 light chain 3 (LC3)-II protein; a marker of autophagy, and formation of autophagosomes in cytoplasm, suggesting that TG2 regulates autophagy. The importance of Beclin-1, an autophagy stimulator, was shown by knocking down Beclin-1, which inhibited rottlerin- and TG2 siRNA-induced autophagy in PDA cells. These findings support that elevated TG2 expression in PDA cells inhibits autophagy leading to development of drug resistance.

PDA generally displays intrinsic resistance to chemo- and radio-therapy, but the molecular mechanisms of resistance are not well understood (Willett et al., 2005). Based on the observations that TG2 expression activates FAK/PI3K/AKT signaling pathway and NF-κB (Mann et al., 2006; Verma, Guha, Wang, et al., 2008; Verma et al., 2006), Verma *et al*. assessed the effect of TG2 inhibition on PDA cell response to chemotherapeutic drug (Verma, Guha, Diagaradjane, et al., 2008). They delivered TG2-specific siRNA-DOPC (1,2-dioleoyl-sn-glycero-3-phosphatidylcholine) liposome to orthotopic xenograft mice

via intravenous injection, with or without administration of gemcitabine via intraperitoneal injection. The mice injected with the combination of TG2 siRNA-DOPC and gemcitabine showed significantly decreased tumor growth and inhibited metastasis. In addition, TG2 inhibition reduced cell proliferation, angiogenesis, and phosphorylation of AKT. Overall, these results support that the inhibition of TG2 sensitizes PDA tumors to gemcitabine.

1.5. Research objectives

Pancreatic ductal adenocarcinoma (PDA) is a very aggressive and lethal disease, which metastasizes rapidly and is resistant to chemotherapeutics. A unique hallmark of the PDA is the presence of dense desmoplastic stroma (DS), which is composed of myofibroblasts, pancreatic stellate cells, collagen, and other extracellular matrix proteins (ECM). Tissue transglutaminase (TG2) is highly expressed in PDA cells and has been reported to be involved in tumor progression and chemotherapy resistance. However, the role of TG2 in PDA stroma is largely unknown. The goal of this study was to understand how up-regulated TG2 in PDA cells contributes to tumor progression and stroma alteration.

Knowing that TG2 is secreted into the ECM, where it crosslinks matrix proteins, I hypothesized that **TG2 secreted from PDA cells promotes PDA tumor progression by modulating the tumor microenvironment (TME)** (**Figure 9**). Specifically, I proposed that **TG2 1) promotes tumor formation and**

progression by 2) modulating composition of PDA stroma and 3) altering cellular signaling in PDA cells, which result in 4) decreased response of tumors to chemotherapy. TG2 in the TME provides a stable and protective tumor milieu for PDA progression through several mechanisms, which were investigated in the following specific aims.

Aim 1: Test the hypothesis that TG2 regulates tumor progression. As abundant TG2 was detected in PDA specimens and in PDA cells, I determined whether TG2 promotes tumor progression. An orthotopic xenograft mouse model was generated by implanting TG2 expressing (control) or knockdown (shTG2) PDA cells directly into the tail of pancreas of female nude mice. Tumor formation and growth were compared between control and shTG2 xenografts.

Aim 2: Test the hypothesis that TG2 alters stroma composition. As the most abundant components of the stroma are stromal cells and collagen type I, I assessed whether TG2 can activate and promote proliferation of fibroblasts, increase deposition of collagen, and induce crosslinking function on collagen, *in vitro* and *in vivo*.

Aim 3: Test the hypothesis that TG2-mediated modulated stroma alters cellular signaling in PDA cells. As the PDA stroma progresses through hyperplastic desmoplasia, its physiological properties become dense and stiff. YAP and TAZ transcription factors regulate cancer cell proliferatioin and survival, and are regulated by mechanotransduction among other mechanisms. I tested

whether YAP and TAZ in the PDA cells are activated by the surrounding TG2-mediated stiff environment, thereby, inducing proliferation of PDA cells.

Aim 4: Test the hypothesis that TG2-mediated modified stroma alters the response of tumors to chemotherapy. The PDA stroma is heterogenous and highly desmoplasic. I determined whether the tumors derived from TG2 expressing PDA cells are protected from the effects of gemcitabine, a common chemotherapeutic agent for PDA.

By testing the hypothesis, we observed involvement of TG2 in pancreatic tumor progression and chemoresistance through stroma modification, supporting that TG2 is a potential therapeutic target within the PDA supportive stroma. From a clinical standpoint, depletion of TG2 in the PDA stroma may improve the response to chemotherapy in PDA patients by providing increased drug penetrance into the tumor milieu and by inhibiting tumor growth and progression.

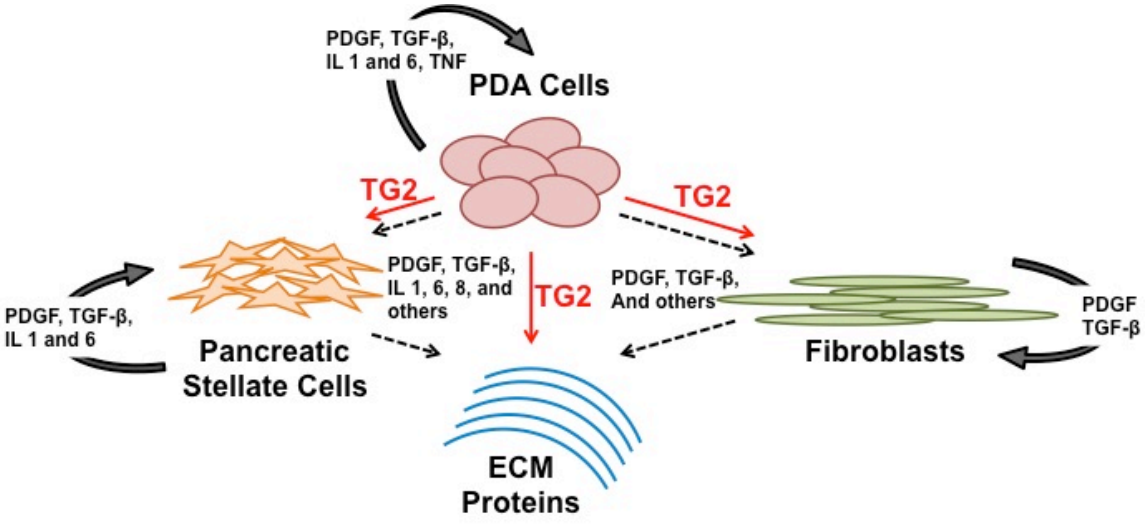

Figure 9. Schematic diagram of hypothesis. TG2 secreted from PDA cells promotes PDA progression by modulating the tumor microenvironment.

CHAPTER 2. MATERIALS AND METHODS

2.1. Antibodies

Western blot (WB): Tissue transglutaminase 2 monoclonal Ab (NeoMarkers, Fremont, CA; #CUB7402), GAPDH monoclonal Ab (Meridian Life Science, Inc., Memphis, TN; #C01448M), YAP1 monoclonal Ab (Abnova, Walnut, CA; #H00010413-M01), phospho-YAP (Ser127) monoclonal Ab (Cell Signaling Technology, Danvers, MA; #13008S), YAP/TAZ monoclonal Ab (Cell Signaling Technology, #8418), donkey anti-rabbit IgG-HRP (GE Healthcare Life Sciences, Pittsburgh, PA; #NA9340V), and goat anti-mouse IgG-HRP (Santa Cruz Biotechnology, Dallas, TX; #sc-2005).

Immunohistochemistry (IHC): Tissue transglutaminase 2 polyclonal Ab (NeoMarkers, #RB-060-P1ABX), Isopeptide (Abcam, Cambridge, MA; #ab424), α-SMA (IHC World, Woodstock, MD; #IW-MA1106), Universal LSABTM2 Kit/HRP, Rabbit/Mouse (Dako North America, Inc., Carpinteria, CA; #K0675), and Liquid DAB+ Substrate Chromogen System (Dako North America, Inc.; #3468).

Immunofluorescence (IF): Tissue transglutaminase 2 monoclonal Ab (same as WB), α-SMA monoclonal Ab (Sigma-Aldrich, St Louis, MO; #F-3777), Collagen I polyclonal Ab (Abcam, #ab34710), YAP/TAZ (same as WB), Cy™5-Conjugated ZyMax™ goat anti-mouse IgG (H+L) (Invitrogen Corporation, Camarillo, CA; #81-6516), Alexa Fluor® 488 goat anti-rabbit IgG (H+L) (Life Technologies, Carlsbad, CA; #A11008), Streptavidin-Alexa Fluor® 647 (Life

Technologies, #S32357), and VECTASHIELD Mounting Medium with DAPI (Vector Laboratories, Burlingame, CA; #H-1200).

2.2. Cell lines and cell cultures

Cell lines: AsPC1, BxPC3, and Paca2 cells were obtained from the American Type Culture Collection (Rockville, MD), and human pancreatic normal epithelial (HPNE) and Panc1 cells were a gift from Prof. Murray Korc of Indiana University Simon Cancer Center (IUSCC) (Shannon HE, 2014). The PDA cells were tested and found to be mycoplasma free by the IUSCC *In Vivo* Therapeutics Core. The human pancreatic cancer associated fibroblasts (hpFibroblasts) were isolated from a human pancreatic tumor and immortalized by transduction of telomerase (hTERT); details will follow in the next section. The normal human dermal fibroblasts (NHF544) were provided by Dr. Dan Spandau from IU School of Medicine, and green fluorescence protein expressing human neonatal dermal fibroblasts (GFP-HNDFs) were purchased from Angioproteomie (Boston, MA; #cAP-0008GFP). Human pancreatic stellate cells (hPSCs) were from ScienCell Research Laboratories (Carlsbad, CA; #3830), and the human mesothelial cell line, LP9, was from the NIA Aging Cell Repository (Camden, NJ).

Cell Culture: AsPC1 and BxPC3 cells were cultured in Roswell Park Memorial Institute (RPMI) 1640 medium (Cellgro, Manassas, VA; #10-040-CV) supplemented with 10% fetal bovine serum (FBS) (Cellgro; #35-011-CV) and 1%

antibiotics (100 U/ml penicillin and 100 µg/ml streptomycin, HyClone Laboratories, Inc., Logan, Utah; #SV30010). Panc1, Paca2, HPNE, hpFibrobasts, NHF544, GFP-HNDFs, hPSCs, and LP9 cells were grown in Dulbecco's modified Eagle's medium (DMEM, Cellgro; #10-013-CV) supplemented with 10% FBS, and 1% antibiotics. Cells were grown at 37°C under 5% CO_2. Serum-free conditioned media (CM) was collected after 24 hour incubation of $5x10^5$ PDA cells in RPMI media by centrifugation of collected media at 1,200 rpm for 5 min prior to transfer of CM to sterile tubes.

2.3. Cell transduction and transfection

TG2 was stably knocked down in AsPC1 and Panc1 cells by transducing cells with MISSION® shRNA Lentiviral Transduction Particles (Sigma; #SHCLNV-NM-004613: TRCN0000000239, 0000000243, 0000272816, 0000272817, and 0000284849), containing short hairpin RNAs (shRNA) targeting TG2 (shTG2) in the presence of polybrene (8µg/mL). As a control (shCtrl), cells were transduced with MISSION® pLKO.1-puro Empty Vector control Transfection Particles (Sigma; #SHC001V). Both shCtrl and shTG2 particles were transduced at a 2.5 multiplicity of infection. Pooled stable clones were collected after selection with puromycin (1 µg/ml), and TG2 knockdown was verified by western blotting.

Transient transfection of short interfering RNA (siRNA) was performed with sequences targeting YAP and TAZ (Santa Cruz Biotechnology, Inc.; #sc-38637 and #sc-38568, respectively) using Lipofectamine® 3000 (Life

technologies, Carlsbad, CA; #L3000008). Dharmacon™ siGENOME™ Control Pool (Dharmacon, Lafayette, CO; #D-001206-13-05) was used as control.

2.4. Co-culture

Co-culture experiments utilized $1x10^4$ cells of GFP-HNDFs mixed with $5x10^3$ PDA cells in 96 wells. GFP-HNDF proliferation was measured daily for 14 days by assessing fluorescence intensity (RFUs) using the SpectraMax Gemini XS microplate fluorometer (Molecular Devices, Sunnyvale, CA) at 485 nm excitation and 538 nm emission. During 14 days of co-culture, with the culture media was replenished every other day.

To determine the effect of PDA cells on activation of fibroblasts and collagen deposition, NHF544 cells ($2.5x10^4$) were cultured in a mixture with PDA cells ($2.5x10^4$) transduced with shRNAs, plated on an 8-well Millicell® EZ $_{SLIDE}$ (Millipore, Billerica, MA; #PEZGS0816). After 24 hours of co-culture, activation of fibroblasts and collagen deposition was analyzed by IF using α-SMA and collagen 1 antibodies, respectively.

To study the proliferation of PDA cells in co-culture with hPSCs, $2x10^5$ hPSCs were seeded in 12-well plates. 24 hours later, $6x10^4$ (Panc1) or $9x10^4$ (AsPC1) cells were added on top of the hPSCs feeder layer and were allowed to proliferate for up to 10 days. Proliferation of PDA cells was assayed by crystal violet staining as described in next section.

2.5. Proliferation assays

Several cell proliferation assays were used: cell counting kit (CCK)-8 assay (Dojindo Molecular Technologies, Inc., Rockville, MD; #CK04), bromodeoxyuridine (BrdU) cell proliferation ELISA (Abcam; #ab126556), and crystal violet staining.

The proliferation of NHF544 and hpFibroblasts on native or crosslinked collagen used CCK-8, according to the manufacturer's instructions. This method measures cell proliferation by determining the amount of yellow-colored formazan dye generated from tetrazolium salt, WST-8, reduced by dehydrogenase activities in live cells. Absorbance at 450 nm was measured using EL800 microplate reader (BioTek Instruments, Inc., Winooski, VT).

The BrdU assay was used to measure proliferation of PDA cells, following the manufacturer's protocol. This assay measures the replicating, live cells by detecting amount of incorporated BrdU in the DNA during S phase of the cell cycle. Incorporated BrdU in the cells was measured at an absorbance of 370 nm by SPECTRAmax® Plus 384 microplate spectrophotometer (Molecular Devices).

Crystal violet staining was utilized to stain the PDA cells grown on the hPSCs feeder layer. Cells were fixed and stained for 20 min at room temperature with Fixing/Staining solution, which contains 0.05% crystal violet (w/v), 1% formaldehyde, 1X PBS, and 1% methanol. The dye was solubilized in methanol, and absorbance at 540 nm was measured on the SPECTRAmax®

Plus 384 spectrophotometer (Molecular Devices). Experiments were performed in 4 replicates and were repeated 2-3 times.

2.6. Western blot analysis

Cells were lysed in Radio-Immunoprecipitation Assay (RIPA) buffer containing Halt™ protease inhibitor cocktail (Thermo Scientific). Equal amounts of proteins were separated by sodium dodecyl sulfate polyacrylamide gel electrophoresis (SDS-PAGE), and transferred to Immuno-Blot polyvinylidene difluoride (PVDF) membranes (Bio-Rad Laboratories, Inc.). After blocking, membranes were blotted with primary antibodies followed by HRP-conjugated secondary antibodies. The protein-antibody complexes were visualized by enhanced chemiluminescence solution (Thermo Scientific), and images were captured by ImageQuant LAS 4000 mini imager with a Chemilux CCD camera (GE Healthcare, Uppsala, Sweden). Densitometry assessment was performed by using ImageJ software. All analyses were repeated at least 3 times.

2.7. Orthotopic pancreatic xenografts

To study tumor growth, $1.5x10^5$ AsPC1 and $2 x10^5$ Panc1 cells, stably transfected with shRNA targeting TG2 or scrambled (control) as mentioned in 2.3. section, suspended in 50 μl of medium were injected directly into the tail of pancreas of 7-8 weeks old female nude mice (nu/nu Balbc) from Harlan

(Indianapolis, IN) using a 27.5 gauge needle under isoflurane anesthesia. The mice were euthanized after three (for Panc1 cells) or 4 weeks (for AsPC1 cells) after cell injection. Twelve mice per group were injected with AsPC1±shTG2 cells and 7 mice per group were injected with Panc1±shTG2 cells. Pancreatic tumors were weighted and measured three-dimensionally and tumor volume was calculated as $4/3*\pi*(L/2)*(W/2)*(H/2)$; where L is length, W is width, and H is height. Metastatic implants were counted.

To study the sensitivity to gemcitabine (Gem) in tumors, the orthotopic xenograft mice with AsPC1±shTG2 cells were prepared as described above and dosed with Gem either one time or twice a week for 4 weeks.

One dose of Gem: Four weeks after cell injection (shCtrl; n=5, shTG2; n=6), Gem at a concentration of 50mg/kg was administered to the mice via intravenous injection, and the mice were euthanized after 2 minutes of Gem administration due to rapid uptake and excretion of Gem in pancreas (Shipley et al., 1992). Tumors and plasma were collected for Gem concentration measurement.

Long-term dose of Gem: Gem at a concentration of 50mg/kg or PBS (control) were administered to the orthotopic xenograft bearing mice (n=7 per group), twice a week for 4 weeks via intraperitoneal injection. At 4-week, the mice were euthanized, and tumor weight, volume, and number of metastases were measured as described above.

Animal experiments were approved by the IU Animal Care and Use Committee, being in compliance with federal regulations.

2.8. Immunohistochemistry (IHC)

Paraffin-embedded de-identified PDA specimens from the IUSCC Tissue Bank were immunostained by using antibodies against TG2 (Neomarkers, 1:200 dilution) and isopeptide (Abcam, Cambridge, MA, 1:100 dilution), after sodium citrate antigen retrieval. Paraffin-embedded pancreatic xenografts were stained similarly, using a TG2 polyclonal antibody (NeoMarkers, 1:50 dilution) and ready to use α-SMA monoclonal antibody (IHC World) for myofibroblasts. Secondary labeling was based on the Avidin/Biotin system (Dako North America, Inc.). Slides were stained with 3-3' diaminobenzidine (DAB) and counterstained with hematoxyllin. Negative controls were run in parallel, with isotype IgG control. H score was calculated as percentage of stained cells multiplied by intensity of staining (graded from 0 to 3+). All slides were reviewed by a board-certified pathologist [Robert Emerson, IUSM]. In total, we stained 75 specimens, of which 52 tumors were parts of a tissue microarray (TMA), 20 were identified as tumors associated with desmoplasia, and 3 were normal pancreas. The IU Institutional Review Board approved the use of de-identified human tissue specimens.

2.9. Immunofluorescence (IF)

Antibodies for TG2 (Neomarkers), α-SMA (Sigma), collagen 1 (Abcam), and YAP/TAZ (Cell Signaling) were used at a 1:100 dilution. PDA cells were cultured on collagen coated (StemCell Technologies, Inc., Vancouver, BC), fibronectin coated (BD Biosciences, Bedford, MA), or uncoated slides (Millicell® EZ $_{SLIDE}$, Millipore). After fixation in 4% paraformaldehyde, cells were permeabilized using 0.1% Triton X-100 in PBS for 5 min and blocked for 1 hour with 3% goat serum in PBS-T (0.1% Tween 20). Subsequently, cells were incubated overnight at 4°C with antibodies for TG2 (Neomarkers), α-SMA (Sigma), collagen 1 (Abcam), and YAP/TAZ (Cell Signaling) at a 1:100 dilution, followed by 1 hour incubation with Cy™5-conjugated anti-mouse secondary antibody (Invitrogen Corporation) and Alexa Fluor® 488 goat anti-rabbit IgG (Life Technologies). To detect matrix-bound TG2, cells were not permeabilized prior to incubation with the TG2 antibody (1:100 dilution), as previously described (Faye et al., 2010). Isotype-specific IgG was a negative control. Nuclei were visualized by 4',6-diamidino-2-phenylindole (DAPI) staining (VECTASHIELD; Vector Laboratories). Analysis used a Zeiss LSM 510 META confocal multiphoton microscope system (Carl Zeiss, Inc., Thornwood, NY, USA) under UV excitation at 635 nm for Cy5, 488 nm for Alexa Fluor® 488, and 405 nm for DAPI.

2.10. Reporter assay

To measure YAP/TAZ transcriptional activity, PDA cells were transfected with pGal4-TEAD4, pGal4-Luciferase, and pTK-Renilla at a ratio of 1:10:1 using DreamFect™ Gold (Oz Biosciences, Inc., San Diego, CA; #DG81000). Plasmids were a gift from Dr. Clark Wells (IUSCC) (Adler et al., 2013). The Dual-Luciferase® Assay System kit (Promega, Madison, WI) determined TEAD4 reporter activity after 48 hours of transfection. To control for transfection efficiency, the luciferase activity was normalized to renilla. Five replicates per group were assessed. Data are presented as means ± standard error (SE) of replicates.

2.11. Reverse transcription PCR (RT-PCR) and quantitative real-time PCR (qRT-PCR)

Total RNA was extracted using RNA STAT-60 Reagent (Tel-Test Inc., Friendswood, TX) and reverse-transcribed using iScript cDNA synthesis kit (Bio-Rad Laboratories, Inc.). The reverse transcriptase product (1 µl) and primers were heated at 94°C for 90-s followed by 24 rounds of amplification for GAPDH and 29 cycles for TG2 (30-s denaturing at 94°C, 30-s annealing at 57°C, and 30-s extension at 72°C) followed by a 10 min final extension at 72°C on a T100™ Thermal Cycler (Bio-Rad Laboratories, Inc.). The RT-PCR product was visualized on an ImageQuant LAS 4000 mini imager (GE Healthcare) after fractionation on a 1% agarose gel. For qRT-PCR, the iTaq Universal SYBR

Green Supermix (Bio-Rad Laboratories, Inc.) on an ABI Prism 7900 platform (Applied Biosystems, Waltham, MA) was used. Primers used for RT-PCR and qRT-PCR are listed in Table 3.

Table 3. Primers for RT-PCR and qRT-PCR

RT-PCR	**TG2**	**Forward**	ACC CGC GTC GTG ACC AAC TAC AAC
		Reverse	GGT GAT ATC CTC CCG CTC GTC TCG
	GAPDH	**Forward**	GAT TCC ACC CAT GGC AAA TTC C
		Reverse	CAC GTT GGC AGT GGG GAC
qRT-PCR	**CTGF**	**Forward**	AGG AGT GGG TGT GTG ACG A
		Reverse	CCA GGC AGT TGG CTC TAA TC
	GAPDH	**Forward**	AGC CAC ATC GCT CAG ACA C
		Reverse	GCC CAA TAC GAC CAA ATC C

Relative target gene expression was calculated using Ct method, $2^{-\Delta Ct}=2^{-[Ct(CTGF)-Ct(GAPDH)]}$, where Ct is the cycle threshold value defined as the fractional cycle number at which the target fluorescent signal passes a fixed threshold. All experiments were performed in duplicates in three independent experiments and results are presented as means ± SE of replicates.

2.12. Collagen crosslinking

Collagen 1 solution (StemCell Technologies, Inc., Vancouver, BC) was treated with TG2 (Sigma) in the presence of 1 mM dithiothreitol (DTT), 5 mM calcium chloride ($CaCl_2$), and 100 mM Tris-HCl (pH 8.0), as previously described (Chau et al., 2005). The collagen mixture was distributed into 96-well plate (50 µl

per well), incubated 90 min at 37°C with lid-on for crosslinking reaction, and dried overnight at 37°C with the lid-off.

2.13. Picrosirius red (PSR) staining

Staining of paraffin-embedded slides used the PSR solution containing 0.1% of Direct red 80 powder (Sigma) dissolved in picric acid (Sigma) for 1 hour at room temperature. Nuclei were stained with Weigert's Hematoxylin (Sigma) for 10 min. The slides were washed twice in 0.5% glacial acetic acid and quickly dehydrated in ethanol and xylene to retain the birefringence of collagen. Imaging with circular polarizing light used the Spot RT Color Carmera System (Diagnostics Instruments, Inc., Sterling Heights, MI) mounted on an inverted Nikon Diaphot 200 microscope (Nikon, Melville, NY).

To quantify the proportion of differently colored collagen fibers, the MetaMorph software (Molecular Devices) was utilized. Original 12-bit images were transformed to 24-bit images by separating colors to 8-bit RGB images and recombining into a 24-bit image. The 24-bit images were resolved into the hue definitions as previously described (26); red 2-9 and 230-256, orange 10-38, yellow 39-51, and green 52-128. The proportion of different colored collagen fibers were calculated by dividing the number of pixels within each hue range by the total number of pixels in all five different hue ranges and expressed as a percentage by multiplying 100. The total collagen content in each image was quantified by dividing the total number of pixels in all five different hue ranges by

total pixels of the image and calculated to percentages. The percentage of total collagen content in experimental group was normalized to control group to compare the total collagen content in two different groups.

2.14. Soluble collagen assay

The amount of soluble collagen in pancreatic xenografts (n=6 per group) was determined by using the Sircol™ Soluble Collagen Assay kit (Biocolor Life Science Assays, Northern Ireland) according to manufacturer's protocol. Frozen tumors (n=6 per group) were homogenized on ice in an extraction buffer containing 50 mM Tris-HCl (pH7.4), 150 mM NaCl, and 0.5% NP40. The homogenates were mixed by rotation for 2 hours at 4°C, followed by sonication on ice followed by 15 min of centrifugation. Protein concentration was measured by Bradford assay, and 500 µg of total protein diluted into PBS were loaded into 96-well plates and dried overnight at 37°C. 150 µl of Sircol dye reagent was added into each well and incubated for 1.5 hour at room temperature. Excess dye was removed, and the plate was washed with 5% acidified water before solubilization in 150 µl of 0.1 M NaOH. Absorbance was measured by BioPhotometer plus (Eppendorf, Hamburg, Germany) at a wavelength of 550 nm. Data are shown as the amount of soluble collagen (µg) present in 500 µg of total protein.

2.15. Hydroxyproline assay

The hydroxyproline colorimetric assay kit purchased from BioVison (Zurich, Switzerland; #K555-100) was used to measure the amount of total collagen in pancreatic xenografts. For preparation of samples, frozen tumors (n=6 per group) were homogenized in 100 µl of dH_2O for every 10 mg of tissue. To each 100 µl of tissue homogenates, 100 µl of 12N HCl was added and hydrolyzed at 120°C for 3 hours with periodical mix by inverting. To remove residue produced after the hydrolysis, the hydrolysates were vortexed and centrifuged at 10,000 x g for 3 min. From the supernatants of hydrolyzed samples, 20 µl was aliquoted to a 96 well plate in duplicates and dried in 37°C oven overnight to remove residual HCl. After the drying process, hydroxyproline standards were prepared on the same 96 well plate, generating concentrations of 0, 0.2, 0.4, 0.6, 0.8, and 1 µg/well in duplicates. For the reaction of the assay, 100 µl of Chloramine T reagent diluted in oxidation buffer was added to each sample and standard and incubated for 5 min at room temperature. Then, 100 µl of DMAB concentrate diluted in perchloric acid/isopropanol solution was added to each well and incubated for 90 min at 60°C oven. Absorbance was measured by SPECTRAmax® Plus 384 microplate spectrophotometer (Molecular Devices) at a wavelength of 560 nm.

2.16. TG2 activity

To determine the localization and enzymatic activity of cellular TG2, PDA cells and fibroblasts cultured on fibronectin (BD BioSciences) or collagen (StemCell Technologies) coated slides were incubated with 500 μM 5-(Biotinamido) pentylamine (5-BP) (ThermoScientific) for 1 hour at 37°C. After washing, cells were fixed with icy cold methanol for 10 min. After blocking in 1% BSA, cells were incubated with Alexa Fluor® 647 streptavidin (Life Technologies) at a dilution of 1:500 for 1 hour.

To assay *in situ* activity of TG2 in tumor tissue, 10 μm cryosections from pancreatic xenografts were dried for 20 min and blocked with 1% BSA. Slides were then incubated at 37°C for 1.5 hour in a buffer containing 5 mM $CaCl_2$, 100 mM Tris-HCl (pH 8.0), in the presence or absence of 1 mM DTT, and 0.001 mM T26 or T26QN (negative control peptide), as previously described (Fukui et al., 2013; K. B. Johnson et al., 2012; Yamane et al., 2010). As another negative control, 5 mM EDTA was added to the buffer. The TG2 enzymatic reaction was stopped by incubating with 25 mM EDTA for 5 min at room temperature. The VECTASHIELD mounting medium contained DAPI (Vector Laboratories). Imaging used a LSM 510 META confocal multiphoton microscope system (Carl Zeiss, Inc.) under UV excitation at 647 nm for Alexa Fluor® 647 streptavidin, 488 nm for FITC, and 405 nm for DAPI.

2.17. Gemcitabine concentration measurement

Gem concentrations in tumor tissue from the animal experiment were analyzed in the Pharmacology Core at Indiana University Simon Cancer Center (IUSCC, Dr. Jones - collaborator). A sensitive and reproducible method was developed to quantify gemcitabine and 2',2' difluorodeoxyuridine (dFdU). This method was used to quantify gemcitabine in plasma and xenografts.

Tumors were harvested 2 min post intravenous gemcitabine injection and were homogenized in phosphate buffer containing tetrahydrouridine (THU), a cytidine deaminase inhibitor, to prevent the degradation of gemcitabine to dFdU. The method that was used to quantify gemcitabine and dFdU employed liquid-liquid extraction, internal standardization (5-azacytidine) and HPLC-MS/MS. A 200 μl of tumor homogenized in THU containing phosphate buffer was extracted with ethyl acetate. The tube was mixed, spun and the ethyl acetate layer was transferred to a separate tube. The ethyl acetate was evaporated to dryness and reconstituted with mobile phase (acetonitrile: 5mM ammonium acetate). An aliquot of the mobile phase was injected into the HPLC and the compounds were separated using a C8 column (5 um; 4.6 X 250 mm Zorbax). The compounds were detected by ESI MS/MS in positive mode (Thermo Quantum Ultra; Thermo Fisher) using 264/112, 265/113, 245/113 as the Q1/Q3 for gemcitabine, dFdU, and 5-azacytidine, respectively. The lower limit of quantification was 1 ng/ml and 30 ng/ml for gemcitabine and dFdU, respectively.

2.18. Statistical analysis

Student's *t* test was used to compare measurements between groups. *P*-values < 0.05 were considered significant.

2.19. Immortalization of human pancreatic cancer associated fibroblasts

This work was done with the help of Dr. Brittney-Shea Herbert at IUSM (Herbert, Hochreiter, Wright, & Shay, 2006).

Preparation of hTERT retroviral vectors for transduction *(done by Shay/Wright lab, UT-Southwestern)***:**

The human telomerase reverse transcriptase (hTERT) coding sequence was cloned into the pBabe retroviral vector containing a neomycin resistance gene. Viral supernatants of empty or +hTERT vector were collected from the ecotropic PE501 packaging cell line after transfection and selection with 4 μg/ml of puromycin. The ecotropic viral supernatants were used to infect the amphotrophic PA317 packaging cell line, followed by selection with 4 μg/ml of puromycin. Then, the amphotropic viral supernatants from PA317 packaging cell line were collected, filtered through a 0.45 μm filter, and used to infect hpFibroblasts.

***Transduction of retroviral hTERT to hpFibroblasts*:**

i) Isolation of hpFibroblasts: Human primary pancreatic cancer associated fibroblasts (hpFibroblasts), F1071; where F indicates fibroblasts and 1071

indicates IU pancreatic tissue bank patient number, were obtained from a PDA specimen collected from the operating room at IUSCC. Briefly, human tumor tissue obtained from the operating room was minced and cultured on a culture dish until the fibroblasts proliferate and spread out. The hpFibroblasts were collected by time difference of trypsinization between hpFibroblasts and other cells, as short time trypsinization detached only hpFibroblasts. The third passage hpFibroblasts were used for immortalization.

ii) Infection: The third passage of hpFibroblasts was grown in 6-well plate until the cells were about 60% confluent. Once the cells were ready, regular medium for hpFibroblasts (DMEM supplemented with 10% FBS and 1% antibiotics), supernatant containing retrovirus (hTERT and pLXSN) and polybrene (0.8 mg/ml) were added. The infecting medium (3ml), representing supernatant from retroviral packaging cells, was diluted into fresh regular medium (3ml) at a ratio of 1:1. Polybrene was added into the diluted infecting medium at the final concentration of 4 µg/ml. The hpFibroblasts were incubated overnight (15 hours) at 37°C under 5% CO_2 with the infecting medium. The next day, the infecting medium was replaced with 3ml of fresh medium, and the cells were incubated 8 hours at 37°C under 5% CO_2 for recovery. The 2^{nd} infection was followed for overnight incubation (15 hours) at 37°C under 5% CO_2. Next morning, the infecting medium was replenished to fresh regular medium, and the hpFibroblasts were grown until they became confluent (10 days).

iii) Selection: Once the cells were confluent, the infected hpFibroblasts were placed under selection with G418 at a final concentration of 200 µg/ml. The

G418-selected hpFibroblasts were tested for telomerase activity by Amruta Phatak in Dr. Herbert's laboratory, using Telomerase Repeat Amplification Protocol (TRAP) assay (Herbert et al., 2006).

iv) Telomerase repeat amplification protocol (TRAP) assay: For the TRAP assay, $10x10^4$ cells of hpFibroblasts were collected. The cells were trypsinized and centrifuged at 3,000g for 5 min at room temperature. The supernatant was removed carefully, and the pellet was resuspended in icy cold NP40 lysis buffer (RNase-/DNase-free) which is composed of 10 mM Tris-HCl (pH 8.0), 1 mM $MgCl_2$, 1 mM EDTA, 1% NP40 (v/v), 0.25 mM sodium deoxycholate, 10% glycerol (v/v), 150 mM NaCl, 5 mM β-mercaptoethanol, and 0.1 mM AEBSF, at the concentrations of 500 and 1,000 cells per µl. A Cy5-labeled oligonucleotide primer for telomerase product was used for the PCR-based TRAP assay. The PCR products were resolved on a polyacrylamide gel and visualized on a PhosphorImager using Image Quant software. Relative telomerase activity was determined as the ratio of the intensity of the telomerase product bands to the internal standard control band.

However, this immortalized hpFibroblasts did not proliferate fast enough. Therefore, in this study, I alternatively used immortalized hpFibroblasts from Dr. Melissa Fishel at IUSM.

CHAPTER 3. RESULTS

3.1. TG2 is abundantly expressed and enzymatically active in PDA cells and in the stroma of PDA tumors

To determine the level of TG2 expression and subcellular localization in pancreatic tumors and in normal pancreas, IHC was performed. We used 52 clinically annotated human PDA specimens on a tissue microarray (TMA) from the IUSCC Tissue Bank. Patient characteristics are presented in Table 4. No TG2 immunostaining was recorded in the stroma of normal pancreas (n=3), and only faint (1+) staining was noted in normal ducts (**Figure 10A**). In contrast, strong (2+ to 3+) TG2 cytoplasmic immunostaining was recorded in 36 out of 52 (69%) specimens, supporting that TG2 expression is increased in PDA compared to normal duct epithelium (**Figure 10B**, *upper left*). TG2 immunostaining was also recorded in the stroma of 44 out of 52 specimens, involving both the cellular (e.g. fibroblasts) as well as the extracellular compartments (84%, **Figure 10B**, *upper right*).

To determine the enzymatic activity of TG2 in the stroma, 20 additional tumors, identified through the IUSCC Tissue Bank as PDA specimens associated with significant desmoplasia, were stained for TG2 and for isopeptide. Isopeptide is a covalent ε-(γ-glutamyl)-lysine bond formed between the donor lysine residue of one protein and the acceptor glutamine residue of another protein as a result of TG2 mediated transamidation. Concordant strong (2+ to 3+) TG2 and

isopeptide staining was recorded in 19 out of 20 additional specimens (**Figure 10B**, *lower*), supporting that TG2 is expressed and active in the pancreatic DS.

Table 4. Clinical characteristics of PDA patients

Patient characteristics (n=52)		Number	Percentage (%)
Stage:	**I**	2	3.8
	IIA	3	5.8
	IIB	46	88.5
	III	1	1.9
Age (median)		62	-
Gender:	**Male**	27	51.9
	Female	25	48.1
Whipple surgery		46	88.5
Post-surgery radiation		33	63.5
Post surgery chemotherapy		52	100

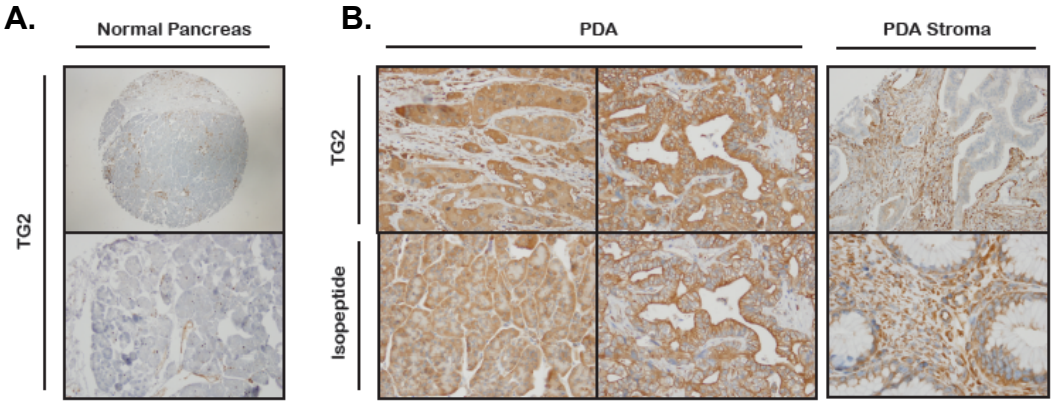

Figure 10. TG2 is highly expressed and active in PDA cells and in the stroma of PDA tumors. **(A)** Immunostaining for TG2 in normal pancreas (*upper;* 40X magnification, *lower;* 200X magnification). **(B)** immunostaining for TG2 (*upper*) and isopeptide (*lower*) in PDA specimens (200X magnification).

3.2. TG2 is secreted by PDA cells and localized in the PDA stroma

First, to measure endogenous TG2 expression levels in HPNE, PDA, stellate cells, and fibroblasts, equal amount of cell lysates from each cell line was used for western immunoblotting (**Figure 11**). Among four different PDA cell lines, AsPC1 and BxPC3 cells expressed relatively abundant TG2, and Panc1 and Paca2 cells expressed relatively low TG2. TG2 expression was also detectable in HPNE cells, but lower than in most PDA cell lines, confirming higher TG2 expression in PDA cells compared to normal pancreatic epithelial cells. Interestingly, stellate cells and fibroblasts also expressed relatively high level of endogenous TG2, corresponding to the TG2 expression observed by IHC in the cellular compartment of the stroma of PDA specimens, mentioned in section 3.1.

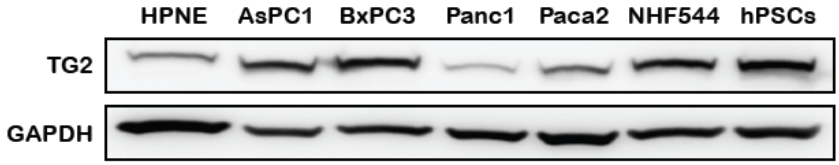

Figure 11. TG2 expression in HPNE, PDA, stellate cells, and fibroblasts. Western blotting for TG2 and GAPDH (internal control). 30 μg of protein per cell line were loaded.

Next, to determine whether TG2 is secreted by PDA cells in the extracellular milieu, we measured TG2 expression by western blotting in conditioned media (CM). For this, equal volume of CM collected from cell cultures were used for western blotting. TG2 was detected in the CM collected from all PDA cells, confirming the secretion of TG2 by PDA cells (**Figure 12**).

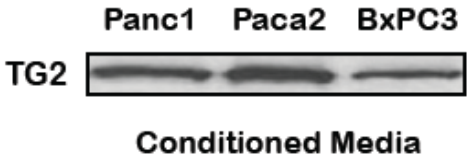

Figure 12. TG2 is secreted by PDA cells into the culture media. Western blotting for TG2 in CM collected from PDA cells. 40 µl of CM per lane was loaded.

In addition, TG2 secretion by PDA cells into the matrix was determined by using IF. Extracellular TG2 was detectable in the matrix deposited by AsPC1, BxPC3, and Panc1 cells (**Figure 13**). These data support the concept that PDA cells secrete TG2 into the ECM, implying the presence of secreted TG2 in the pancreatic tumor milieu.

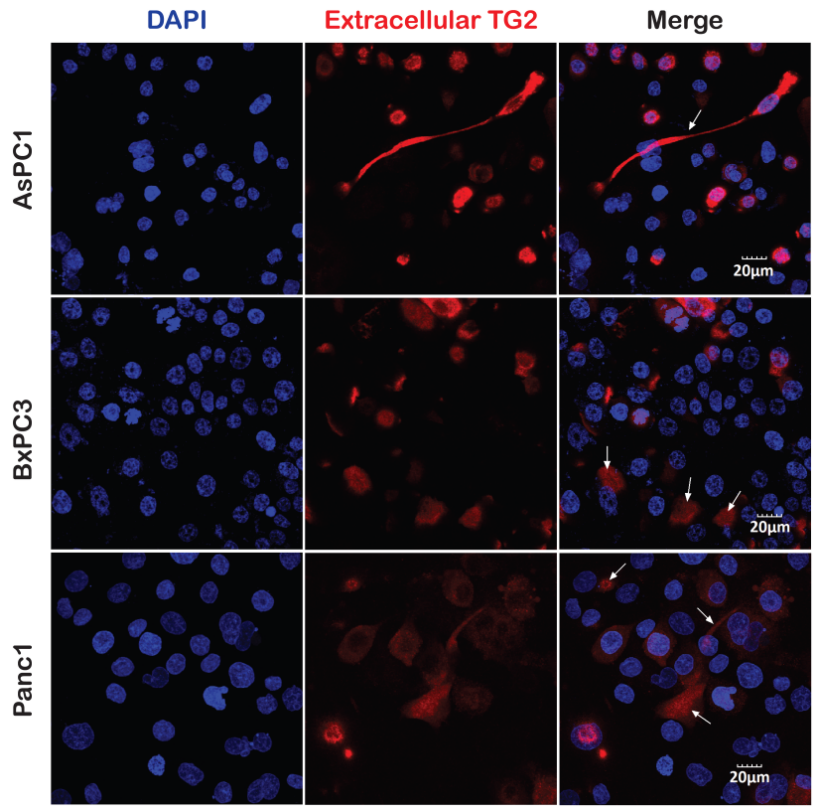

Figure 13. Detection of extracellular TG2. IF for extracellular TG2 (Cy5, red) deposited by AsPC1, BxPC3, and Panc1 cells onto the collagen matrix. Arrows point the TG2 deposited in the ECM. Nuclei are visualized by DAPI staining.

To assess cellular localization and enzymatic activity of TG2, incorporation of 5-BP and T26 was utilized. 5-BP and T26 are known TG2 substrates, which incorporate into amine free proteins as a result of crosslinking activity of TG2.

As shown in **Figure 14**, TG2 was abundantly expressed in the cytosol and on the plasma membrane of AsPC1 and Panc1 cells. In addition, enzymatic activity of TG2 was detectable by incorporated 5-BP in the cytoplasm of both cell types.

However, TG2 was abundantly expressed, but was enzymatically inactive in fibroblasts (**Figure 14** and **Figure 15A**) and in LP9 normal mesothelial cells (**Figure 15B**), suggesting that the enzymatic activity of TG2 may be differentially regulated in cancer vs. normal cells. Specificity of the substrate incorporation assay is supported by lack of IF signal when cells were incubated with the mutant T26QN peptide (not a TG2 substrate, **Figure 15B**) or with EDTA (**Figure 15A**), a chelator of Ca^{2+}.

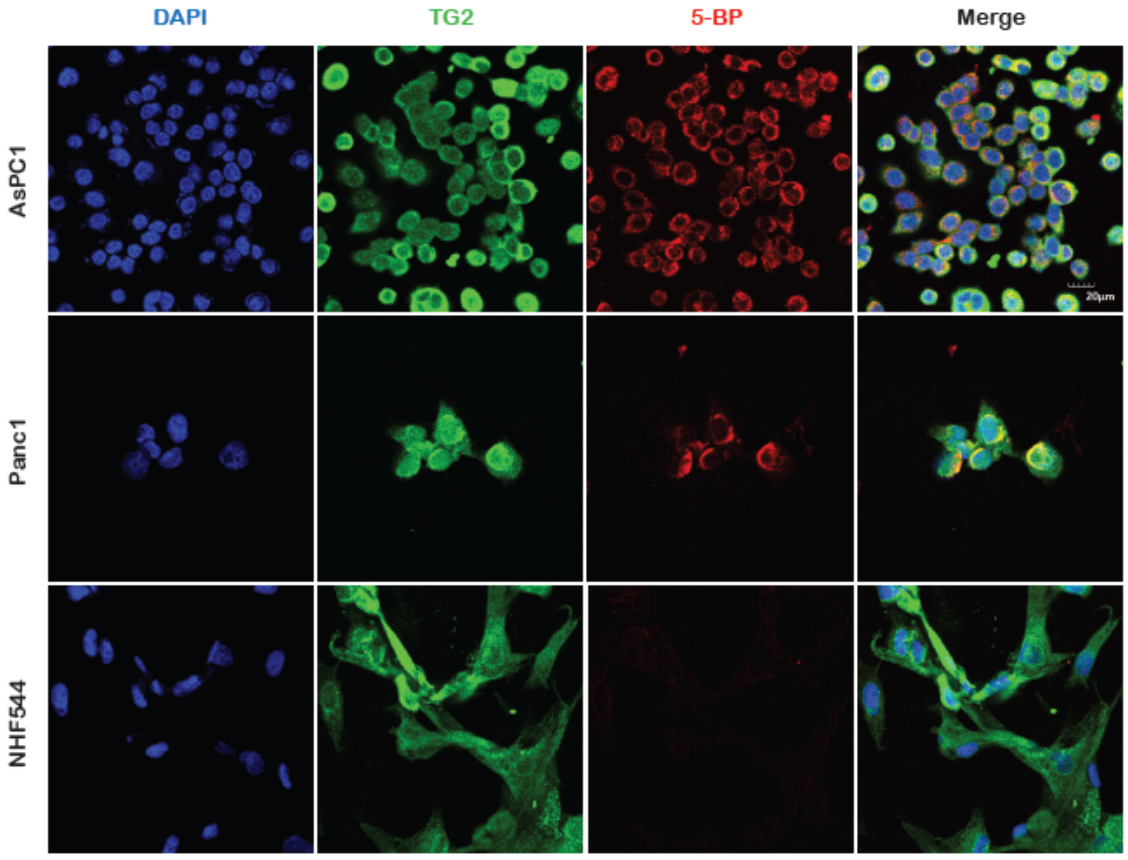

Figure 14. TG2 is secreted into the pancreatic TME by PDA cells and is enzymatically active. **(A)** Western blotting for TG2 and GAPDH (internal control) in PDA cells and fibroblasts. **(B)** Western blotting for TG2 in CM (30µl/lane) collected from PDA cells. **(C)** IF for TG2 (Alexa Fluor® 488, green) and 5-BP (Alexa Fluor® 647 Streptavidin, red) in AsPC1, Panc1 and NHF544 cells (600X magnification). Nuclei are visualized by DAPI.

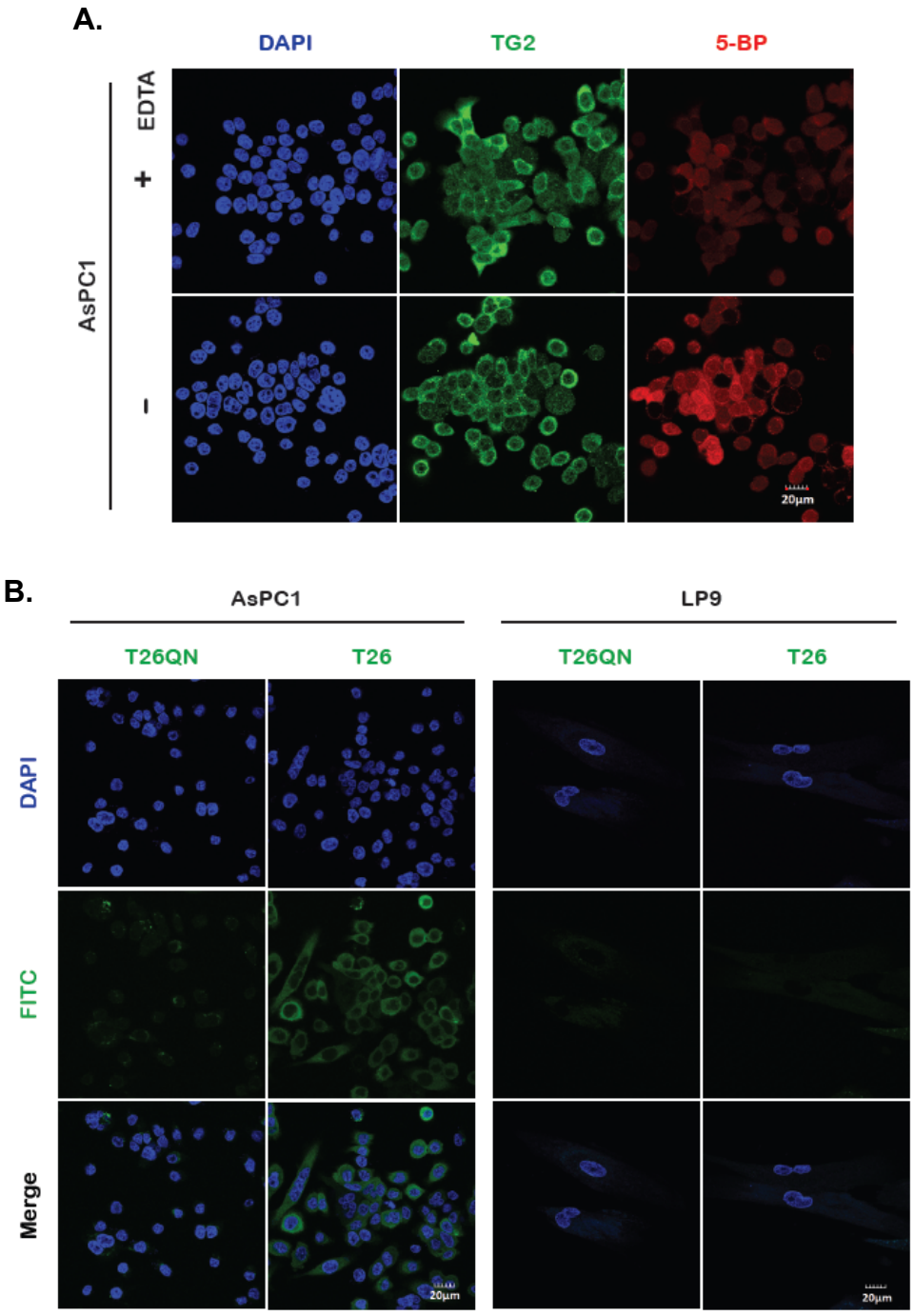

Figure 15. TG2 is enzymatically active in PDA cells. **(A)** IF staining for TG2 (Alexa Fluor® 488, green) and 5-BP (Alexa Fluor® 647 Streptavidin, red) in AsPC1 cells (600X magnification). Incubation with 1 mM EDTA was used as a negative control (inhibits TG2 enzymatic activity). Nuclei are visualized by DAPI staining. **(B)** IF staining using FITC-labeled T26, and T26QN (negative control) in AsPC1 and LP9 mesothelial cells (600X magnification). Nuclei are visualized by DAPI staining.

3.3. TG2 knockdown in PDA cells

To proceed with functional studies of TG2, TG2 was knocked down in AsPC1 and Panc1 cells by stably transducing shRNA targeting TG2 (shTG2). TG2 protein and *mRNA* expression levels were significantly downregulated in shTG2 transduced cells compared to cells transduced with scrambled shRNA (shCtrl, **Figure 16A**). TG2 secretion in the CM was also decreased in shTG2 compared to shCtrl transduced PDA cells (**Figure 16B**).

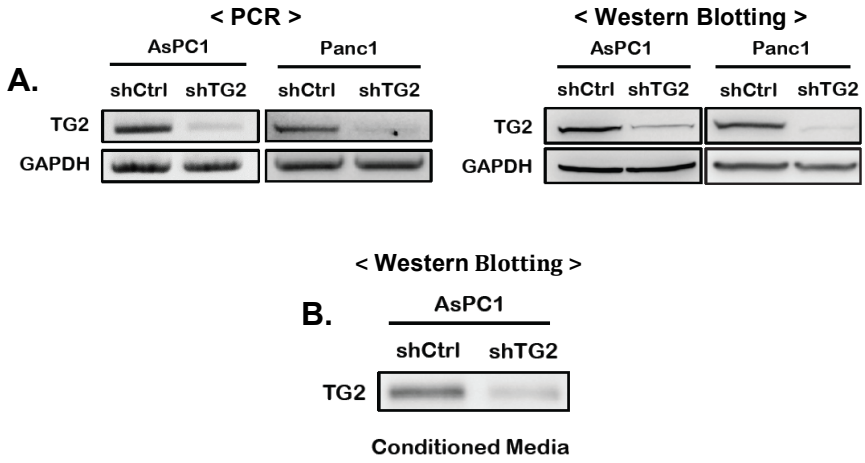

Figure 16. Knockdown of TG2 in PDA cells. **(A)** TG2 expression measured by RT-PCR (*left*) and western blotting (*right*) in AsPC1 and Panc1 cells stably transduced with shRNA targeting TG2 (shTG2) or control shRNA (shCtrl). **(B)** Western blotting for TG2 in CM collected from AsPC1 +shCtrl and +shTG2 cells.

3.4. TG2 knockdown in PDA cells does not affect proliferation and colony formation, *in vitro*

To determine the effect of TG2 knockdown on PDA cells, shRNA transduced PDA cell lines described in section 3.3 were used. First, we

compared proliferation of PDA cells +shCtrl and +shTG2. No significant difference in the proliferation was observed (**Figure 17**). Next, we determined the ability to form colonies of PDA cells depending on TG2 expression level. Knockdown of TG2 in PDA cells did not inhibit the clonogenic potential compared to that of control cells (**Figure 18**). Together, these results show that knockdown of TG2 in PDA cells does not directly affect cell proliferation and colony formation.

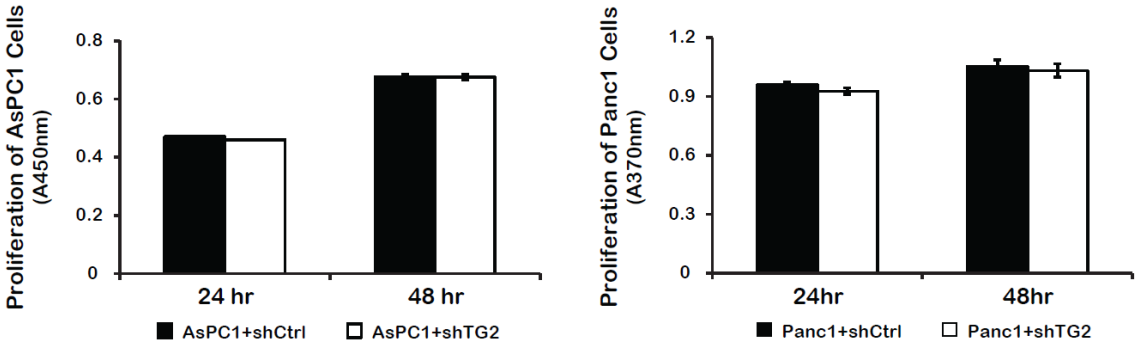

Figure 17. Effect of TG2 knockdown on PDA cell proliferation. Proliferation of AsPC1+shCtrl and +shTG2 cells (*left*, CCK-8 assay) and of Panc1+shCtrl and +shTG2 cells (*right*, BrdU assay). Bars represent average measurements ± SE.

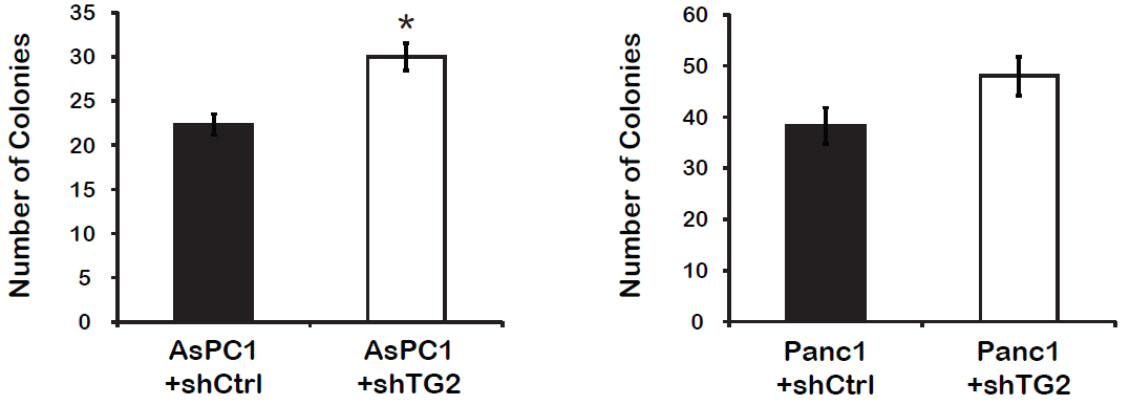

Figure 18. Effect of TG2 knockdown on PDA cell colony formation. Clonogenic assay compares colony formation between AsPC1+shCtrl and AsPC1+shTG2 cells (*left*, n=3 per group, $p = 0.02$) and Panc1+shCtrl and Panc1+shTG2 cells (*right,* n=3 per group, $p = 0.14$). Bars represent average measurements ± SE; * $p < 0.05$.

3.5. TG2 knockdown in PDA cells inhibits tumor growth, *in vivo*

To measure the effects of TG2 on tumor growth and metastasis, orthotopic human pancreatic cancer xenograft mouse model was generated by injecting PDA cells +shCtrl and +shTG2 (shown in section 3.3.) directly into the tail of pancreas of nude female mice. Tumors were harvested at the 4th (AsPC1) and the 3rd (Panc1) week after PDA cell implantation, and used for the following analyses.

The average tumor volume and weight were significantly decreased in xenografts derived from AsPC1+shTG2 cells compared to AsPC1+shCtrl cells (**Figure 19A**, *left* and *middle* panels, p = 0.02 and p = 0.04, respectively). There was no significant difference in the number of macro-metastases visible and countable on the omentum and peritoneal surfaces between the two groups (Figure 19A, *right* panel, p = 0.70). The stable knockdown of TG2 in AsPC1+shTG2 xenografts compared to controls was confirmed by IHC and was quantified by H scores (**Figure 19B**, p = 0.004), which was calculated as percentage of stained cells multiplied by intensity of staining (grade from 0 to 3+).

Likewise, decrease in the average tumor volume and weight was observed in xenografts derived from Panc1+shTG2 cells compared to Panc1+shCtrl cells (**Figure 20A**, *left* and *middle* panels, p = 0.01 and p = 0.006, respectively). The number of macro-metastases on the omentum and peritoneal surfaces was also significantly decreased in Panc1+shTG2 tumor bearing mice

compared to controls (**Figure 20A**, *right* panel, $p = 0.03$). Stable knockdown of TG2 was confirmed by IHC quantification (**Figure 20B**, $p = 0.007$).

Interestingly, the effect of TG2 knockdown on decreased tumor growth and metastasis was more pronounced in tumors derived from Panc1 compared to AsPC1 cells. This phenomenon is possibly due to the shorter doubling times of Panc1 cells (18±1 hours) vs. AsPC1 cells (24±1 hours) (Porcelli et al., 2013), which led to increased growth of Panc1+shCtrl tumors. In addition, as Panc1 cells express relatively low TG2 compared to AsPC1 cells, the effect of TG2 knockdown in Panc1 cells may have been more prominent and remarkably inhibited Panc1+shTG2 tumor growth compared to AsPC1 tumors. Taken together, these data demonstrate that TG2 expression levels in PDA cells are strongly correlated with tumor growth, *in vivo*.

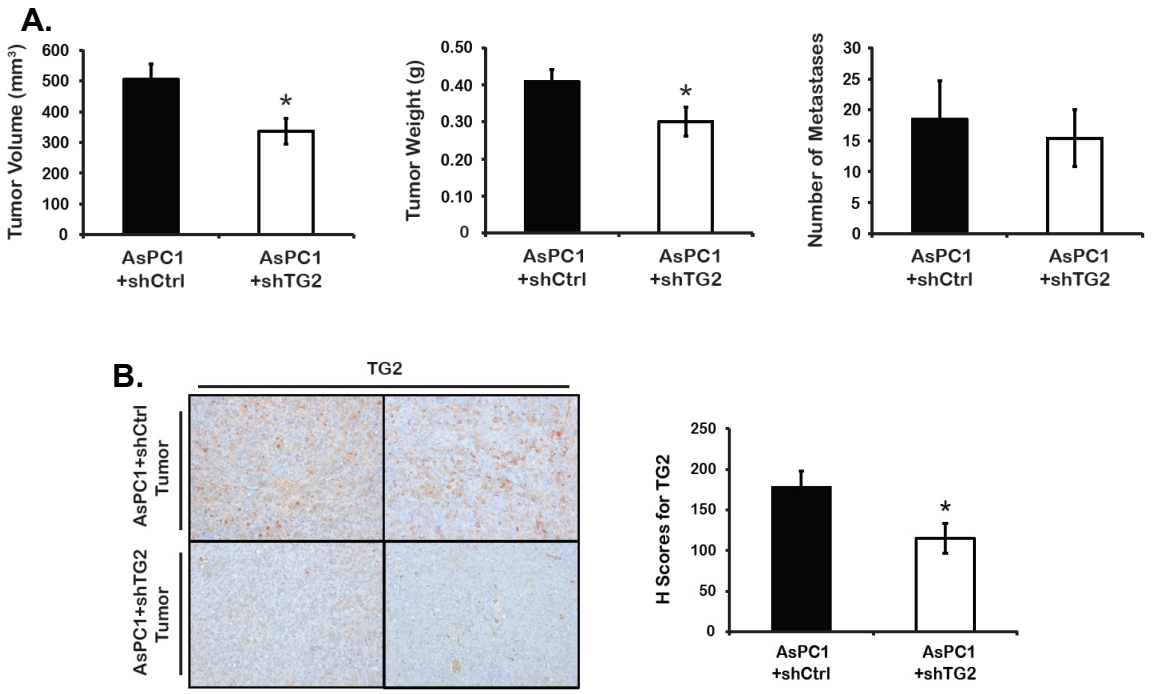

Figure 19. TG2 knockdown inhibits tumor growth in AsPC1 orthotopic xenograft mouse model. **(A)** Average tumor volume (*left*, $p = 0.02$), weight (*middle*, $p = 0.04$), and number of metastases (*right*, $p = 0.70$) of xenografts derived from AsPC1+shCtrl (n=11) and +shTG2 (n=12) cells. **(B)** IHC for TG2 in AsPC1+shCtrl and AsPC1+shTG2 xenografts (*left*). Quantitated H scores of TG2 expression in tumors (*right*, n=10 per group, $p = 0.004$). * H score = percentage of stained cells x intensity of staining (grade from 0 to 3+). Bars represent average H scores ± SE; * $p < 0.05$.

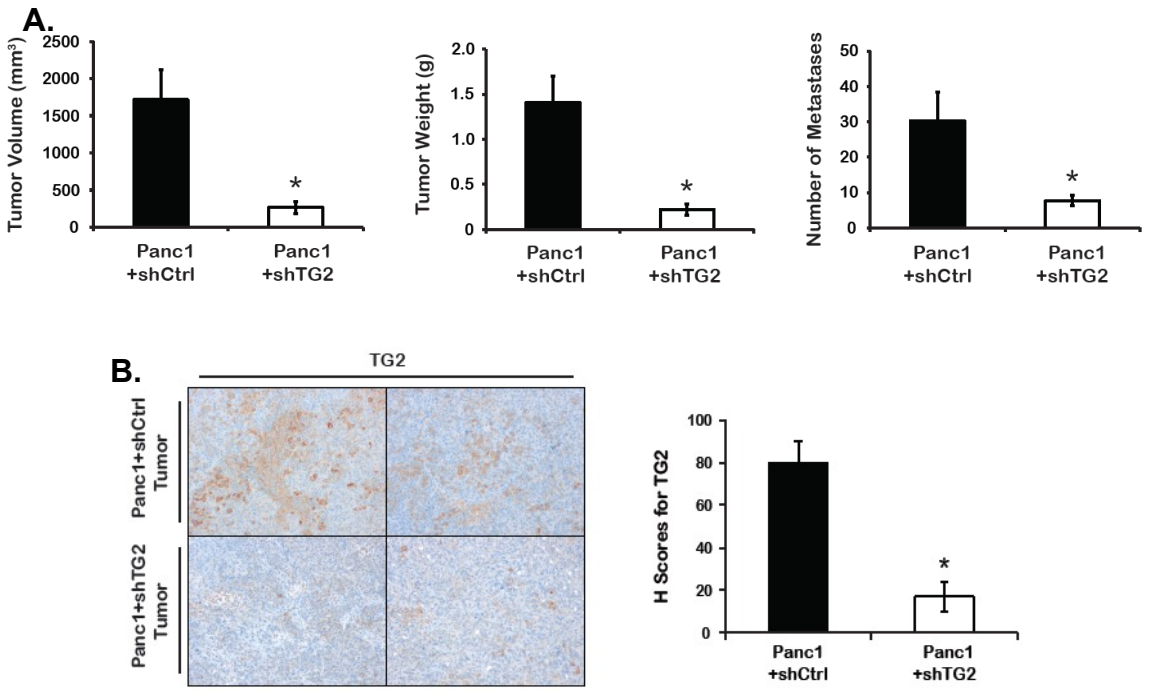

Figure 20. TG2 knockdown inhibits tumor growth in Panc1 orthotopic xenograft mouse model. **(A)** Average tumor volume (*left*, p = 0.01), weight (*middle*, p = 0.006), and number of metastases (*right*, p = 0.03) derived from Panc1+shTG2 and +shCtrl cells (n=7 per group). **(B)** IHC for TG2 in Panc1+shCtrl and PanC1+shTG2 xenografts (*left*). Quantitated H scores of TG2 expression in tumors (*right panels*, n=3 per group, p=0.007).

3.6. TG2 is enzymatically active in PDA tumors

Under normal physiological conditions, TG2 is enzymatically inactive *in vitro* and *in vivo*. Various stressors, such as injury or hypoxia, are required to activate TG2 (M. Siegel et al., 2008). To determine whether TG2 is catalytically active in the pancreatic TME, we measured incorporation of the FITC-labeled T26 peptide, which is specifically crosslinked to ECM proteins by TG2 (K. B. Johnson et al., 2012). Enzymatically active TG2 was detectable both intra- and extra-cellularly in AsPC1 and Panc1 xenograft tumor sections (**Figure 21**), suggesting that the enzyme is active in the pancreatic milieu. Incubation with the

T26 peptide in the presence of EDTA and with the mutant T26QN peptide, which is not a TG2 substrate, were used as negative controls to prove specificity.

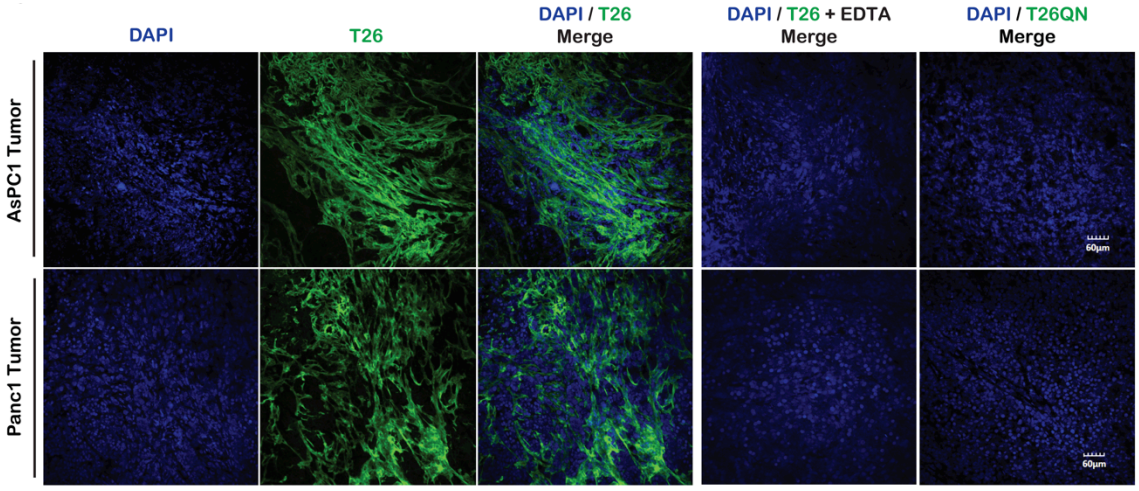

Figure 21. TG2 is enzymatically active in the PDA stroma. IF using FITC-labeled T26, FITC-labeled T26 and EDTA (negative control), and T26QN (negative control) in AsPC1 and Panc1 xenografts (200X magnification).

In addition, according to Jin *et al*., extracellular TG2 is catalytically inactive even in open, active conformation due to oxidation between the Cys residues in the catalytic core. Therefore, reducing agents, such as DTT or thioredoxin, are needed to activate TG2 (Jin et al., 2011).

To exclude the possibility that TG2 might be artificially activated by DTT during the assay, we incubated T26 in the absence of DTT in the reaction buffer. Enzymatic activity of TG2 was detectable in the PDA xenografts even in the absence of DTT (**Figure 22**), supporting that TG2 is enzymatically active, *in situ*.

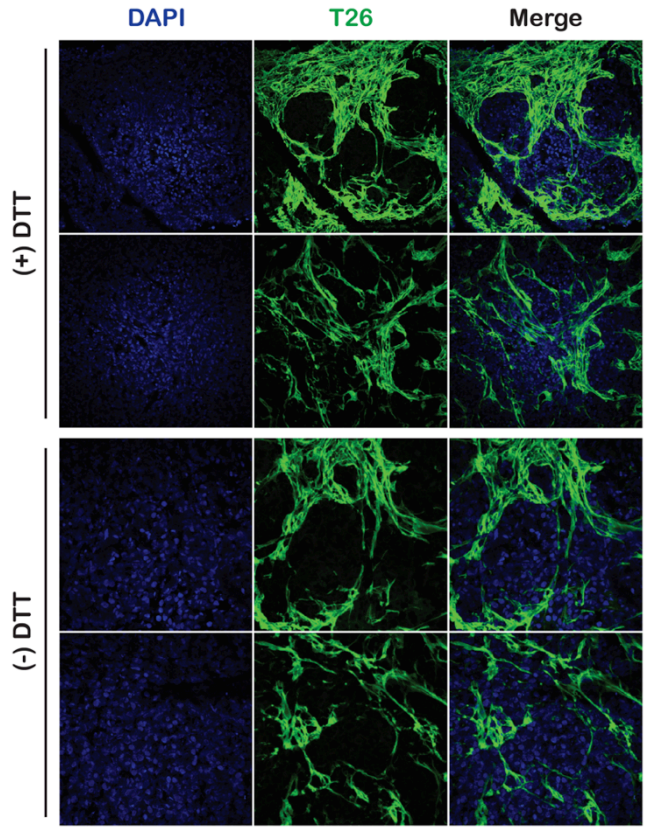

Figure 22. TG2 is enzymatically active, *in situ*, in the PDA xenografts. IF using FITC-labeled T26, in the presence and the absence of 1 mM DTT in Panc1 xenografts (200X magnification).

3.7. Enzymatically active TG2 crosslinks collagen in PDA tumors

One of the known TG2 substrates is collagen I, a critical component of the pancreatic DS (Mahadevan & Von Hoff, 2007). To determine whether collagen I was crosslinked by TG2 in the pancreatic TME, we used PSR staining which distinguishes the thickness of collagen fibers. Birefringence of PSR staining under polarizing microscope is highly specific for collagen fibers, which appear red, orange, yellow, or green in order of decreasing thickness (Rich & Whittaker, 2005).

Birefringence of collagen fibers in AsPC1+shCtrl tumors was mostly bright orange, red, and yellow, while that in AsPC1+shTG2 tumors was mostly green and yellow (**Figures 23A**), suggesting that collagen I fibers are thicker in tumors derived from TG2 expressing cancer cells. Moreover, the area of birefringence corresponding to collagen was more extensive in AsPC1+shCtrl tumors compared to AsPC1+shTG2 xenografts (**Figure 23B**, $p = 0.001$), demonstrating increased collagen deposition in TG2 expressing tumors. As shown in **Figure 23**, most collagen was deposited around pancreatic ducts and at the edge of tumors. Likewise, Panc1+shCtrl tumors also contained higher proportion of thicker collagen compared to Panc1+shTG2 tumor. However, overall birefringence of collagen in Panc1 tumors was less than in AsPC1 tumors (data not shown).

To verify that this correlation is relevant to human pancreatic tumors, PSR staining of high-TG2 and low-TG2 PDA specimens was carried out (n=6 per group). First, IHC of TG2 was perfomed on a human pancreatic cancer TMA, and the specimens were grouped into high-TG2 and low-TG2 expressing groups based on H scores. The same TMA was stained with PSR, and collagen thickness was analyzed based on different birefringence colors. Then, the correlation of TG2 expression level and crosslinked collagen content was compared. Likewise, the proportion of red and orange birefringence was significantly higher in high-TG2 tumor, while that of yellow and green was significantly higher in low-TG2 tumors (**Figure 24A**, $p < 0.001$). These data suggest that TG2 expression levels are strongly correlated with the percentage of crosslinked collagen. Moreover, the area of birefringence corresponding to

collagen was more extensive in high-TG2 tumors compared to low-TG2 tumors (**Figure 24B**, p = 0.001).

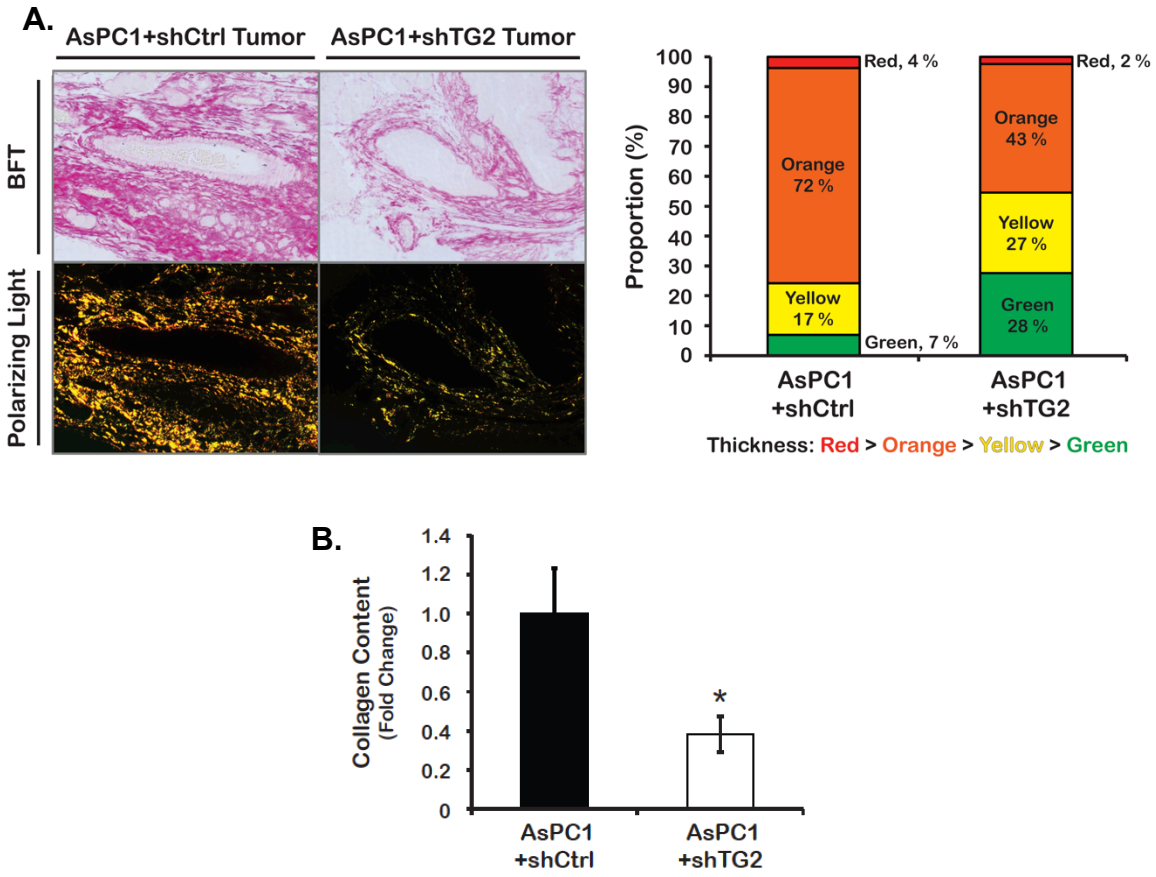

Figure 23. Enzymatically active TG2 crosslinks collagen in the PDA stroma. **(A)** Representative PSR staining determines thickness of collagen fibers in AsPC1+shCtrl and AsPC1+shTG2 tumors (*left*); *upper* - bright field transmission (BFT) microscopy, *lower* - polarizing light microscopy (200X magnification). Quantification of collagen fiber thicknesses based on differences in birefringence in AsPC1+shCtrl and AsPC1+shTG2 xenografts (*right*). **(B)** Quantitative assessment of collagen content based on the area of collagen birefringence per microscopic field. Bars represent average fold changes ± SE; n=11 images per group, p < 0.001.

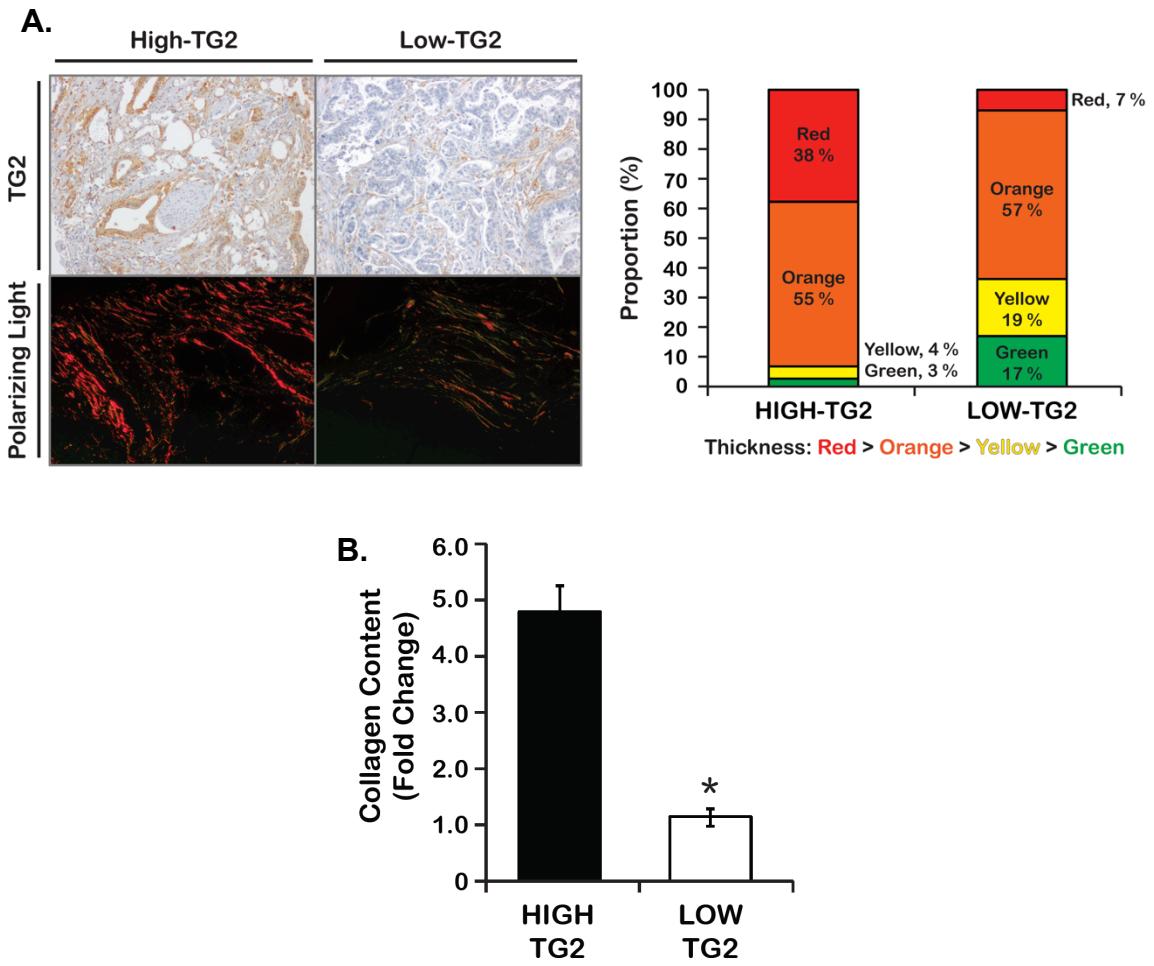

Figure 24. Higher expression level of TG2 is correlated with higher percentage of crosslinked collagen in human PDA specimens. **(A)** Representative PSR staining determines thickness of collagen fibers in high-TG2 and low-TG2 tumors (*left*); *upper* - IHC for TG2 (100X magnification), *lower* - polarizing light microscopy (200X magnification). Quantification of collagen fiber thicknesses based on differences in birefringence in high-TG2 and low-TG2 PDA specimens (*right*). **(B)** Quantitative assessment of collagen content based on the area of collagen birefringence per microscopic field. Bars represent average fold changes ± SE; n=6 images per group, $p < 0.0001$.

To measure the amount of non-crosslinked, soluble collagen in the pancreatic xenografts derived from +shCtrl and +shTG2 PDA cells, sircol soluble collagen assay was performed using protein extracts from the xenografts. Soluble collagen content was significantly higher ($p = 0.001$) in AsPC1+shTG2

compared to AsPC1+shCtrl tumors (**Figure 25**, *left*, n=6 per group) and in Panc1+shTG2 compared to Panc1+shCtrl xenografts (**Figure 25**, *right*, p = 0.005, n=6 per group). These data add to the observations that TG2 secreted from PDA cells promotes collagen crosslinking reaction in the pancreatic stroma.

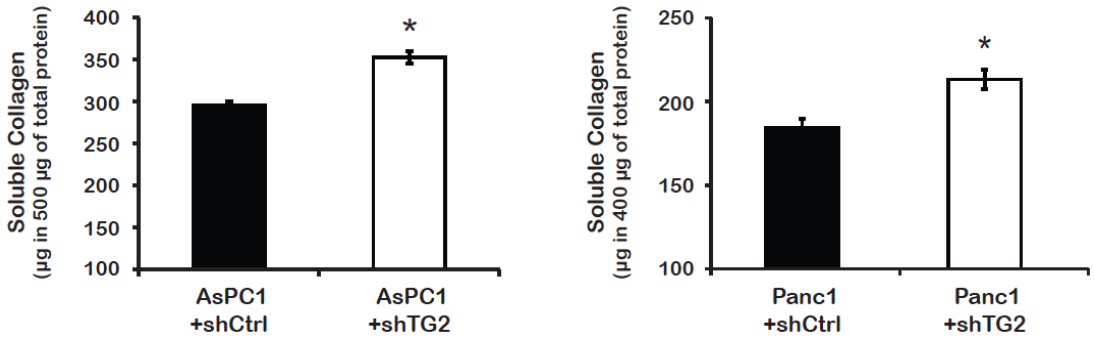

Figure 25. Soluble collagen measured by the Sircol assay in AsPC1+shCtrl (n=6) and AsPC1+shTG2 (n=5, *left*, p = 0.001) and Panc1+shCtrl and Panc1+shTG2 tumors (n=6 per group, *right*, p = 0.005). Bars represent average measurements of the groups ± SE. * denotes $p < 0.05$.

Additionally, to measure the total collagen content in the AsPC1+shCtrl and AsPC1+shTG2 xenografts, hydroxyproline assay was used. Hydroxyproline is a major component of collagen, and its distribution is highly restricted to collagen. Therefore, hydroxyproline content reflects amount of collagen in the sample. The amount of hydroxyproline present in the hydrolysates of AsPC1+shCtrl and +shTG2 was similar, demonstrating no difference in the amount of total collagen between AsPC1+shCtrl and AsPC1+shTG2 xenografts (**Figure 26**).

Collectively, these data suggest that TG2 secreted from PDA cells promotes collagen crosslinking reaction in PDA tumors.

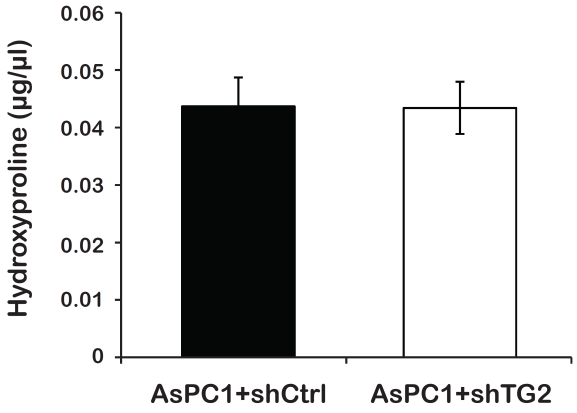

Figure 26. Total collagen content is the same in pancreatic xenografts derived from control and TG2 knocked down PDA cells. Hydroxyproline assay measures collagen content in the hydrolysates of AsPC1+shCtrl and +shTG2 xenografts (n=6 per group, $p > 0.9$). 20 µl from 200 µl of hydrolysate was used for the assay. Bars represent average measurements ± SE.

3.8. TG2-mediated crosslinked collagen promotes proliferation of fibroblasts

To determine the functional significance of native and TG2-mediated crosslinked collagen to the proliferation of fibroblasts, NHF544 fibroblasts were grown on plates with no vs. native collagen and native vs. TG2-mediated crosslinked collagen. The proliferation of NHF544 fibroblasts, measured by CCK-8 assay, was increased on collagen coated compared to uncoated plates (**Figure 27**, *left* panel, $p < 0.04$) and even more on TG2-mediated crosslinked collagen compared to native collagen (**Figure 27**, *right* panel, $p < 0.03$).

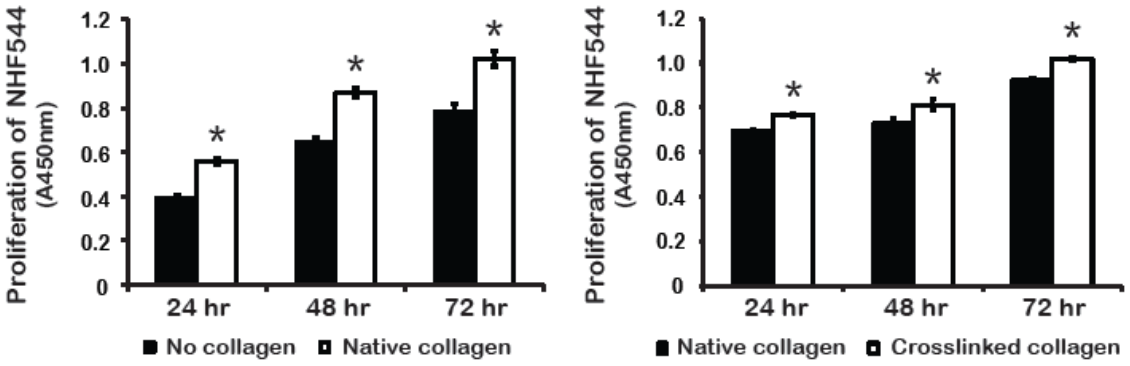

Figure 27. Proliferation of fibroblasts is promoted by collagen and furthermore by TG2-mediated crosslinked collagen. CCK-8 assay measures proliferation of NHF544 fibroblasts grown on collagen coated or uncoated plates (*left*, $p < 0.04$) and on native or TG2-mediated crosslinked collagen (*right*, $p < 0.03$). Bars represent average measurements ± SE.

Likewise, the proliferation of immortalized human PDA-associated fibroblasts (hpFibroblasts) was augmented on collagen coated compared to uncoated plates (**Figure 28***, left* panel, $p = 0.01$) and furthermore on TG2-mediated crosslinked collagen compared to native collagen (**Figure 28***, right* panel, $p < 0.001$).

Taken together, these data suggest that collagen and crosslinked collagen in the matrix promote fibroblast proliferation.

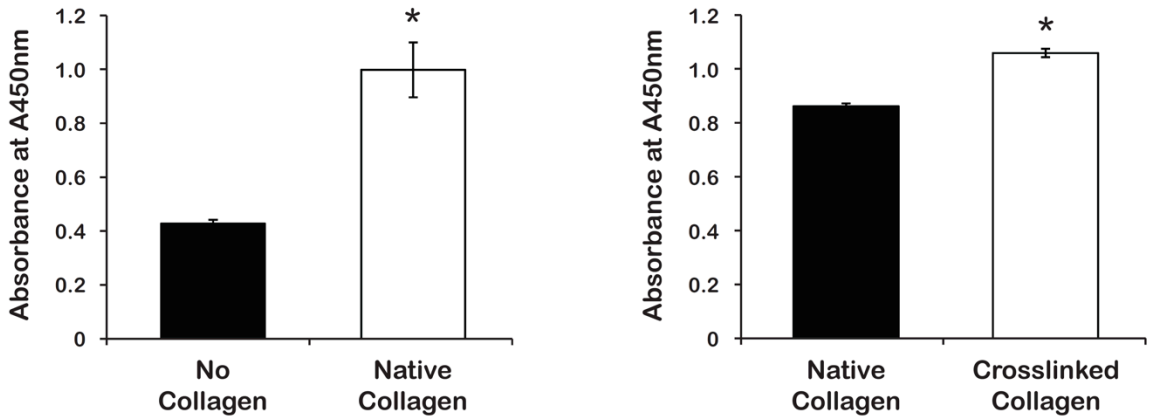

Figure 28. Proliferation of hpFibroblasts is promoted by collagen and furthermore by TG2-mediated crosslinked collagen. CCK-8 assay measures proliferation of hpFibroblasts cultured on collagen coated or uncoated plates (*left*, $p = 0.01$) and on native or on TG2-mediated crosslinked collagen (*right*, $p < 0.001$). The proliferation assay was performed 48 hours after the cell culture. Bars represent average measurements ± SE. hpFibroblasts were obtained and provided by Dr. Melissa Fishell at IUSM.

3.9. TG2 expressing PDA cells promote proliferation of fibroblasts

Next, to study the effect of TG2 secreted by PDA cells on stromal cell proliferation, co-culture experiments were performed. GFP-expressing human normal dermal fibroblasts (GFP-HNDFs) were co-cultured with AsPC1+shCtrl or +shTG2 cells, and the proliferation of fibroblasts was determined by measuring green fluorescence emitted from the fibroblasts. The direct co-culture of GFP-HNDFs with TG2 expressing AsPC1 cells significantly promoted proliferation of the fibroblasts over a 14-day period compared to the co-culture with AsPC1+shTG2 cells (**Figure 29**, $p < 0.03$). The proliferation of fibroblasts in co-culture with cancer cells expressing and secreting low levels of TG2 (AsPC1+shTG2) was not different from proliferation of fibroblasts cultured alone,

suggesting that secretion of TG2 in co-culture models augments the fibrotic response.

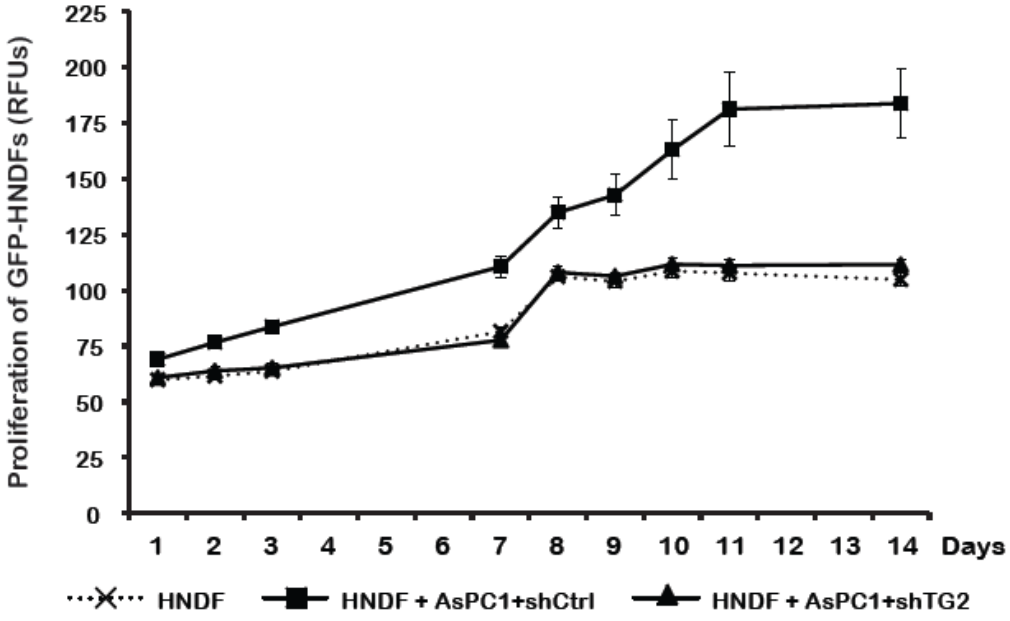

Figure 29. TG2 expressing PDA cells promote proliferation of fibroblast in a co-culture. Proliferation of GFP-HNDFs in co-culture with AsPC1+shCtrl or AsPC1+shTG2 cells or grown alone for 14 days ($p < 0.03$). Green fluorescence was measured at Ex. 485nm and Em. 538nm.

To determine the direct effect of TG2 on stromal cell proliferation, different concentrations (0, 1, and 2.5 µg/ml) of wild-type (active) and mutant ($C^{277}S$; inactive) recombinant TG2 were added into the growth medium of stromal cells in the absence of PDA cells. In contrast to the co-culture results, active recombinant TG2 did not alter fibroblast or stellate cell proliferation (**Figure 30**), measured by BrdU assay. These results suggest that TG2 acts in concert with other factors in the matrix produced by PDA cells to stimulate fibroblasts proliferation.

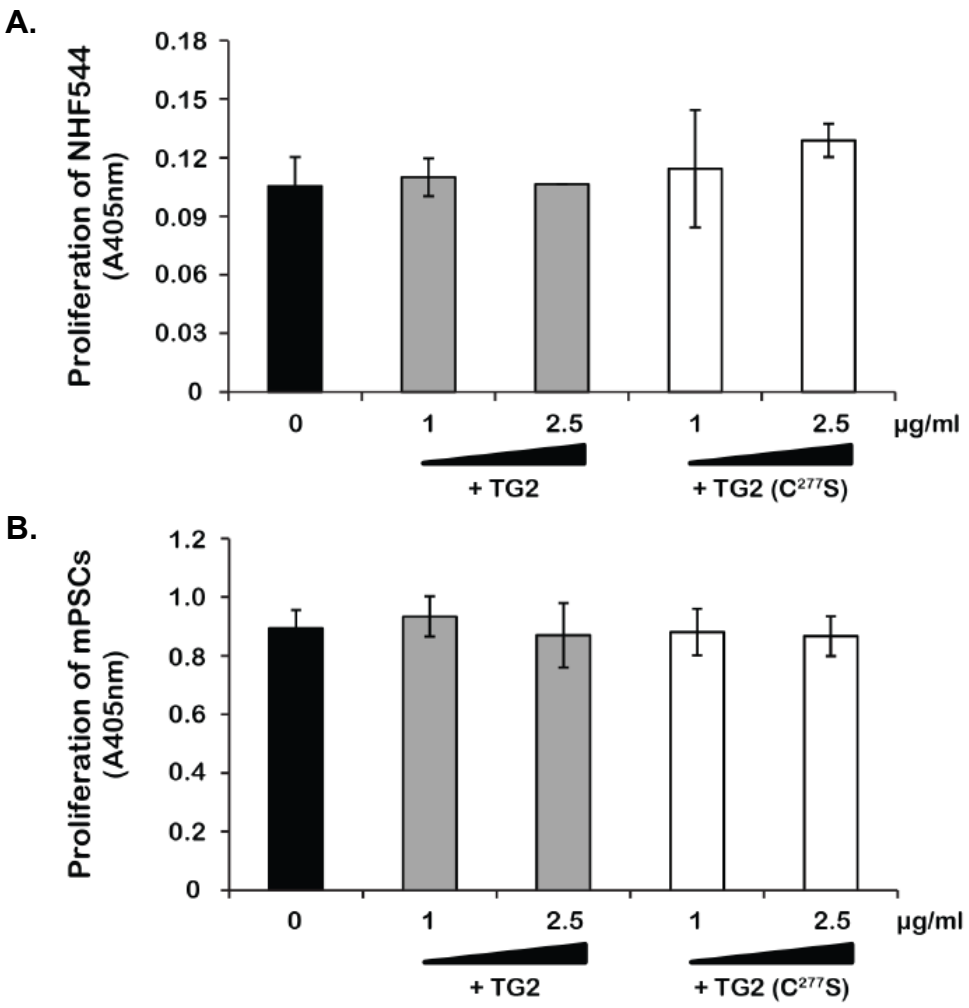

Figure 30. Externally added recombinant TG2 does not alter proliferation of fibroblast and mouse pancreatic stellate cells (mPSCs). BrdU assay measures proliferation of **(A)** NHF544 and **(B)** mPSCs treated for 48 hours with various concentrations (0, 1, and 2.5 µg/ml) of purified recombinant TG2 (active) and mutant $C^{277}S$ TG2 (inactive) (n=3 per group, $p > 0.3$). Bars represent average measurements ± SE.

3.10. TG2 expressing PDA cells activate fibroblasts

To determine whether fibroblasts are activated in the presence of PDA cells, co-culture experiments were performed, followed by IF for α-SMA, a marker for active fibroblasts. Co-culture of NHF544 cells with AsPC1 and Panc1 cells caused increased expression of α-SMA in fibroblasts (**Figure 31A**).

As we observed activation of fibroblasts in the presence of PDA cells, and as activation of fibroblasts is known to promote collagen production, we next determined whether TG2 secreted by PDA cells contributes to fibroblast activation. To assess the significance of TG2 to fibroblast activation, NHF544 fibroblasts were co-cultured with +shCtrl and +shTG2 PDA cells, and collagen deposition by fibroblasts was analyzed by IF. Increased collagen I staining was observed in NHF544 fibroblasts when co-cultured with TG2 expressing AsPC1 and Panc1 control (+shCtrl) cells, compared to fibroblasts co-cultured with AsPC1 and Panc1 +shTG2 cells (**Figure 31B**).

In addition, activated fibroblasts were measured *in vivo* in AsPC1+shCtrl or AsPC1+shTG2 xenografts by IHC for α-SMA and were quantified by H score. The number of α-SMA expressing, activated fibroblasts was significantly higher in AsPC1+shCtrl compared to +shTG2 xenografts (**Figure 32**, $p < 0.05$).

Collectively, these data show that in the pancreatic TME, TG2 secreting PDA cells promote the growth, the activation, and the collagen deposition by fibroblasts.

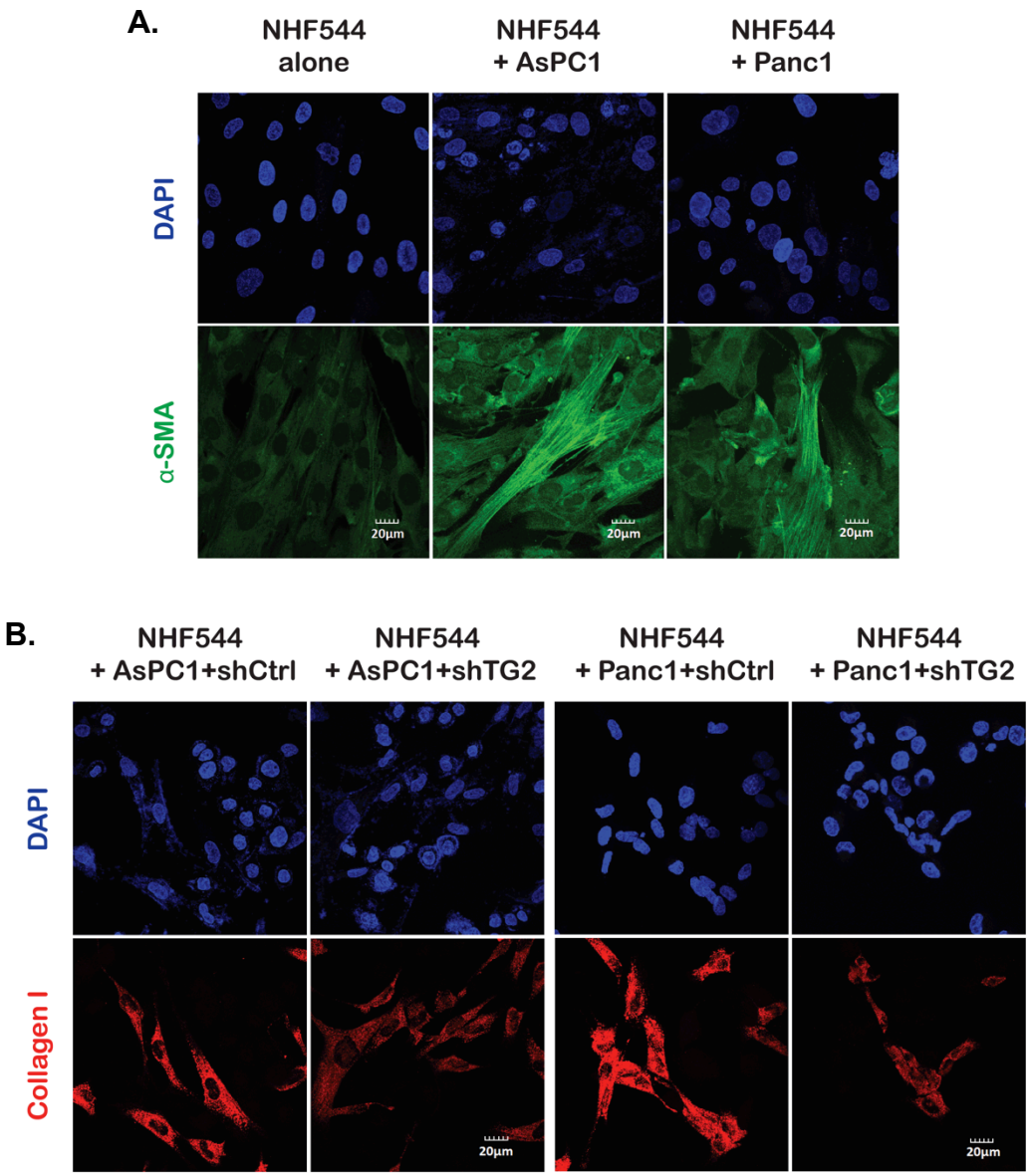

Figure 31. TG2 activates fibroblasts promoting collagen production. **(A)** IF for α-SMA (Alexa Fluor® 488, green) in NHF544 cultured alone (*left*) or co-cultured with AsPC1 (*middle*) or Panc1 cells (*right*). **(B)** IF for collagen I (Cy5, red) in NHF544 co-cultured with AsPC1+shCtrl or +shTG2 (*left*) or with Panc1+shCtrl and +shTG2 cells (*right*). Nuclei are visualized by DAPI (600X magnification).

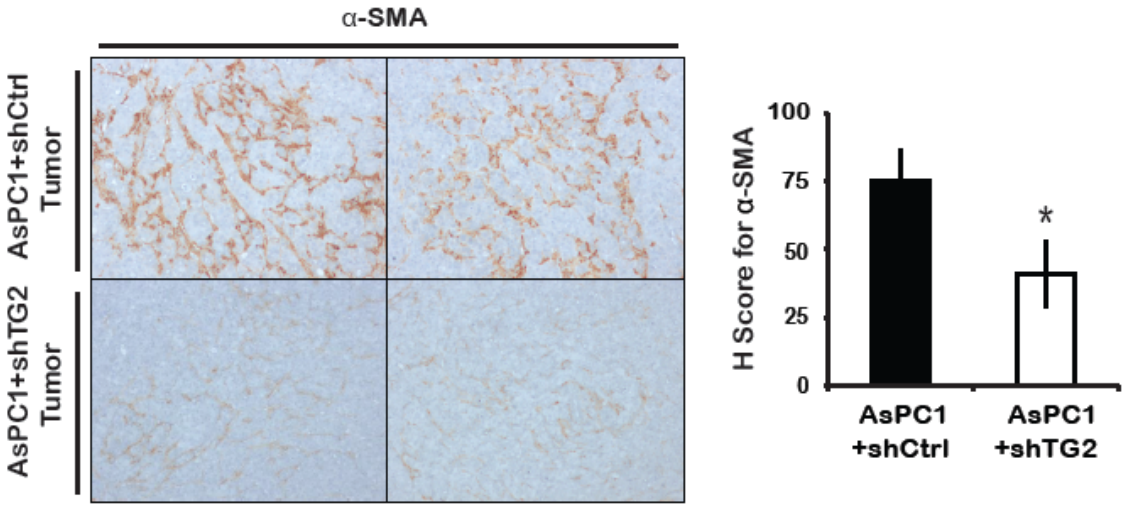

Figure 32. TG2 activates fibroblasts in mouse PDA xenografts. IHC for α-SMA identifies activated fibroblasts in AsPC1+shCtrl (n=10) and +shTG2 (n=7) xenografts (*left*). H scores quantify fibrosis (*right*, $p < 0.05$). Bars represent average quantification ± SE. * denotes $p < 0.05$.

3.11. Collagen and stromal cells promote growth of PDA cells

Next, we tested whether stromal alterations induced by TG2 conversely regulate the growth of PDA cells. First, the proliferation of PDA cells grown on collagen-coated vs. uncoated plates was measured by using the BrdU assay. The proliferation of AsPC1 and Panc1 cells was promoted when cells were cultured on collagen-coated plates compared to uncoated (**Figure 33A**, $p < 0.03$).

In addition, proliferation of PDA cells grown on feeder layer of hPSCs vs. no feeder layer was analyzed by using crystal violet staining. The proliferation of PDA cells grown on hPSC feeder layer was enhanced compared to when they were cultured without feeder layer (**Figure 33B**, $p < 0.006$).

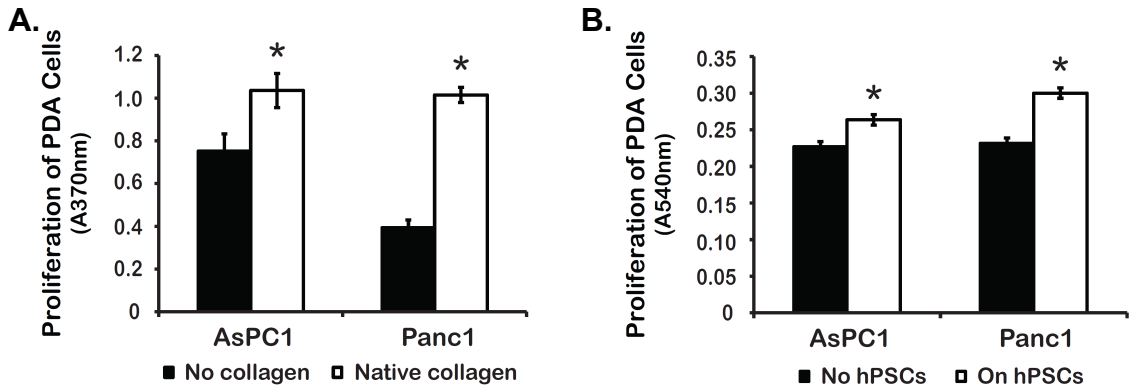

Figure 33. Collagen and stromal cells promote proliferation of PDA cells. **(A)** BrdU assay measures proliferation of AsPC1 and Panc1 cells grown on collagen-coated or uncoated plates ($p < 0.03$). **(B)** Crystal violet staining measures proliferation of AsPC1 and Panc1 cells cultured on a feeder layer of hPSCs or without feeder layer ($p < 0.006$). Bars represent average of 4 replicate measurements for each group ± SE. * denotes $p < 0.05$.

Taken together, these results demonstrate that TG2 secreted by PDA cells in the tumor milieu modulates the PDA stroma by promoting activation, proliferation, and collagen deposition of fibroblast and by crosslinking collagen. These stromal modifications conversely promote proliferation of PDA cells and provide a supportive environment for continuing tumor growth.

3.12. Knockdown of TG2 in PDA cells decreased proliferation, *in vivo*

Based on our findings showing that 1) pancreatic tumors contain activated stromal cells and crosslinked collagen, 2) those tumor components promote PDA cell proliferation *in vitro*, and 3) knockdown of TG2 in PDA cells decreases tumor growth *in vivo*, but 4) does not affect PDA cell proliferation and colony formation *in vitro*, we wanted to determine whether knockdown of TG2 in PDA cells has an

effect on PDA cell proliferation *in vivo*. To assess this, IHC staining for Ki67, a marker for proliferation, on pancreatic xenografts derived from AsPC1+shCtrl or AsPC1+shTG2 cells was performed. Proliferation of PDA cells in the xenografts was quantified by counting the Ki67 positive PDA cells in five randomly chosen fields per sample.

Interestingly, in contrast to the *in vitro* result, which showed no effect of TG2 knockdown on PDA cell proliferation, the number of Ki67 positive PDA cells in AsPC1+shTG2 xenografts was significantly decreased, *in vivo*, compared to that of controls (**Figure 34**).

Taken altogether, our findings demonstrate that the effects of TG2 on tumor growth are not due to the direct effects on PDA cells, but by the combined TG2 effects on the PDA stroma, which in turn regulate PDA cell proliferation and tumor progression.

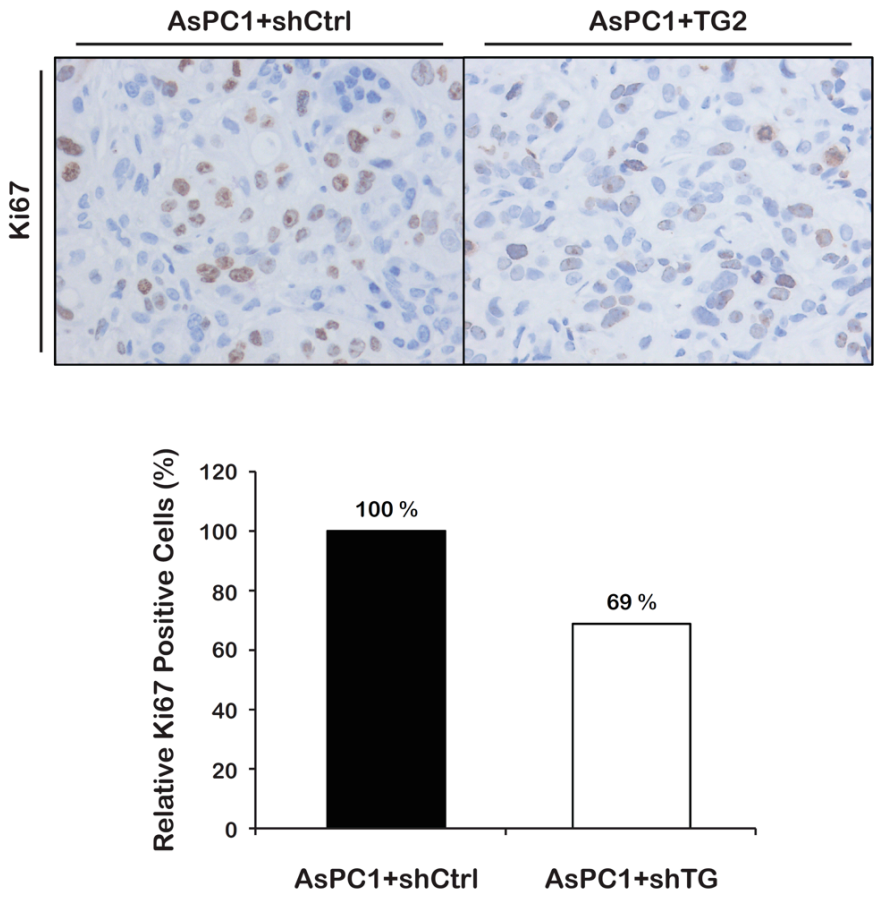

Figure 34. Knockdown of TG2 in PDA cells decreased proliferation *in vivo*. IHC stains for Ki67 in AsPC1+shCtrl and +shTG2 xenografts (*upper*). Graph represents relative percentage of Ki67 positive cells in AsPC1+shCtrl and +shTG2 xenografts (*lower*; n=3 per group, $p = 0.042$). Five randomly selected fields per sample were analyzed for Ki67 positive cells.

3.13. Matrix induced YAP/TAZ activation promotes PDA cell proliferation

As the pancreatic stroma becomes infiltrated by crosslinked collagen and activated fibroblasts, its stiffness increases. A mechanism activated by the physical properties of the ECM is the process of mechanotransduction, which translates mechanical stimuli into biochemical signals. The major factors activated by mechanical cues are the Yes-associated protein (YAP) and the

transcriptional co-activator with PDZ-binding motif (TAZ), which in turn regulate cancer cell growth. YAP and TAZ are known transcription factors involved in the Hippo signaling pathway. Activation of Hippo signaling pathway via MST1/2 and LATS1/2 kinases phosphorylates YAP (p-YAP), which becomes inactive and undergoes proteosomal degradation (B. Zhao, Li, Lei, & Guan, 2010). However, when Hippo signaling pathway is switched off, non-phosphorylated, active YAP translocates into the nucleus and promotes its target gene expression leading to cell proliferation.

However, besides the role of YAP and TAZ in Hippo signaling pathway, Dupont *et al*. have reported that YAP and TAZ are also involved in mechanotransduction, which proceeds independently of the Hippo signaling pathway (Dupont et al., 2011). They have shown that cells can be affected by the stiffness of the ECM via YAP and TAZ activation. Activated YAP and TAZ in a stiff environment translocate into the nucleus and promote cell proliferation, while inactive YAP and TAZ in cells embedded in a soft matrix remain in the cytoplasm.

On the basis of the report by Dupont *et al*., we determined the effect of collagen on YAP/TAZ activation in PDA cells. First, we determined cellular localization of YAP/TAZ in PDA cells grown on collagen-coated vs. uncoated plates by using IF. We noted increased nuclear YAP/TAZ localization in Panc1 and AsPC1 cells plated on collagen-coated plates compared to uncoated plates (**Figure 35A** and **35B**), indicating that higher proportion of YAP/TAZ is activated in PDA cells when cultured on collagen vs. no collagen.

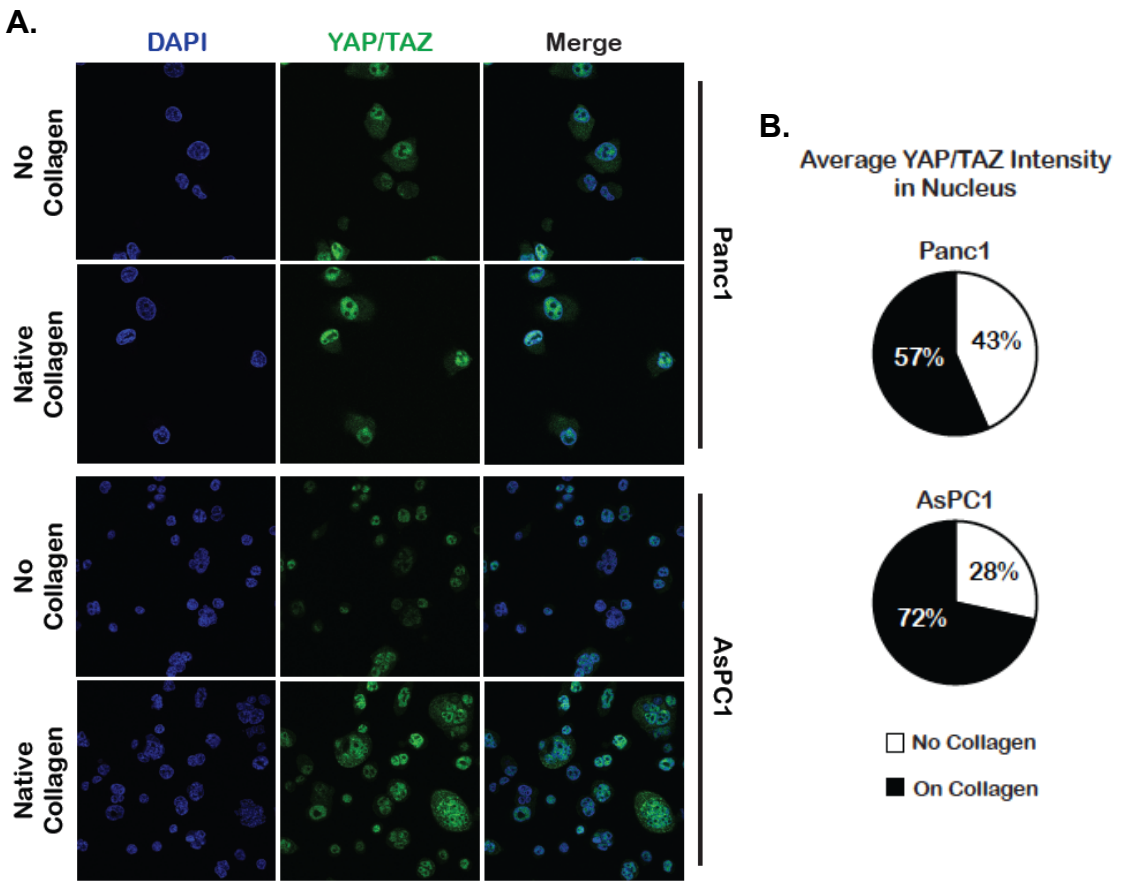

Figure 35. Collagen increases nuclear localization of YAP/TAZ in PDA cells. **(A)** IF for YAP/TAZ (Alexa Fluor® 488, green) in Panc1 and AsPC1 cells grown on collagen-coated or uncoated slides (600X magnifications). **(B)** Pie charts show the relative percentage of nuclear YAP/TAZ in Panc1 and AsPC1 cells plated on collagen-coated or uncoated plates. Nuclear localization of YAP/TAZ in PDA cells was quantified by averaging the intensity of green fluorescence in the nucleus of each cell, which was analyzed via MetaMorph software.

Next, we analyzed p-YAP (inactive) level in PDA cells grown on collagen-coated vs. uncoated plates by using western blotting. Decreased levels of p-YAP and increased ratio of total-YAP/p-YAP were detected in PDA cells plated on collagen-coated compared to uncoated plates (**Figure 36**), confirming the IF result that YAP is activated in PDA cells when cultured on collagen vs. no collagen.

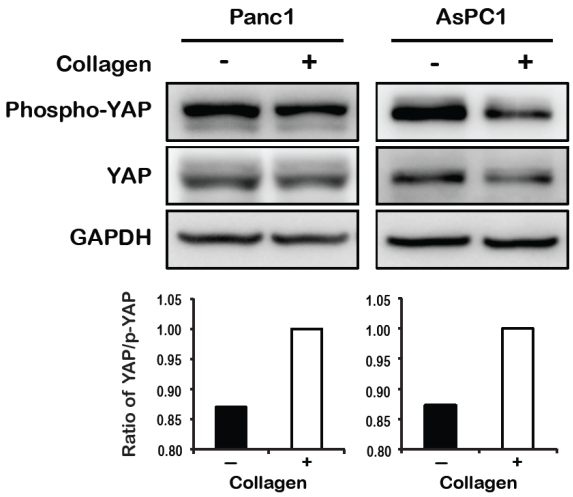

Figure 36. Collagen decreases phosphorylation of YAP in PDA cells. Western blotting (*upper*) shows total-YAP and p-YAP in Panc1 and AsPC1 cells plated on collagen-coated or uncoated plates and bars *(lower)* represent the ratio of total-YAP/p-YAP.

Collectively, these data suggest that YAP/TAZ transcription factors are activated in PDA cells by the presence of collagen matrix, and also possibly by the collagen matrix, which has become stiff due to the collagen crosslinking by TG2 secreted from PDA cells.

Based on the possibility that TG2, secreted by PDA cells, crosslinks and renders the collagen matrix stiff, we next determined the involvement of TG2 to YAP/TAZ activation in PDA cells grown on collagen. Panc1+shCtrl and +shTG2 and AsPC1+shCtrl and +shTG2 cells were cultured on collagen-coated slides. First, IF was used to visualize cellular localization of YAP/TAZ in PDA cells ±shTG2 plated on collagen. Increased nuclear localization was recorded in TG2 expressing control Panc1 and AsPC1 cells compared to +shTG2 PDA cells (**Figure 37A** and **37B**), suggesting that TG2 is involved in activation of YAP/TAZ in PDA cells grown on collagen.

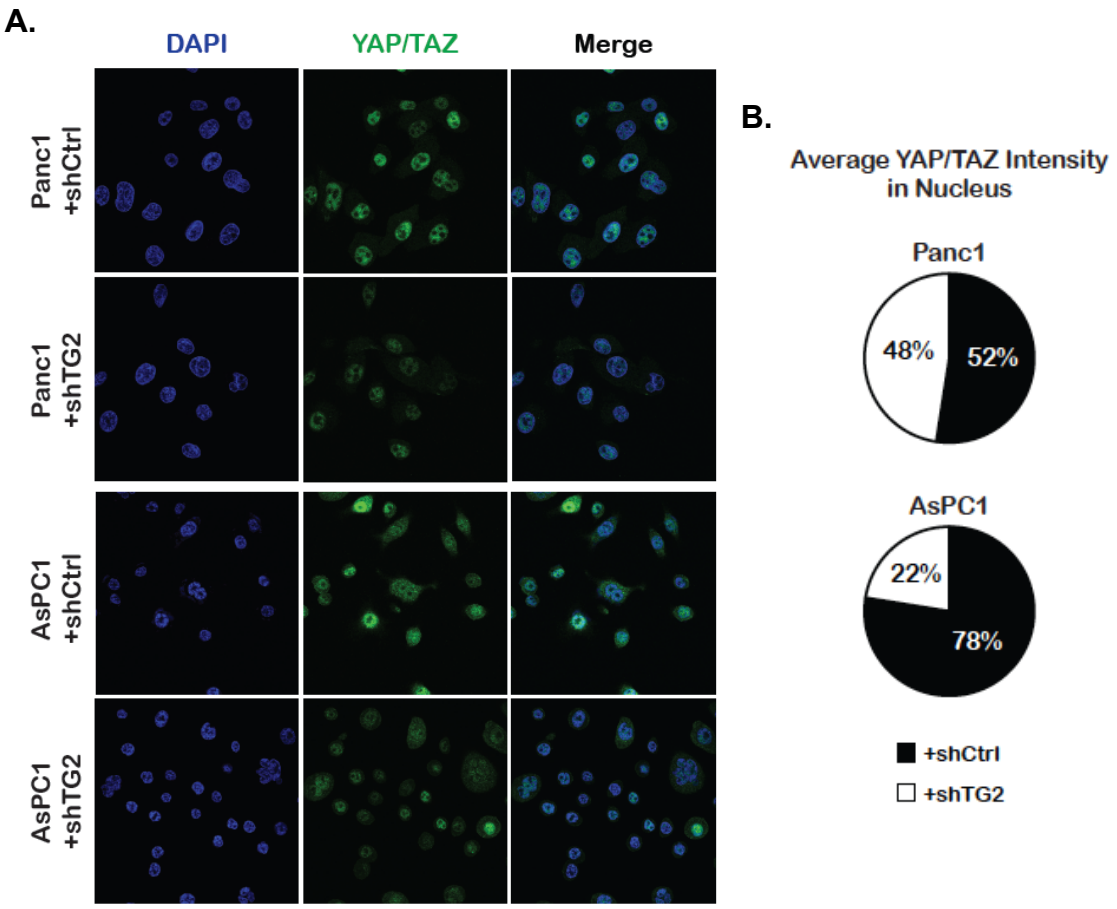

Figure 37. TG2 increases nuclear localization of YAP/TAZ in PDA cells grown on collagen. **(A)** IF for YAP/TAZ (Alexa Fluor® 488, green) in Panc1+shCtlr and +shTG2 and AsPC1+shCtrl and +shTG2 cells grown on collagen (600X magnification). **(B)** Pie charts show the relative percentage of nuclear YAP/TAZ in Panc1+shCtrl and +shTG2 cells grown on collagen. Nuclear localization of YAP/TAZ in PDA cells was quantified by averaging the intensity of green fluorescence in the nucleus of each cell, which was analyzed via MetaMorph software.

Next, we measured p-YAP in PDA cells ±shTG2 plated on collagen by using western blotting. Decreased levels of p-YAP and increased ratio of total-YAP/p-YAP were observed in Panc1+shCtrl compared to +shTG2 cells (**Figure 38**), confirming IF result that TG2 is involved in activation of YAP/TAZ in PDA cells cultured on collagen.

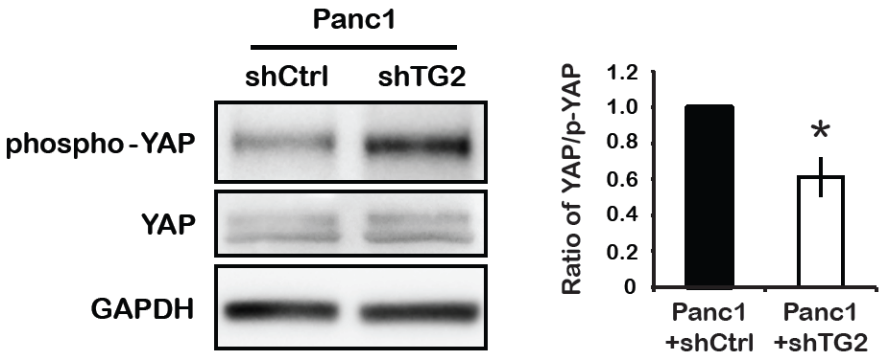

Figure 38. TG2 decreases phosphorylation of YAP in PDA cells grown on collagen. Western blotting (*left*) shows total-YAP and p-YAP in Panc1+shCtrl or Panc1+shTG2 grown on collagen. Bars (*right*) represent the ratio of total-YAP/p-YAP.

Next, to determine whether nuclear localization of YAP/TAZ corresponds to increased transcriptional activity, we measured the transcriptional activity of YAP in Panc1 cells cultured on collagen by using the TEAD4 reporter assay. TEAD4 reporter assay is processed through production of Gal4-TEAD4 fusion protein, which recruits YAP to the promoter of firefly luciferase reporter resulting in induction of luciferase expression. Therefore, high luminescent signal will be detected in the presence of YAP/TAZ, while no signal will be detected in the absence of YAP/TAZ. Luciferase activity in TEAD4 reporter assay was increased in Panc1+shCtrl compared to Panc1+shTG2 cells cultured on collagen (**Figure 39**, p = 0.009), confirming the activation of YAP/TAZ in TG2 expressing cells.

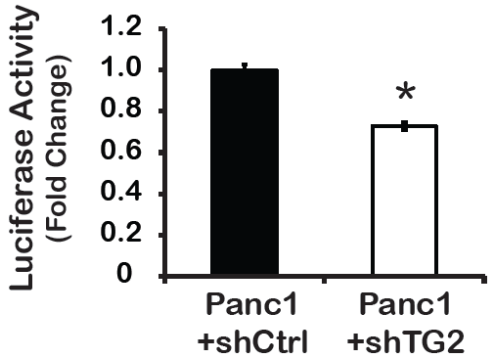

Figure 39. TG2 activates YAP in PDA cells grown on collagen. TEAD4 reporter assay in Panc1+shCtrl and Panc1+shTG2 cells grown on collagen (n=5, p = 0.009). Firefly luciferase activity was normalized to *renilla* luciferase. Bars represent averages of 5 replicates per group ± SE; * denotes $p < 0.05$.

The activation of YAP/TAZ results in up-regulation of specific target genes. To assess YAP/TAZ transcriptional activity, we measured the mRNA levels of *connective tissue growth factor* (*CTGF*), which is a known YAP/TAZ target gene, by utilizing qRT-PCR. Increased *CTGF mRNA* level (**Figure 40**, p = 0.04) was observed in Panc1+shCtrl cells compared to Panc1+shTG2 cells grown on collagen, confirming activation of YAP/TAZ in TG2 expressing cells.

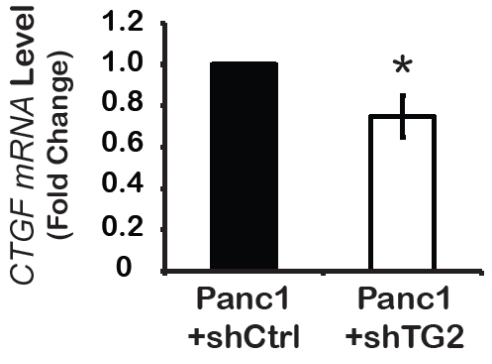

Figure 40. Activation of YAP/TAZ promotes expression of *CTGF* gene in PDA cells grown on collagen. QRT-PCR measures *CTGF mRNA* levels in Panc1+shCtrl and Panc1+shTG2 cells grown on collagen (p = 0.04). Bars represent average fold changes ± SE. * denotes $p < 0.05$.

Collectively, these data suggest that TG2 expressed in PDA cells is involved in activation of YAP and TAZ in PDA cells grown on collagen matrix, possibly by crosslinking collagen and increasing the environment stiffness. Further studies focused on measurement of collagen matrix stiffness are needed to delineate the specific mechanism by which TG2 activates YAP/TAZ.

Lastly, to determine the significance of YAP and TAZ to PDA cell proliferation, transient knockdown of YAP and TAZ was performed by transfecting siRNA targeting both transcription factors. First, knockdown of YAP and TAZ in PDA cells by siRNAs was confirmed by western blotting (**Figure 41**).

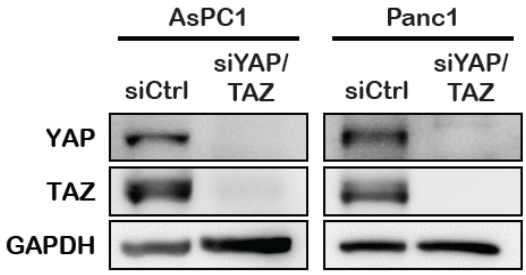

Figure 41. Knockdown of YAP/TAZ in PDA cells by transient siRNA transfection. Western immunoblotting for YAP and TAZ in AsPC1 and Panc1 cells transfected with siRNA targeting YAP and TAZ. GAPDH served as a loading control.

Next, we measured proliferation of control (+siCtrl) and +siYAP/TAZ PDA cells by performing BrdU assay. Knockdown of YAP/TAZ decreased proliferation of PDA cells compared to control cells grown on collagen (**Figure 42**, $p < 0.01$), confirming that YAP and TAZ are important players involved in cell proliferation.

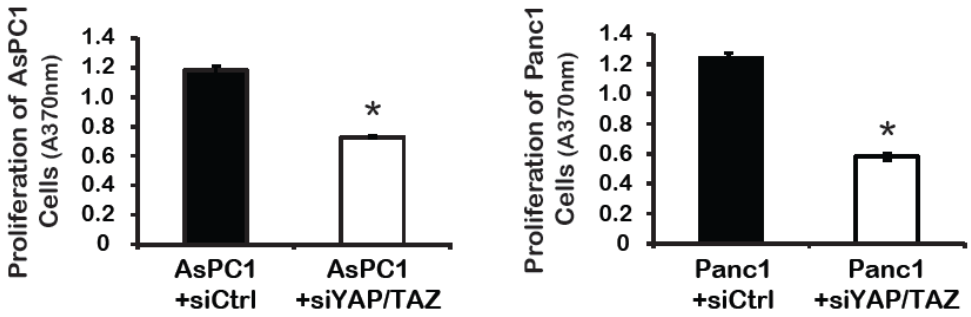

Figure 42. Knockdown of YAP/TAZ in PDA cells decreases cell proliferation. BrdU assay measures proliferation of AsPC1 (*left*) and Panc1 (*right*) cells transfected with siRNA targeting YAP and TAZ (n=4 per group, $p < 0.01$). Bars represent average of 4 replicates ± SE; * denotes $p < 0.05$.

Taken together, these data demonstrate that the transcription factors, YAP and TAZ, are activated in TG2 expressing PDA cells grown on collagen, and that their activation regulates cell proliferation. These findings outline a new mechanism by which cancer cell proliferation is modulated by TG2 through signals reflected from the tumor cells into the surrounding stroma.

3.14. Effect of TG2 knockdown on response to gemcitabine in PDA cells and in tumors

3.14.1. Knockdown of TG2 does not affect response to gemcitabine in PDA cells, *in vitro*

To determine whether knockdown of TG2 in PDA cells alters sensitivity of PDA cells to gemcitabine, AsPC1+shCtrl or +shTG2 cells (**Figure 16**) were treated with gemcitabine in dose-dependent manner for 48 hours, and the

number of proliferating, live cells was quantified by CCK-8 assay. The number of surviving AsPC1+shTG2 cells after gemcitabine treatment was not different from that of AsPC1+shCtrl cells (**Figure 43**), suggesting that the knockdown of TG2 does not sensitize PDA cells to gemcitabine.

In addition, proliferation of both AsPC1+shCtrl and +shTG2 cells was constant at the IC_{50} level in the presence of gemcitabine (**Figure 43**), indicating that gemcitabine blocks cell proliferation, consistent with its known mechanism of action (Shipley et al., 1992).

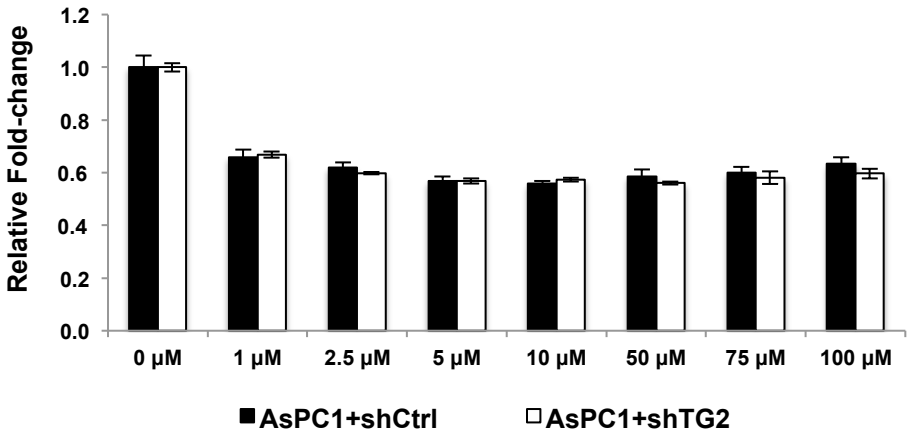

Figure 43. Knockdown of TG2 does not affect response to gemcitabine in PDA cells. CCK-8 assay measures proliferation of AsPC1+shCtrl and +shTG2 cells after 48 hours of gemcitabine treatment in dose-dependent manner (1-100 µM). Bars represent average fold changes of triplicates ± SE.

3.14.2. Co-culture of PDA cells with fibroblasts decreases sensitivity of PDA cells to gemcitabine, *in vitro*

As we have observed 1) increased proliferation of PDA cells cultured on a feeder layer of stromal cells and 2) dense PDA stroma with active stromal cells, we hypothesized that fibroblasts could protect PDA cells from gemcitabine, leading to continuous proliferation of PDA cells.

To test this, we performed co-culture of GFP-expressing AsPC1 cells with NHF544 fibroblasts at a ratio of 1:1. Proliferation of AsPC1 cells was determined by measuring green fluorescence emitted from the AsPC1 cells during the 96-hour time course. As shown in **Figure 44**, AsPC1 cells proliferated more when in co-culture with fibroblasts compared to AsPC1 cells cultured alone (*left*, $p < 0.05$).

In addition, 96-hour gemcitabine treatment at a high concentration (200 μM) in the co-culture of AsPC1 with fibroblasts did not attenuate the proliferation of AsPC1 cells during the 96-hour time course. On the other hand, the number of surviving AsPC1 cells was decreased in the presence of gemcitabine when cultured alone, consistent with the known anti-proliferative effects of gemcitabine (**Figure 44**, *right*, $p < 0.05$).

Overall, these data suggest that fibroblasts present in the co-culture protect PDA cells from the effects of gemcitabine.

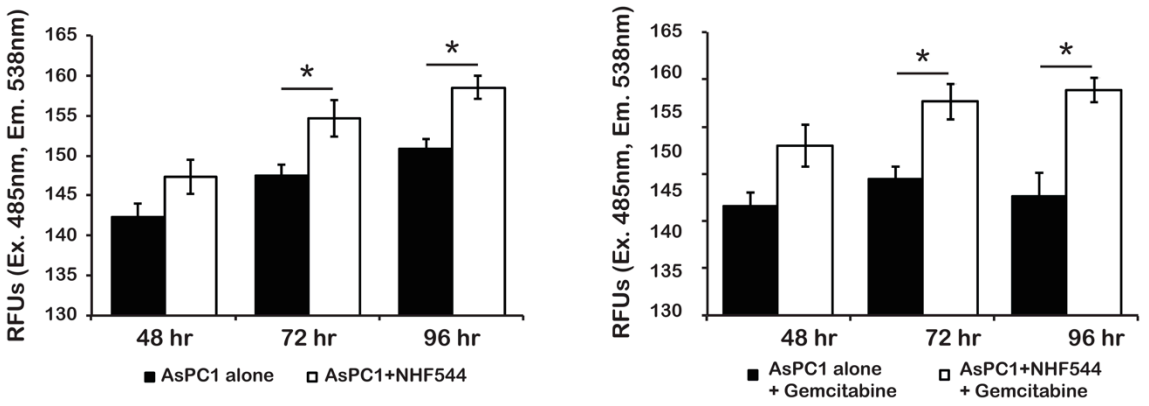

Figure 44. Fibroblasts protect PDA cells from gemcitabine treatment. Proliferation of AsPC1+GFP cells in co-culture with fibroblasts or grown alone (*left*) and treated with gemcitabine (*right*) for 4 days. Green fluorescence in AsPC1+GFP cells was measured at Ex. 485nm and Em. 538nm. Bars represent average RFUs of triplicates ± SE. * denotes $p < 0.05$.

3.14.3. Knockdown of TG2 in PDA cells inhibits tumor growth and sensitizes tumors to gemcitabine

Based on our previous results showing decreased fibrosis in shTG2 PDA cell-derived xenografts and decreased sensitivity to gemcitabine in PDA cells when co-cultured with stromal cells, we tested whether knockdown of TG2 in PDA cells induces sensitivity to gemcitabine in PDA tumors. To test this, we used orthotopic pancreatic xenograft mouse model derived from AsPC1+shCtrl or +shTG2 cells, treated with gemcitabine twice a week for 4 weeks at a dose of 25 mg/kg via intraperitoneal injection (n=7 per PBS group and n=8 per gemcitabine group).

In concordance with previous data, average tumor volumes and weights were significantly decreased in xenografts derived from AsPC1+shTG2 cells compared to controls (**Figure 45**, *upper*, $p = 0.002$ and $p = 0.001$, respectively),

while there was no significant difference in the number of macro-metastases between the two groups (**Figure 45**, *lower*, $p = 0.55$).

Gemcitabine treatment decreased the average tumor size and weight in both AsPC1+shCtrl and AsPC1+shTG2 derived xenografts compared to PBS (**Figure 45**, *upper*, $p < 0.002$). Furthermore, average tumor size and weight were significantly lower in AsPC1+shTG2 derived xenografts treated with gemcitabine compared to controls treated with gemcitabine (**Figure 45**, *upper*, $p = 0.04$ and $p = 0.03$, respectively).

In addition, treatment of gemcitabine in mice bearing AsPC1+shTG2 xenografts significantly decreased number of macro-metastasis compared to mice carrying AsPC1+shCtrl tumors (**Figure 45**, *lower*, $p = 0.005$). Together, these data suggest that the knockdown of TG2 inhibits tumor growth and sensitizes tumors to gemcitabine, *in vivo*.

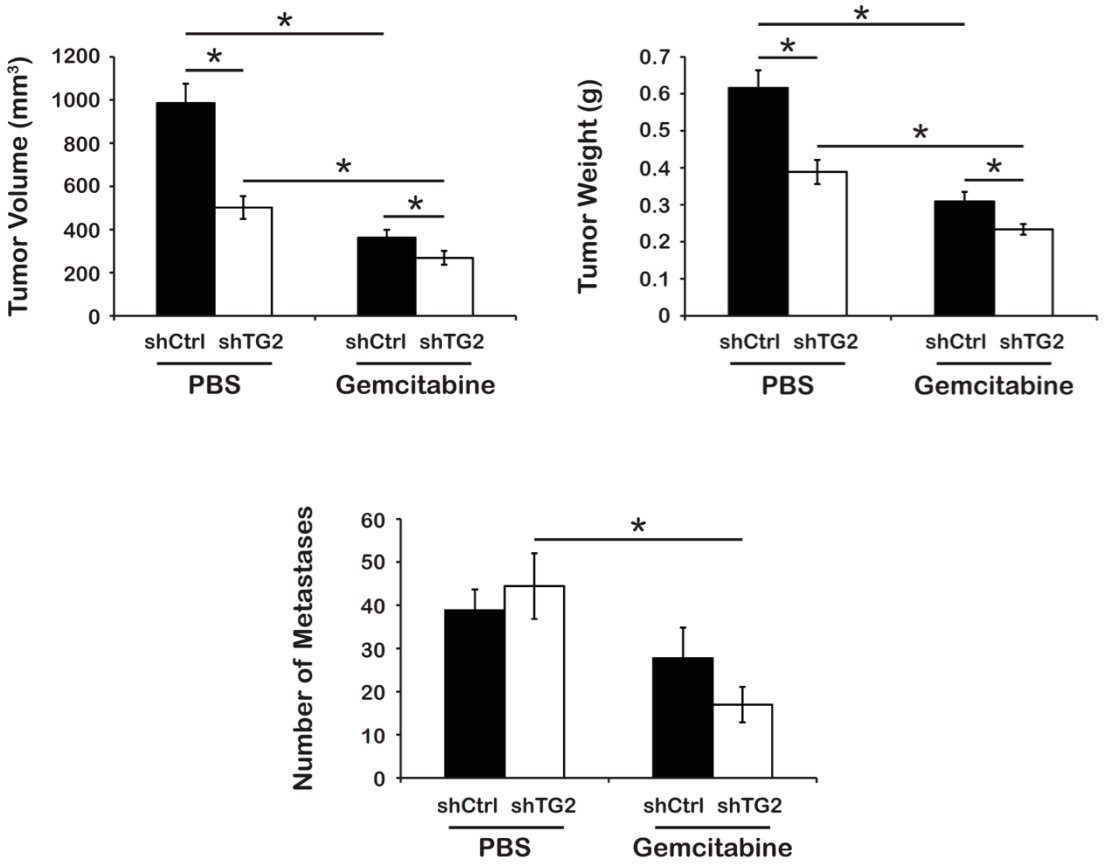

Figure 45. Knockdown of TG2 in PDA cells decreases tumor growth and sensitizes tumors to gemcitabine. Average tumor volume, weight, and number of metastases of xenografts derived from AsPC1+shCtrl and +shTG2 cells and treated with gemcitabine or PBS. n=7 per PBS groups and n=8 per gemcitabine groups. Bars represent average measurements ± SE; * denotes $p < 0.05$.

3.14.4. Knockdown of TG2 in PDA cells does not affect penetrance of gemcitabine in tumor tissues

Based on our findings showing decreased fibrosis in shTG2 tumors, we hypothesized that the more pronounced gemcitabine effects in shTG2 tumors is due to increased penetrance of gemcitabine in the shTG2 tumors compared to control tumors. To determine the gemcitabine concentrations in tumor tissues depending on TG2 expression levels, we used orthotopic pancreatic xenograft

mouse model derived from AsPC1+shCtrl and +shTG2 cells. After 4 weeks of PDA cell implantation, the mice were given a single dose of gemcitabine (25 mg/kg) via intravenous injection and tumors were harvested within 2 minutes. The uptake of gemcitabine in pancreas occurs within minutes after intravenous administration, and gemcitabine is rapidly excreted (Kristjansen, Brown, Shipley, & Jain, 1996; Shipley et al., 1992), justifying the time point chosen. Concentrations of gemcitabine and its derivative, 2',2'-difluorodeoxyuridine (dFdU), in tumor tissues were quantified by HPLC-MS/MS [collaboration with Dr. Jones in the pharmacology core at IUSCC].

The sum of gemcitabine and dFdU concentrations in tumor tissues was slightly higher, but not reaching statistical significance, between the AsPC1+shTG2 and AsPC1+shCtrl tumors (**Figure 46**, n=6 per group, p = 0.4). This non-significant trend might be explained by high variability within the groups, consisting of only 6 mice. We cannot completely exclude that TG2 knockdown does not alter gemcitabine penetrance into tumor tissue.

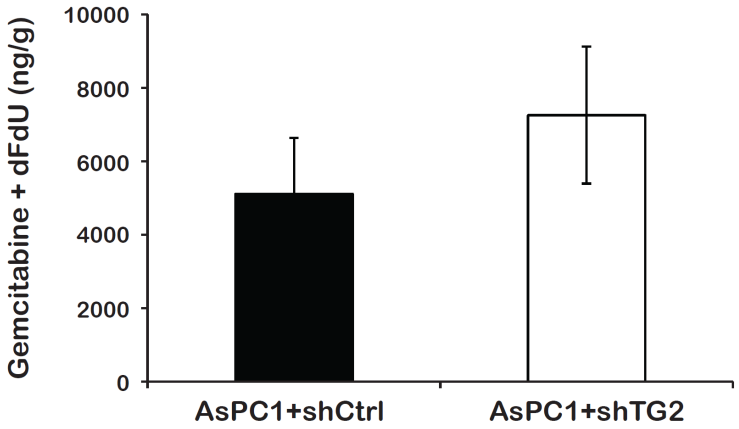

Figure 46. Gemcitabine concentration in tumor tissue is not affected by TG2 knockdown in PDA cells. Sum of gemcitabine and dFdU concentration per tumor weight (ng/g) in AsPC1+shCtrl and +shTG2 xenografts (n=6 per group, p = 0.4). Bars represent average quantification ± SE.

3.15. Knockdown of TG2 does not affect microvessel density

As we have shown that AsPC1+shTG2 tumors respond more efficiently to gemcitabine compared to controls, we questioned whether delivery of gemcitabine was increased in shTG2 tumors altered vascularization. To determine the number of vessels present in the ±shTG2 pancreatic xenografts, IHC staining for CD31, a marker for angiogenesis, was performed in shCtrl and shTG2 pancreatic xenografts. The number of CD31 positive vessels was counted by a board-certified pathologist [Robert Emerson, IUSM].

A trend towards an increase in microvessel density (MVD) was observed in shTG2 tumors compared to controls (**Figure 47**, n=6 per group, p = 0.2), suggesting that perhaps tumors are better vascularized in the absence of TG2. However, this did not reach statistical significance and requires future validation.

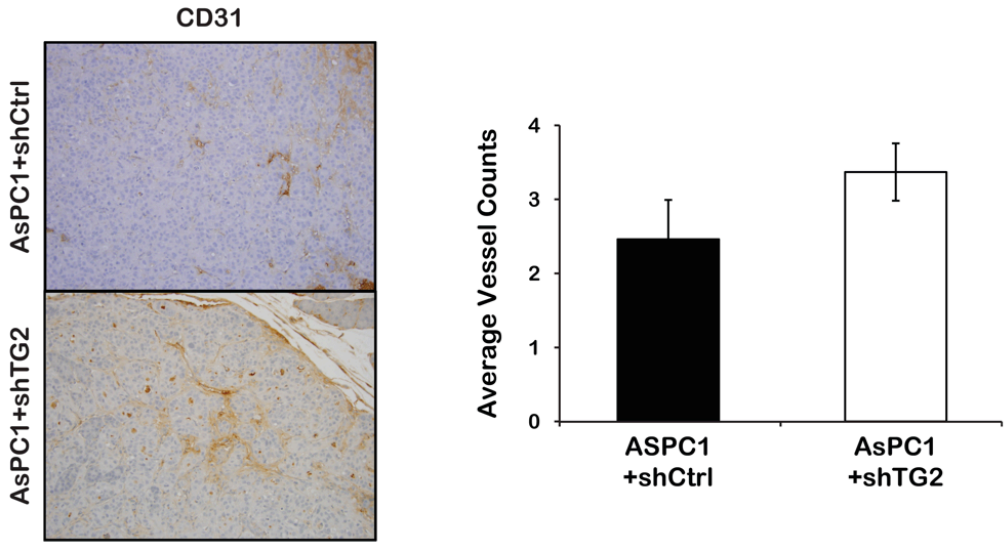

Figure 47. Knockdown of TG2 in PDA cells does not affect MVD in tumors. Average of number of vessels counted in AsPC1+shCtrl and +shTG2 xenografts (n=6 per group, p = 0.2). Brown staining represents $CD31^+$ microvessels. Bars represent average vessel counts ± SE.

In all, our data suggest that knockdown of TG2 in PDA cells sensitizes tumors to gemcitabine, possibly by inducing angiogenesis and delivery of gemcitabine in tumor tissue. Future studies focusing on validation of TG2-mediated vascularization and gemcitabine penetrance in tumors are required to delineate mechanism by which TG2 increases tumor response to gemcitabine. Additionally, TG2 induced proliferation of fibroblasts in the matrix may provide a protective effect and favor continued tumor growth.

CHAPTER 4. DISCUSSION

4.1. Summary of results

Our findings outline how changes in the pancreatic cancer stroma induced by TG2 secreted from PDA cells alter tumor growth. We show that overexpressed TG2 in PDA cells and in tumors is secreted into the culture medium and the tumor milieu, respectively. TG2 secreted from PDA cells is catalytically active and crosslinks collagen in the matrix. In addition, the secreted TG2 and the TG2-mediated crosslinked collagen activate fibroblasts, promoting their proliferation and increasing collagen production. Eventually, this promotes tumor growth, *in vivo*. These effects are abolished by TG2 knockdown with shRNA, which causes reduced amount of thick, crosslinked collagen and decreased number of active fibroblasts. TG2 knockdown, *in vivo*, also inhibits tumor growth. Furthermore, we showed that the fibrosis-rich stiff pancreatic tumors activate YAP/TAZ signaling, promoting PDA cell proliferation. Taken together, these data demonstrate the effects of enzymatically active TG2 on the pancreatic TME and their subsequent consequences on cancer cell proliferation and tumor growth, supporting future studies targeting the crosslinking activity of TG2 to disrupt tumor progression.

4.2. TG2 expression in PDA cells and in tumors

Previously, it has been reported that TG2 is overexpressed in epithelial cancers, such as ovarian and breast cancers (Condello et al., 2014; Lorand &

Graham, 2003; Mehta et al., 2004). TG2 is also overexpressed in pancreatic cancer (Verma, Guha, Diagaradjane, et al., 2008; Verma, Guha, Wang, et al., 2008).

Mehta and co-workers have previously reported that, TG2 is highly expressed in 42 out of 75 (56%) drug resistant and metastatic human PDA tumors and in all of 12 human PDA cell lines analyzed (Verma et al., 2006). Consistent with these reports, we show abundant expression of TG2 in 36 out of 52 (69%) PDA specimens, supporting increased TG2 expression in PDA compared to the normal duct epithelium. We also show that 4 different human PDA cell lines express higher levels of TG2 compared to pancreatic normal epithelial cells. Those 4 different cell lines expressed variable TG2 levels; relatively abundant TG2 in AsPC1 and BxPC3 cell lines and relatively low TG2 in Panc1 and Paca2 cell lines. These differences may be due to different characteristics of the cells' tumor of origin.

We also show that TG2 is secreted in the ECM. Similar to reports by Lorand and Graham (Lorand & Graham, 2003) describing that TG2 is secreted in the ECM and is involved in the ECM assembly, we observed abundant TG2 localization in the ECM of PDA tumors. This is the first report showing that TG2 secreted from PDA cells is localized especially in the PDA stroma.

TG2 lacks leader peptide or hydrophobic domain, which are typically present for secreted proteins to be exported (Gentile et al., 1991; Liu et al., 2002). Surprisingly, however, localization of TG2 was observed not only in the

cytoplasm, but also on the cell surface and extracellular space of undamaged endothelial and smooth muscle cells, macrophages, fibroblasts, and osteoblasts (Iismaa et al., 2009; Lorand & Graham, 2003).

Some reports proposed that the externalization of TG2 occurs through intracellular trafficking toward the cell surface, while others suggested that it is mediated through interaction with other transmembrane proteins, such as integrins or adrenergic receptors (Lorand & Graham, 2003), or with extracellular binding partners, such as fibronectin and heparin sulfate proteoglycans (Gaudry et al., 1999; Scarpellini et al., 2009). Belkin *et al*. has proposed that TG2 externalizes through trafficking of perinuclear recycling endosomes, which requires initial tethering of TG2 to endosomal phosphoinositides, subsequent tight binding to endosomal membrane, and fusion with plasma membrane (Belkin, 2011). In addition, Belkin *et al*. have shown that this secretion can be inhibited by nitric oxide, which is involved in angiogenesis (Santhanam et al., 2011). However, the mechanism of TG2 secretion across lipid bilayers of membrane remains disputed.

4.3. TG2 activity in the PDA stroma

It is known that the functions of TG2 are tightly controlled by environmental factors that cause allosteric structural changes and alter the accessibility of the catalytic domain. High Ca^{2+} concentrations in the ECM allow the protein to adopt an open conformation that exposes the catalytic core, while

high intracellular GTP forces a closed, enzymatically inactive structure (Pinkas et al., 2007). These conformational changes suggest that TG2 should be catalytically inactive in the intracellular environment under normal physiological conditions.

However, here we show that TG2 is enzymatically active in the pancreatic TME based on analyzes testing incorporation of 5-BP and T26 small peptides. 5-BP is a biotinylated amine, which gets incorporated onto glutamine residues on accessible TGase substrates. T26 is a FITC-labeled glutamine donor substrate specific for TG2. In the presence of catalytically active TG2, both 5-BP and T26 are crosslinked and incorporated in proteins harboring free amine groups. Here we showed that TG2 is catalytically active in PDA cells and in the stroma where it crosslinks collagen, and possibly other ECM substrates.

However, we did not detect 5-BP incorporation in human dermal fibroblasts and T26 incorporation in mesothelial LP9 cells under normal physiological conditions, suggesting that TG2 is enzymatically inactive in these normal cells. On the other hand, incorporation of 5-BP was detectable in the cytoplasm and on the membrane of PDA cells. TGase activity was inhibited by EDTA, a Ca^{2+} chelator that is known to inhibit the catalytic activity of TGases. In addition, incorporation of T26 into proteins in the cytoplasm and on the membrane of PDA cells was observed, confirming that TG2 is enzymatically active in malignant PDA cells. However, under low intracellular Ca^{2+} and high GTP concentrations, TG2 should be catalytically inactive. Our findings showing intracellular TG2 crosslinking activity inside cancer cells suggest that the enzyme

may be abnormally activated in transformed cells. The factors causing TG2 activation within PDA cells remain not known and future studies are needed to delineate the mechanism.

In situ TG2 activity was also detected in pancreatic xenografts by using the T26 assay. T26 incorporation was observed both intra- and extra-cellularly in AsPC1 and Panc1 xenograft sections, supporting that secreted TG2 from PDA cells is enzymatically active in the tumor milieu. Khosla's group previously reported that extracellular TG2 is enzymatically inactivated through oxidation, which forms disulfide bonds between Cys^{370} and Cys^{371} residues. Reducing factors, such as dithiothreitol (DTT) and thioredoxin (Trx), are required to restore TG2 enzymatic activity (Jin et al., 2011).

To exclude the possibility that TG2 may be activated spuriously in this assay, we carried out the assay in the absence of DTT. We still observed incorporation of T26 in the ECM in the absence of DTT in the reaction solution, supporting that TG2 is enzymatically active *in situ* in these tissues. We do not know whether other reducing factors are endogenously present in the pancreatic milieu and could cause TG2 activation. Further studies are needed to elucidate the observed phenomenon.

In addition to that report, they also reported that extracellular TG2 is catalytically inactive, but can be transiently activated upon tissue injury (Siegel et al., 2008). Therefore, it is tempting to speculate that tissue injury including hypoxia inflicted by tumorigenesis may be inducing TG2 enzymatic activity *in vivo*

(Filiano, Bailey, Tucholski, Gundemir, & Johnson, 2008). In addition, metabolic or physical factors involved in oxidative stress and Ca^{2+} homeostasis, for example, may be expressed or function differently in transformed compared to normal cells. Interestingly, a previous report by Verma *et al*. suggested that IκBα, the NF-κB inhibitory subunit, is a direct substrate of TG2 enzymatic activity in PDA cells (Verma et al., 2006), although direct evidence of TG2 activity was not provided in that report.

4.4. Stromal alterations induced by TG2

The ECM of the pancreatic stroma is prominently composed of collagens, non-collagen glycoproteins, growth factors, and modulators of the cell-matrix interaction (Duner, Lopatko Lindman, Ansari, Gundewar, & Andersson, 2010; Feig et al., 2012). Among prominent ECM proteins, collagen I, III, and fibronectin are the major components of the pancreatic DS (Gress et al., 1995; Lunardi et al., 2014; Mahadevan & Von Hoff, 2007), and they are potential substrates for TG2.

Here we also show that collagen I, a known TG2 substrate, was crosslinked by TG2 leading to the formation of a dense matrix in the pancreatic milieu. TG2 expressing PDA cell-derived pancreatic xenografts contained higher proportion of thick, crosslinked collagen, lesser amount of soluble, non-crosslinked collagen, and the same amount of total collagen compared to shTG2 xenografts, confirming that TG2 secreted by PDA cells into the tumor milieu crosslinks collagen, making it stable and insoluble.

In addition, we showed that the TG2-mediated crosslinked collagen promoted the growth of fibroblasts. Proliferation of fibroblasts, *in vitro*, was induced by native collagen and furthermore by TG2-mediated crosslinked collagen. We also showed that TG2 expressing PDA cells promoted the growth and the activation of fibroblasts. Co-culture of fibroblasts with TG2 expressing PDA cells increased activation, proliferation, and collagen deposition of the fibroblasts compared to the co-culture with TG2 KD cells. Likewise, higher content of active fibroblasts (α-SMA positive) was detected in the control pancreatic xenogragfts compared to shTG2 xenografts. Our findings are consistent with a previous report demonstrating that collagen crosslinked by TG2 stimulated the proliferation of dermal fibroblasts (Chau et al., 2005) and with studies demonstrating the involvement of TG2 in wound healing and in pathologic fibrotic responses in the lung or liver (Collighan & Griffin, 2009; Olsen et al., 2014; Olsen et al., 2011; Shweke et al., 2008; E. A. Verderio, Johnson, & Griffin, 2004).

We also showed that these alterations of collagen and fibroblasts conversely stimulated the growth of PDA cells. Proliferation of PDA cells was promoted when cells were grown on collagen vs. no collagen and on feeder layer of hPSCs vs. no hPSCs. In addition, higher PDA cell proliferation rate, as measured by Ki67 staining, was detected *in vivo* in the TG2 expressing cell-derived pancreatic xenografts compared to shTG2 xenografts.

In contrast, knockdown of TG2 in PDA cells did not alter their proliferation and clonogenic potential, *in vitro*. These findings suggested that the effects of

TG2 on tumor growth are not explained by direct effect on cancer cells, but by TG2-mediated alterations of the stroma, which in turn regulate tumor progression.

In contrast to the activation and proliferation of fibroblasts observed in the co-culture with TG2 expressing PDA cells, addition of active recombinant TG2 did not affect the proliferation of the fibroblasts. This finding suggests that TG2 acts in concert with other factors secreted in the ECM.

Taken together, our findings demonstrate that PDA cells secreting TG2 in the tumor milieu promote fibroblast activation and proliferation as well as collagen crosslinking, leading to stromal alterations, which in turn promote tumor growth.

In addition to our findings, we suspect that the enzyme has other substrates in the pancreatic ECM and that their modifications through crosslinking could contribute to the distinct architecture of the DS, which in turn fosters tumor progression.

To sum up, we report a significant decrease in the number of activated myofibroblasts and thick collagen fibers in tumors derived from shTG2 transduced cells, and show that these stromal alterations directly affect proliferation of fibroblasts and cancer cells. The protective role of the pancreatic stroma to cancer cells has been previously recognized and linked to the resistance of pancreatic tumors to chemo and radiotherapy (Erkan, 2013; Garrido-Laguna et al., 2011; Gore & Korc, 2014). Our data implicate for the first

time TG2 as a modulator of the pancreatic TME through its protein crosslinking properties.

4.5. TG2 promotes pancreatic tumor growth

Here we demonstrate that TG2 knockdown by shRNA in pancreatic cancer cells inhibits tumor growth. We showed decreased average volume and weight of shTG2 tumors compared to control tumors. This result is consistent with a previous study reported by Mehta and colleagues (Verma, Guha, Diagaradjane, et al., 2008). They used TG2-specific siRNA-DOPC liposome to knockdown TG2 in an orthotopic mouse model. The siRNAs were delivered via intravenous injection, and this led to inhibition of pancreatic tumor growth along with decreased tumor vascularity (Verma, Guha, Diagaradjane, et al., 2008).

However, in contrast to their report, we did not observe changes in multi-vessel density between TG2 expressing and TG2 knockdown tumors. This contradictory result may have resulted from different approaches in TG2 knockdown. Non-specific delivery of siRNA targeting TG2 via intravenous route in their model may have affected all TG2 expressing cells (including endothelial cells), while TG2 knockdown was restricted to PDA cells in our model. Therefore, it is possible that TG2 knockdown in endothelial cells in their model led to the anti-angiogenic effect observed.

4.6. TG2 induces YAP activation in PDA cells

Here we link for the first time TG2 to activation of the transcriptional regulators, YAP and TAZ, in cancer cells. YAP/TAZ are known transcription factors involved in the Hippo signaling pathway, a pathway strongly implicated in cell survival and proliferation and activated in epithelial cancers (Cordenonsi et al., 2011; Zeng & Hong, 2008). Independent of the canonical Hippo signaling pathway, YAP/TAZ can be regulated by the physical properties of the ECM and are involved in mechanotransduction, translating mechanical cues into relevant biological signals (Dupont et al., 2011). Recent reports have implicated YAP activation in pancreatic tumor progression downstream or independent of mutant Kras (Kapoor et al., 2014; Zhang et al., 2014). Zhang *et al*. reported that pancreas-specific deletion of YAP in mutant *Kras* ($Kras^{G12D}$) mice inhibited the progression of neoplastic PDA lesion to PDA, and that YAP is an important transcriptional factor downstream of Kras/MAPK signaling pathway, promoting neoplastic cell proliferation of PDA progression (Zhang et al., 2014). In addition, Kapoor *et al*. reported that overexpression of Yap1 induces PDA recurrence independent of *Kras* mutation and MAPK signaling pathway by forming a Yap1/Tead2 complex that interacts with E2F transcriptional factor, resulting in activation of cell cycle and DNA replication (Kapoor et al., 2014). Here we propose that the pancreatic matrix rendered denser by TG2 through collagen crosslinking and stimulation of a fibrotic response provides positive proliferative feedback to the cancer cells by stimulating YAP/TAZ signaling.

We show that the matrix, specifically collagen, activates YAP/TAZ in PDA cells leading to their nuclear localization and induces target gene (CTGF) expression. In addition, nuclear localization of YAP/TAZ correlates with TG2 expression level in PDA cells. Higher intensity of nuclear YAP/TAZ was detected in TG2 expressing control PDA cells compared to TG2 knocked-down cells, and in abundant-TG2 expressing cells (AsPC1) compared to low-TG2 expressing (Panc1) cells. We speculate that these effects may have resulted from stimuli triggered by the stiff collagen matrix, crosslinked by secreted TG2 from PDA cells. However, a limitation of our study is that we were not able to measure the actual mechanical forces of the matrix. Therefore, we cannot exclude that signals other than tissue stiffness, directly modulated by TG2 or by the matrix, contribute to YAP activation. Future studies should be performed to determine the stiffness of the tumor and the collagen matrix in the presence of TG2 or when TG2 is inhibited.

In addition, we show that knockdown of YAP/TAZ in PDA cells grown on collagen correlates to decreased cell proliferation, suggesting that YAP/TAZ are directly involved in regulation of PDA cell proliferation.

Collectively, our findings outline a new mechanism by which PDA cell proliferation is modulated by TG2 through signals reflected from the tumor into the surrounding stroma (**Figure 48**).

These observations led us to propose that the stimulatory growth signals conveyed by TG2 require the stroma, which “deflects” mechanical or biological cues from the tumor milieu into an active oncogenic program.

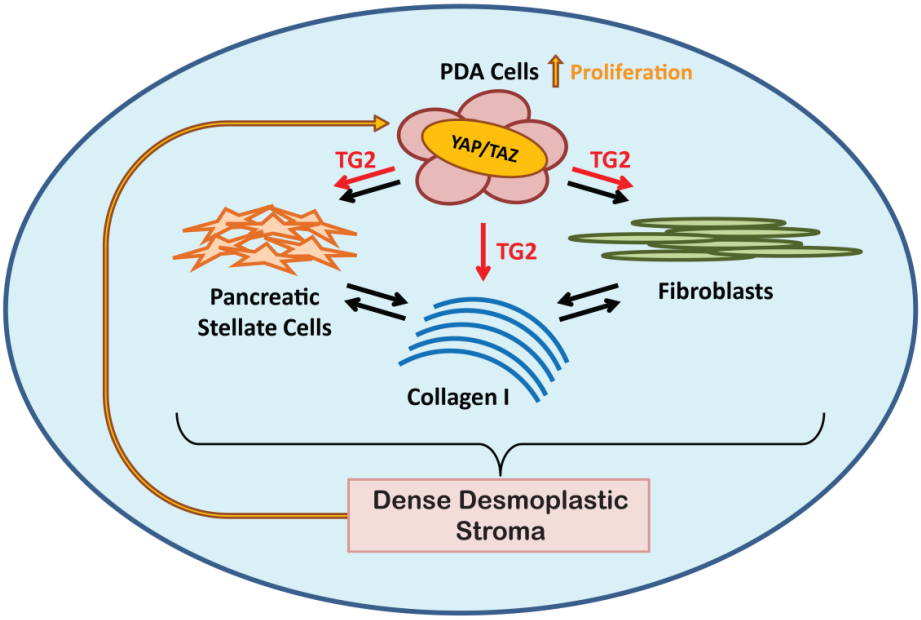

Figure 48. Proposed mechanism by which TG2 promotes tumor growth. TG2 expressed and secreted by PDA cells in the tumor microenvironment modulates the stroma by activating stromal cells and crosslinking collagen, resulting in a fibrosis-rich stroma. This dense stroma protects PDA cells from gemcitabine and activates YAP/TAZ in PDA cells, promoting cell proliferation and tumor growth.

4.7. Effect of TG2 on gemcitabine response in PDA cells and in tumors:

Here we show that the TG2-mediated desmoplasia of the PDA stroma limits the gemcitabine effect. Treatment of mice bearing AsPC1+shCtrl or AsPC1+shTG2 xenografts with gemcitabine significantly decreased the average tumor volume and weight compared to PBS (control) treatment. In addition, gemcitabine treatment significantly decreased the average tumor volume and the

weight of AsPC1+shTG2 xenografts compared to AsPC1+shCtrl xenografts, suggesting that knockdown of TG2 enhanced sensitivity of tumors to gemcitabine, possibly by diminishing the desmoplasia of the stroma. Our findings are consistent with a previous report by Verma *et al*. showing that siRNA-mediated knockdown of TG2 inhibited PDA tumor growth and enhanced gemcitabine therapeutic efficacy (Verma, Guha, Diagaradjane, et al., 2008).

We also show that gemcitabine treatment of mice bearing AsPC1+shTG2 xenografts significantly decreased number of metastases compared to the PBS treatment, while there was no effect of gemcitabine treatment on number of metastases in the mice bearing AsPC1+shCtrl xenografts. Interestingly, metastatic propensity was not inhibited by TG2 knockdown alone, but gemcitabine treatment in addition to TG2 knockdown showed synergistic effect in decreasing the number of metastases in the tumor bearing mice. These findings may be related to less fibrotic stroma due to TG2 knockdown, which in turn provides improved penetrance of gemcitabine.

Our findings demonstrating decreased metastatic propensity of the combination of TG2 knockdown and gemcitabine treatment is consistent with the previous report by Verma *et al*. (Verma, Guha, Diagaradjane, et al., 2008). However, we were not able to show inhibition of metastasis only by knockdown of TG2 in PDA cells, while the other authors have observed dramatic decrease in metastasis by TG2 knockdown alone. As mentioned earlier, this difference may have resulted as a consequence of the different approaches of TG2 downregulation, which nonspecifically affected TG2 expression in their model

leading to anti-angiogenic effects and the subsequent inhibition of cell proliferation, tumor growth, and metastasis.

In addition, and in contrast to their results, we did not observe changes in microvessel density between TG2 expressing and TG2 knockdown tumors. This indicates not only that restricted TG2 knockdown in PDA cells is not sufficient to alter angiogenesis in PDA tumors, but also that enhanced gemcitabine effect in the shTG2 tumors is not related to altered delivery of the drug through vessels.

Here we also show that uptake of gemcitabine in AsPC1+shCtrl and AsPC1+shTG2 xenografts, 2 minutes after intravenous administration, is not significantly different. This may have resulted from similar microvessel density between the shCtrl and the shTG2 tumors, which contributed to the same delivery of gemcitabine into tissues.

However, even though the gemcitabine concentrations between the two groups were not statistically significant, there was a trend of higher gemcitabine concentration in shTG2 tumors. As tumors were harvested only 2 minutes after one dose of gemcitabine administration, some variability in gemcitabine tissue distribution may have occurred. In addition, only 6 mice per group were used for this study. As *in vivo* experiments with mice have high variability, increasing the number of specimens could decrease the observed variability.

In vitro, we also show that knockdown of TG2 in PDA cells itself does not significantly affect sensitivity to gemcitabine. However, PDA cells in a co-culture with fibroblasts were protected from gemcitabine treatment compared to the PDA

cells cultured alone. These findings indicate that the dense, fibrotic stroma resulting from the TG2-mediated activate fibroblasts and crosslinked collagen may be linked to chemoresistance in pancreatic cancer. This stroma protects PDA cells from gemcitabine and promotes continuous proliferation of PDA cells and tumor growth.

Taken together, this is the first report describing the effects of TG2 on the pancreatic TME, and its subsequent consequences on cancer cell proliferation and tumor growth. Our study demonstrates that TG2 expressing PDA cells form larger pancreatic tumors, enriched in thick collagen fibers and in active fibroblasts. The dense stroma of TG2 expressing PDA tumors protects PDA cells from gemcitabine and conveys signals leading to YAP/TAZ activation in cancer cells promoting cell proliferation and tumor growth (**Figure 48**). Our findings support the involvement of enzymatically active TG2 in the progression of PDA and future studies targeting the crosslinking activity of TG2 to disrupt tumor progression.

CHAPTER 5. FUTURE DIRECTIONS

The 5-BP and T26 incorporation experiment showed that TG2 is enzymatically active only in PDA cells but not in the normal fibroblasts and mesothelial cells. However, the factors causing TG2 activation within PDA cells remain unknown. Therefore, future studies are needed to delineate the mechanism.

In addition, we hypothesized that stiffness of the collagen matrix leads to activation of YAP and TAZ in PDA cells grown on collagen. However, a limitation of our study was that the actual mechanical forces of the matrix could not be measured. Therefore, we cannot exclude that signals other than tissue stiffness, directly modulated by TG2 or by the matrix, contribute to YAP activation. Future studies are required to determine the stiffness of the tumor and the collagen matrix in the presence or knockdown of TG2.

In this study, we focused on the involvement of TG2 in the alteration of collagen and stromal cells in the tumor milieu. However, as the pancreatic stroma is heterogenous with various cytokines, growth factors, and extracellular matrix proteins, it is possible that other factors in the ECM may be involved in modulation of PDA stroma leading to tumor progression and chemoresistance. Therefore, future studies are needed to identify other factors involved in the stroma alteration in concert with TG2.

Lastly, effects of TG2 enzymatic inhibitors on tumor progression and response to chemotherapy will be explored.

REFERENCES

Achyuthan, K., & Greenberg, C. (1987). Identification of a guanosine triphosphate-binding site on guinea pig liver transglutaminase. Role of GTP and calcium ions in modulating activity. *Journal of Biological Chemistry, 262*(4), 1901-1906.

Adler, J. J., Johnson, D. E., Heller, B. L., Bringman, L. R., Ranahan, W. P., Conwell, M. D., . . . Wells, C. D. (2013). Serum deprivation inhibits the transcriptional co-activator YAP and cell growth via phosphorylation of the 130-kDa isoform of Angiomotin by the LATS1/2 protein kinases. *Proc Natl Acad Sci U S A, 110*(43), 17368-17373.

Aeschlimann, D., & Thomazy, V. (2000). Protein crosslinking in assembly and remodelling of extracellular matrices: the role of transglutaminases. *Connect Tissue Res, 41*(1), 1-27.

Akar, U., Ozpolat, B., Mehta, K., Fok, J., Kondo, Y., & Lopez-Berestein, G. (2007). Tissue transglutaminase inhibits autophagy in pancreatic cancer cells. *Molecular Cancer Research, 5*(3), 241-249.

Akimov, S. S., & Belkin, A. M. (2001). Cell surface tissue transglutaminase is involved in adhesion and migration of monocytic cells on fibronectin. *Blood, 98*(5), 1567-1576.

Azrak, R. G., Cao, S., Slocum, H. K., Toth, K., Durrani, F. A., Yin, M. B., . . . Rustum, Y. M. (2004). Therapeutic synergy between irinotecan and 5-fluorouracil against human tumor xenografts. *Clinical Cancer Research, 10*(3), 1121-1129.

Baek, K. J., Das, T., Gray, C. D., Desai, S., Hwang, K.-C., Gacchui, R., . . . Im, M.-J. (1996). A 50 KDa protein modulates guanine nucleotide binding of transglutaminase II. *Biochemistry, 35*(8), 2651-2657.

Barnes, R. N., Bungay, P. J., Elliott, B. M., Walton, P. L., & Griffin, M. (1985). Alterations in the distribution and activity of transglutaminase during tumour growth and metastasis. *Carcinogenesis, 6*(3), 459-463.

Belkin, A. M. (2011). Extracellular TG2: emerging functions and regulation. *FEBS J, 278*(24), 4704-4716.

Biankin, A. V., Waddell, N., Kassahn, K. S., Gingras, M. C., Muthuswamy, L. B., Johns, A. L., . . . Grimmond, S. M. (2012). Pancreatic cancer genomes reveal aberrations in axon guidance pathway genes. *Nature, 491*(7424), 399-405.

Blackford, A., Parmigiani, G., Kensler, T. W., Wolfgang, C., Jones, S., Zhang, X., . . . Hruban, R. H. (2009). Genetic mutations associated with cigarette smoking in pancreatic cancer. *Cancer Res, 69*(8), 3681-3688.

Bours, V., Dejardin, E., Goujon-Letawe, F., Merville, M.-P., & Castronovo, V. (1994). The NF-κB transcription factor and cancer: high expression of NF-κB-and IκB-related proteins in tumor cell lines. *Biochem Pharmacol, 47*(1), 145-149.

Bruce, S. E., & Peters, T. J. (1983). The subcellular localization of transglutaminase in normal liver and in glucagon-treated and partial hepatectomized rats. *Biosci Rep, 3*(12), 1085-1090.

Burris, H. A., Moore, M. J., Andersen, J., Green, M. R., Rothenberg, M. L., Madiano, M. R., . . . VanHoff, D. D. (1997). Improvements in survival and clinical benefit with gemcitabine as first-line therapy for patients with advanced pancreas cancer: A randomized trial. *Journal of Clinical Oncology, 15*(6), 2403-2413.

Campbell, S. L., Khosravi-Far, R., Rossman, K. L., Clark, G. J., & Der, C. J. (1998). Increasing complexity of Ras signaling. *Oncogene, 17*(11 Reviews), 1395-1413.

Cao, L., Shao, M., Schilder, J., Guise, T., Mohammad, K., & Matei, D. (2012). Tissue transglutaminase links TGF-β, epithelial to mesenchymal transition and a stem cell phenotype in ovarian cancer. *Oncogene, 31*(20), 2521-2534.

Chau, D. Y., Collighan, R. J., Verderio, E. A., Addy, V. L., & Griffin, M. (2005). The cellular response to transglutaminase-cross-linked collagen. *Biomaterials, 26*(33), 6518-6529. doi: 10.1016/j.biomaterials.2005.04.017.

Cheung, W., Darfler, M. M., Alvarez, H., Hood, B. L., Conrads, T. P., Habbe, N., . . . Maitra, A. (2008). Application of a global proteomic approach to archival precursor lesions: deleted in malignant brain tumors 1 and tissue transglutaminase 2 are upregulated in pancreatic cancer precursors. *Pancreatology, 8*(6), 608-616.

Collighan, R. J., & Griffin, M. (2009). Transglutaminase 2 cross-linking of matrix proteins: biological significance and medical applications. *Amino Acids, 36*(4), 659-670.

Condello, S., Morgan, C. A., Nagdas, S., Cao, L., Turek, J., Hurley, T. D., & Matei, D. (2014). beta-Catenin-regulated ALDH1A1 is a target in ovarian cancer spheroids. *Oncogene, 34*(18), 2297-2308.

Conroy, T., Desseigne, F., Ychou, M., Bouche, O., Guimbaud, R., Becouarn, Y., . . . Intergroup, P. (2011). FOLFIRINOX versus gemcitabine for metastatic pancreatic cancer. *N Engl J Med, 364*(19), 1817-1825.

Cordenonsi, M., Zanconato, F., Azzolin, L., Forcato, M., Rosato, A., Frasson, C., . . . Piccolo, S. (2011). The Hippo transducer TAZ confers cancer stem cell-related traits on breast cancer cells. *Cell, 147*(4), 759-772.

Cunningham, D., Chau, I., Stocken, D. D., Valle, J. W., Smith, D., Steward, W., . . . Neoptolemos, J. P. (2009). Phase III randomized comparison of gemcitabine versus gemcitabine plus capecitabine in patients with advanced pancreatic cancer. *J Clin Oncol, 27*(33), 5513-5518.

Di Venere, A., Rossi, A., De Matteis, F., Rosato, N., Agro, A. F., & Mei, G. (2000). Opposite effects of Ca(2+) and GTP binding on tissue transglutaminase tertiary structure. *J Biol Chem, 275*(6), 3915-3921.

Duner, S., Lopatko Lindman, J., Ansari, D., Gundewar, C., & Andersson, R. (2010). Pancreatic cancer: the role of pancreatic stellate cells in tumor progression. *Pancreatology, 10*(6), 673-681.

Dupont, S., Morsut, L., Aragona, M., Enzo, E., Giulitti, S., Cordenonsi, M., . . . Piccolo, S. (2011). Role of YAP/TAZ in mechanotransduction. *Nature, 474*(7350), 179-183.

Erkan, M. (2013). Understanding the stroma of pancreatic cancer: co-evolution of the microenvironment with epithelial carcinogenesis. *J Pathol, 231*(1), 4-7.

Erkan, M., Hausmann, S., Michalski, C. W., Fingerle, A. A., Dobritz, M., Kleeff, J., & Friess, H. (2012). The role of stroma in pancreatic cancer: diagnostic and therapeutic implications. *Nat Rev Gastroenterol Hepatol, 9*(8), 454-467.

Faye, C., Inforzato, A., Bignon, M., Hartmann, D., Muller, L., Ballut, L., . . . Ricard-Blum, S. (2010). Transglutaminase-2: a new endostatin partner in the extracellular matrix of endothelial cells. *Biochem. J, 427*, 467-475.

Feig, C., Gopinathan, A., Neesse, A., Chan, D. S., Cook, N., & Tuveson, D. A. (2012). The pancreas cancer microenvironment. *Clin Cancer Res, 18*(16), 4266-4276.

Ferrari, D., & Soling, H. (1999). The protein disulphide-isomerase family: unravelling a string of folds. *Biochem. J, 339*, 1-10.

Fesus, L., & Piacentini, M. (2002). Transglutaminase 2: an enigmatic enzyme with diverse functions. *Trends Biochem Sci, 27*(10), 534-539.

Fesus, L., & Szondy, Z. (2005). Transglutaminase 2 in the balance of cell death and survival. *FEBS Lett, 579*(15), 3297-3302.

Filiano, A. J., Bailey, C. D., Tucholski, J., Gundemir, S., & Johnson, G. V. (2008). Transglutaminase 2 protects against ischemic insult, interacts with HIF1beta, and attenuates HIF1 signaling. *FASEB J, 22*(8), 2662-2675.

Fok, J. Y., Ekmekcioglu, S., & Mehta, K. (2006). Implications of tissue transglutaminase expression in malignant melanoma. *Mol Cancer Ther, 5*(6), 1493-1503.

Freedman, R. B., Hirst, T. R., & Tuite, M. F. (1994). Protein disulphide isomerase: building bridges in protein folding. *Trends in biochemical sciences, 19*(8), 331-336.

Frese, K. K., Neesse, A., Cook, N., Bapiro, T. E., Lolkema, M. P., Jodrell, D. I., & Tuveson, D. A. (2012). nab-Paclitaxel potentiates gemcitabine activity by reducing cytidine deaminase levels in a mouse model of pancreatic cancer. *Cancer Discov, 2*(3), 260-269.

Fukahi, K., Fukasawa, M., Neufeld, G., Itakura, J., & Korc, M. (2004). Aberrant expression of neuropilin-1 and-2 in human pancreatic cancer cells. *Clinical Cancer Research, 10*(2), 581-590.

Fukui, M., Kuramoto, K., Yamasaki, R., Shimizu, Y., Itoh, M., Kawamoto, T., & Hitomi, K. (2013). Identification of a highly reactive substrate peptide for transglutaminase 6 and its use in detecting transglutaminase activity in the skin epidermis. *FEBS J, 280*(6), 1420-1429.

Gandhi, V., & Plunkett, W. (1990). Modulatory activity of 2',2'-difluorodeoxycytidine on the phosphorylation and cytotoxicity of arabinosyl nucleosides. *Cancer Res, 50*(12), 3675-3680.

Garrido-Laguna, I., Uson, M., Rajeshkumar, N. V., Tan, A. C., de Oliveira, E., Karikari, C., . . . Hidalgo, M. (2011). Tumor engraftment in nude mice and enrichment in stroma- related gene pathways predict poor survival and resistance to gemcitabine in patients with pancreatic cancer. *Clin Cancer Res, 17*(17), 5793-5800.

Gaudry, C. A., Verderio, E., Aeschlimann, D., Cox, A., Smith, C., & Griffin, M. (1999). Cell Surface Localization of Tissue Transglutaminase Is Dependent on a Fibronectin-binding Site in Its N-terminal -Sandwich Domain. *Journal of Biological Chemistry, 274*(43), 30707-30714.

Gentile, V., Saydak, M., Chiocca, E. A., Akande, O., Birckbichler, P. J., Lee, K. N., . . . Davies, P. J. (1991). Isolation and characterization of cDNA clones to mouse macrophage and human endothelial cell tissue transglutaminases. *J Biol Chem, 266*(1), 478-483.

Ghosh, S., May, M. J., & Kopp, E. B. (1998). NF-κB and Rel proteins: evolutionarily conserved mediators of immune responses. *Annual review of immunology, 16*(1), 225-260.

Gore, J., & Korc, M. (2014). Pancreatic cancer stroma: friend or foe? *Cancer Cell, 25*(6), 711-712.

Grenard, P., Bresson-Hadni, S., El Alaoui, S. d., Chevallier, M., Vuitton, D. A., & Ricard-Blum, S. (2001). Transglutaminase-mediated cross-linking is involved in the stabilization of extracellular matrix in human liver fibrosis. *Journal of hepatology, 35*(3), 367-375.

Gress, T. M., Müller-Pillasch, F., Lerch, M. M., Friess, H., Büchler, M., & Adler, G. (1995). Expression andin-situ localization of genes coding for extracellular matrix proteins and extracellular matrix degrading proteases in pancreatic cancer. *International Journal of Cancer, 62*(4), 407-413.

Griffin, M., Casadio, R., & Bergamini, C. M. (2002). Transglutaminases: nature's biological glues. *Biochem J, 368*(Pt 2), 377-396.

Grzesiak, J. J., & Bouvet, M. (2006). The alpha2beta1 integrin mediates the malignant phenotype on type I collagen in pancreatic cancer cell lines. *Br J Cancer, 94*(9), 1311-1319.

Haixia, W., Qikui, C., Liuping, J., & Li, W. (2005). Expression and Significance of Cyclooxygenase-2 in Human Pancreatic Carcinomas. *The Chinese-German Journal of Clinical Oncology, 4*(2), 121-123.

Hanahan, D., & Weinberg, R. A. (2000). The Hallmarks of Cancer. *Cell, 100*(1), 57-70.

Hanahan, D., & Weinberg, R. A. (2011). Hallmarks of cancer: the next generation. *Cell, 144*(5), 646-674.

Hang, J., Zemskov, E. A., Lorand, L., & Belkin, A. M. (2005). Identification of a novel recognition sequence for fibronectin within the NH2-terminal beta-sandwich domain of tissue transglutaminase. *J Biol Chem, 280*(25), 23675-23683.

Hasegawa, G., Suwa, M., Ichikawa, Y., Ohtsuka, T., Kumagai, S., Kikuchi, M., . . . Saito, Y. (2003). A novel function of tissue-type transglutaminase: protein disulphide isomerase. *Biochem J, 373*(Pt 3), 793-803.

Heinemann, V., Boeck, S., Hinke, A., Labianca, R., & Louvet, C. (2008). Meta-analysis of randomized trials: evaluation of benefit from gemcitabine-based combination chemotherapy applied in advanced pancreatic cancer. *BMC Cancer, 8*, 82.

Helming, K. C., Wang, X., Wilson, B. G., Vazquez, F., Haswell, J. R., Manchester, H. E., . . . Roberts, C. W. (2014). ARID1B is a specific vulnerability in ARID1A-mutant cancers. *Nat Med, 20*(3), 251-254.

Herbert, B.-S., Hochreiter, A. E., Wright, W. E., & Shay, J. W. (2006). Nonradioactive detection of telomerase activity using the telomeric repeat amplification protocol. *Nat Protoc, 1*(3), 1583-1590.

Herman, J. F., Mangala, L. S., & Mehta, K. (2006). Implications of increased tissue transglutaminase (TG2) expression in drug-resistant breast cancer (MCF-7) cells. *Oncogene, 25*(21), 3049-3058.

Hertel, L. W., Boder, G. B., Kroin, J. S., Rinzel, S. M., Poore, G. A., Todd, G. C., & Grindey, G. B. (1990). Evaluation of the antitumor activity of gemcitabine (2',2'-difluoro-2'-deoxycytidine). *Cancer Res, 50*(14), 4417-4422.

Hezel, A. F., Kimmelman, A. C., Stanger, B. Z., Bardeesy, N., & Depinho, R. A. (2006). Genetics and biology of pancreatic ductal adenocarcinoma. *Genes Dev, 20*(10), 1218-1249.

Hidalgo, M., Cascinu, S., Kleeff, J., Labianca, R., Lohr, J. M., Neoptolemos, J., . . . Heinemann, V. (2015). Addressing the challenges of pancreatic cancer: future directions for improving outcomes. *Pancreatology, 15*(1), 8-18.

Hlatky, L., Hahnfeldt, P., & Folkman, J. (2002). Clinical application of antiangiogenic therapy: microvessel density, what it does and doesn't tell us. *J Natl Cancer Inst, 94*(12), 883-893.

Hruban, R. H., Adsay, N. V., Albores-Saavedra, J., Anver, M. R., Biankin, A. V., Boivin, G. P., . . . Tuveson, D. A. (2006). Pathology of genetically engineered mouse models of pancreatic exocrine cancer: consensus report and recommendations. *Cancer Res, 66*(1), 95-106.

Hruban, R. H., & Klimstra, D. S. (2014). Adenocarcinoma of the pancreas. *Semin Diagn Pathol, 31*(6), 443-451.

Hruban, R. H., Wilentz, R. E., & Kern, S. E. (2000). Genetic Progression in the Pancreatic Ducts. *The American Journal of Pathology, 156*(6), 1821-1825.

Huang, P., Chubb, S., Hertel, L. W., Grindey, G. B., & Plunkett, W. (1991). Action of 2',2'-difluorodeoxycytidine on DNA synthesis. *Cancer Res, 51*(22), 6110-6117.

Iacobuzio-Donahue, C. A., Ashfaq, R., Maitra, A., Adsay, N. V., Shen-Ong, G. L., Berg, K., . . . Kern, S. E. (2003). Highly expressed genes in pancreatic ductal adenocarcinomas A comprehensive characterization and comparison of the transcription profiles obtained from three major technologies. *Cancer Res, 63*(24), 8614-8622.

Ihle, N. T., Byers, L. A., Kim, E. S., Saintigny, P., Lee, J. J., Blumenschein, G. R., . . . Powis, G. (2012). Effect of KRAS oncogene substitutions on protein behavior: implications for signaling and clinical outcome. *J Natl Cancer Inst, 104*(3), 228-239.

Iismaa, S. E., Mearns, B. M., Lorand, L., & Graham, R. M. (2009). Transglutaminases and disease: lessons from genetically engineered mouse models and inherited disorders. *Physiol Rev, 89*(3), 991-1023.

Ijichi, H. (2012). Inhibition of CXCLs/CXCR2 axis in the tumor microenvironment might be a potent therapeutics for pancreatic cancer. *Oncoimmunology, 1*(4), 569-571.

Ikenaga, N., Ohuchida, K., Mizumoto, K., Cui, L., Kayashima, T., Morimatsu, K., . . . Tanaka, M. (2010). CD10+ pancreatic stellate cells enhance the progression of pancreatic cancer. *Gastroenterology, 139*(3), 1041-1051, 1051 e1041-1048.

Im, M., & Graham, R. (1990). A novel guanine nucleotide-binding protein coupled to the alpha 1-adrenergic receptor. I. Identification by photolabeling or membrane and ternary complex preparation. *Journal of Biological Chemistry, 265*(31), 18944-18951.

Im, M., Riek, R., & Graham, R. (1990). A novel guanine nucleotide-binding protein coupled to the alpha 1-adrenergic receptor. II. Purification, characterization, and reconstitution. *Journal of Biological Chemistry, 265*(31), 18952-18960.

Infante, J. R., Matsubayashi, H., Sato, N., Tonascia, J., Klein, A. P., Riall, T. A., . . . Goggins, M. (2007). Peritumoral fibroblast SPARC expression and patient outcome with resectable pancreatic adenocarcinoma. *Journal of Clinical Oncology, 25*(3), 319-325.

Inoue, A., Yamamoto, N., Kimura, M., Nishio, K., Yamane, H., & Nakajima, K. (2014). RBM10 regulates alternative splicing. *FEBS Lett, 588*(6), 942-947.

Janiak, A., Zemskov, E. A., & Belkin, A. M. (2006). Cell surface transglutaminase promotes RhoA activation via integrin clustering and suppression of the Src–p190RhoGAP signaling pathway. *Mol Biol Cell, 17*(4), 1606-1619.

Jin, X., Stamnaes, J., Klock, C., DiRaimondo, T. R., Sollid, L. M., & Khosla, C. (2011). Activation of extracellular transglutaminase 2 by thioredoxin. *J Biol Chem, 286*(43), 37866-37873.

Johnson, K. B., Petersen-Jones, H., Thompson, J. M., Hitomi, K., Itoh, M., Bakker, E. N., . . . Watts, S. W. (2012). Vena cava and aortic smooth muscle cells express transglutaminases 1 and 4 in addition to transglutaminase 2. *Am J Physiol Heart Circ Physiol, 302*(7), H1355-1366.

Johnson, T. S., Skill, N. J., El Nahas, A. M., Oldroyd, S. D., Thomas, G. L., Douthwaite, J. A., . . . Griffin, M. (1999). Transglutaminase transcription and antigen translocation in experimental renal scarring. *Journal of the American Society of Nephrology, 10*(10), 2146-2157.

Jones, S., Zhang, X., Parsons, D. W., Lin, J. C., Leary, R. J., Angenendt, P., . . . Kinzler, K. W. (2008). Core signaling pathways in human pancreatic cancers revealed by global genomic analyses. *Science, 321*(5897), 1801-1806.

Junn, E., Ronchetti, R. D., Quezado, M. M., Kim, S.-Y., & Mouradian, M. M. (2003). Tissue transglutaminase-induced aggregation of α-synuclein: Implications for Lewy body formation in Parkinson's disease and dementia with Lewy bodies. *Proceedings of the National Academy of Sciences, 100*(4), 2047-2052.

Kanda, M., Matthaei, H., Wu, J., Hong, S. M., Yu, J., Borges, M., . . . Goggins, M. (2012). Presence of somatic mutations in most early-stage pancreatic intraepithelial neoplasia. *Gastroenterology, 142*(4), 730-733 e739.

Kapoor, A., Yao, W., Ying, H., Hua, S., Liewen, A., Wang, Q., . . . DePinho, R. A. (2014). Yap1 activation enables bypass of oncogenic Kras addiction in pancreatic cancer. *Cell, 158*(1), 185-197.

Karin, M., Cao, Y., Greten, F. R., & Li, Z.-W. (2002). NF-κB in cancer: from innocent bystander to major culprit. *Nature Reviews Cancer, 2*(4), 301-310.

Kim, D.-S., Park, S.-S., Nam, B.-H., Kim, I.-H., & Kim, S.-Y. (2006). Reversal of drug resistance in breast cancer cells by transglutaminase 2 inhibition and nuclear factor-κB inactivation. *Cancer Res, 66*(22), 10936-10943.

Kim, S.-Y., Jeitner, T. M., & Steinert, P. M. (2002). Transglutaminases in disease. *Neurochemistry international, 40*(1), 85-103.

Klein, A. P., Brune, K. A., Petersen, G. M., Goggins, M., Tersmette, A. C., Offerhaus, G. J., . . . Hruban, R. H. (2004). Prospective risk of pancreatic cancer in familial pancreatic cancer kindreds. *Cancer Res, 64*(7), 2634-2638.

Koay, E. J., Baio, F. E., Ondari, A., Truty, M. J., Cristini, V., Thomas, R. M., . . . Fleming, J. B. (2014). Intra-tumoral heterogeneity of gemcitabine delivery and mass transport in human pancreatic cancer. *Phys Biol, 11*(6), 065002.

Koay, E. J., Truty, M. J., Cristini, V., Thomas, R. M., Chen, R., Chatterjee, D., . . . Fleming, J. B. (2014). Transport properties of pancreatic cancer describe gemcitabine delivery and response. *J Clin Invest, 124*(4), 1525-1536.

Korc, M. (2007). Pancreatic cancer-associated stroma production. *Am J Surg, 194*(4 Suppl), S84-86.

Kotsakis, P., & Griffin, M. (2007). Tissue transglutaminase in tumour progression: friend or foe? *Amino Acids, 33*(2), 373-384.

Kristjansen, P., Brown, T. J., Shipley, L. A., & Jain, R. K. (1996). Intratumor pharmacokinetics, flow resistance, and metabolism during gemcitabine infusion in ex vivo perfused human small cell lung cancer. *Clinical Cancer Research, 2*(2), 359-367.

Kuo, T. F., Tatsukawa, H., & Kojima, S. (2011). New insights into the functions and localization of nuclear transglutaminase 2. *FEBS J, 278*(24), 4756-4767.

Lee, K. N., Birckbichler, P. J., & Patterson, M. K. (1989). GTP hydrolysis by guinea pig liver transglutaminase. *Biochem Biophys Res Commun, 162*(3), 1370-1375.

Li, D., Xie, K., Wolff, R., & Abbruzzese, J. L. (2004). Pancreatic cancer. *The Lancet, 363*(9414), 1049-1057.

Liu, S., Cerione, R. A., & Clardy, J. (2002). Structural basis for the guanine nucleotide-binding activity of tissue transglutaminase and its regulation of transamidation activity. *Proc Natl Acad Sci U S A, 99*(5), 2743-2747.

Locher, C., Fabre-Guillevin, E., Brunetti, F., Auroux, J., Delchier, J. C., Piedbois, P., & Zelek, L. (2008). Fixed-dose rate gemcitabine in elderly patients with

advanced pancreatic cancer: an observational study. *Crit Rev Oncol Hematol, 68*(2), 178-182.
Lorand, L., & Graham, R. M. (2003). Transglutaminases: crosslinking enzymes with pleiotropic functions. *Nat Rev Mol Cell Biol, 4*(2), 140-156.
Lunardi, S., Muschel, R. J., & Brunner, T. B. (2014). The stromal compartments in pancreatic cancer: are there any therapeutic targets? *Cancer Lett, 343*(2), 147-155.
Maehama, T., & Dixon, J. E. (1998). The tumor suppressor, PTEN/MMAC1, dephosphorylates the lipid second messenger, phosphatidylinositol 3, 4, 5-trisphosphate. *Journal of Biological Chemistry, 273*(22), 13375-13378.
Mahadevan, D., & Von Hoff, D. D. (2007). Tumor-stroma interactions in pancreatic ductal adenocarcinoma. *Mol Cancer Ther, 6*(4), 1186-1197.
Mann, A. P., Verma, A., Sethi, G., Manavathi, B., Wang, H., Fok, J. Y., . . . Mehta, K. (2006). Overexpression of tissue transglutaminase leads to constitutive activation of nuclear factor-κB in cancer cells: delineation of a novel pathway. *Cancer Res, 66*(17), 8788-8795.
Matei, D., Graeber, T. G., Baldwin, R. L., Karlan, B. Y., Rao, J., & Chang, D. D. (2002). Gene expression in epithelial ovarian carcinoma. *Oncogene, 21*(41), 6289-6298.
Mchta, K. (2005). Mammalian transglutaminases: a family portrait. *Progress in experimental tumor research, 38*, 1-18.
Mehta, K. (2009). Biological and therapeutic significance of tissue transglutaminase in pancreatic cancer. *Amino Acids, 36*(4), 709-716.
Mehta, K., Fok, J., Miller, F. R., Koul, D., & Sahin, A. A. (2004). Prognostic significance of tissue transglutaminase in drug resistant and metastatic breast cancer. *Clin Cancer Res, 10*(23), 8068-8076.
Mehta, K., Kumar, A., & Kim, H. I. (2010). Transglutaminase 2: a multi-tasking protein in the complex circuitry of inflammation and cancer. *Biochem Pharmacol, 80*(12), 1921-1929.
Mhaouty-Kodja, S. (2004). Ghα/tissue transglutaminase 2: an emerging G protein in signal transduction. *Biology of the Cell, 96*(5), 363-367.
Mishra, S., Melino, G., & Murphy, L. J. (2007). Transglutaminase 2 kinase activity facilitates protein kinase A-induced phosphorylation of retinoblastoma protein. *Journal of Biological Chemistry, 282*(25), 18108-18115.
Mishra, S., & Murphy, L. J. (2004). Tissue transglutaminase has intrinsic kinase activity: identification of transglutaminase 2 as an insulin-like growth factor-binding protein-3 kinase. *J Biol Chem, 279*(23), 23863-23868.
Mishra, S., & Murphy, L. J. (2006). The p53 oncoprotein is a substrate for tissue transglutaminase kinase activity. *Biochem Biophys Res Commun, 339*(2), 726-730.
Mishra, S., Saleh, A., Espino, P. S., Davie, J. R., & Murphy, L. J. (2006). Phosphorylation of histones by tissue transglutaminase. *Journal of Biological Chemistry, 281*(9), 5532-5538.
Miyamoto, H., Murakami, T., Tsuchida, K., Sugino, H., Miyake, H., & Tashiro, S. (2004). Tumor-stroma interaction of human pancreatic cancer: acquired

resistance to anticancer drugs and proliferation regulation is dependent on extracellular matrix proteins. *Pancreas, 28*(1), 38-44.

Mizushima, N. (2007). Autophagy: process and function. *Genes & development, 21*(22), 2861-2873.

Moore, M. J., Goldstein, D., Hamm, J., Figer, A., Hecht, J. R., Gallinger, S., . . . National Cancer Institute of Canada Clinical Trials, G. (2007). Erlotinib plus gemcitabine compared with gemcitabine alone in patients with advanced pancreatic cancer: a phase III trial of the National Cancer Institute of Canada Clinical Trials Group. *J Clin Oncol, 25*(15), 1960-1966.

Nakanishi, C., & Toi, M. (2005). Nuclear factor-κB inhibitors as sensitizers to anticancer drugs. *Nature Reviews Cancer, 5*(4), 297-309.

Nakaoka, H., Perez, D. M., Baek, K. J., Das, T., Husain, A., Misono, K., . . . Graham, R. M. (1994). Gh: a GTP-binding protein with transglutaminase activity and receptor signaling function. *Science, 264*(5165), 1593-1596.

Noiva, R., & Lennarz, W. (1992). Protein disulfide isomerase. A multifunctional protein resident in the lumen of the endoplasmic reticulum. *J Biol Chem, 267*(6), 3553-3556.

Ohlund, D., Franklin, O., Lundberg, E., Lundin, C., & Sund, M. (2013). Type IV collagen stimulates pancreatic cancer cell proliferation, migration, and inhibits apoptosis through an autocrine loop. *BMC Cancer, 13*, 154.

Olive, K. P., Jacobetz, M. A., Davidson, C. J., Gopinathan, A., McIntyre, D., Honess, D., . . . Allard, D. (2009). Inhibition of Hedgehog signaling enhances delivery of chemotherapy in a mouse model of pancreatic cancer. *Science, 324*(5933), 1457-1461.

Olsen, K. C., Epa, A. P., Kulkarni, A. A., Kottmann, R. M., McCarthy, C. E., Johnson, G. V., . . . Sime, P. J. (2014). Inhibition of transglutaminase 2, a novel target for pulmonary fibrosis, by two small electrophilic molecules. *Am J Respir Cell Mol Biol, 50*(4), 737-747.

Olsen, K. C., Sapinoro, R. E., Kottmann, R. M., Kulkarni, A. A., Iismaa, S. E., Johnson, G. V., . . . Sime, P. J. (2011). Transglutaminase 2 and its role in pulmonary fibrosis. *Am J Respir Crit Care Med, 184*(6), 699-707.

Orban, J. M., Wilson, L. B., Kofroth, J. A., El-Kurdi, M. S., Maul, T. M., & Vorp, D. A. (2004). Crosslinking of collagen gels by transglutaminase. *Journal of biomedical materials research Part A, 68*(4), 756-762.

Ozdemir, B. C., Pentcheva-Hoang, T., Carstens, J. L., Zheng, X., Wu, C. C., Simpson, T. R., . . . Kalluri, R. (2014). Depletion of carcinoma-associated fibroblasts and fibrosis induces immunosuppression and accelerates pancreas cancer with reduced survival. *Cancer Cell, 25*(6), 719-734.

Park, K.-S., Kim, H.-K., Lee, J.-H., Choi, Y.-B., Park, S.-Y., Yang, S.-H., . . . Hong, K.-M. (2010). Transglutaminase 2 as a cisplatin resistance marker in non-small cell lung cancer. *Journal of cancer research and clinical oncology, 136*(4), 493-502.

Pavillard, V., Formento, P., Rostagno, P., Formento, J. L., Fischel, J. L., Francoual, M., . . . Milano, G. (1998). Combination of irinotecan (CPT11) and 5-fluorouracil with an analysis of cellular determinants of drug activity. *Biochem Pharmacol, 56*(10), 1315-1322.

Petersen, G. M., de Andrade, M., Goggins, M., Hruban, R. H., Bondy, M., Korczak, J. F., . . . Klein, A. P. (2006). Pancreatic cancer genetic epidemiology consortium. *Cancer Epidemiol Biomarkers Prev, 15*(4), 704-710.

Pinkas, D. M., Strop, P., Brunger, A. T., & Khosla, C. (2007). Transglutaminase 2 undergoes a large conformational change upon activation. *PLoS Biol, 5*(12), e327.

Porcelli, L., Quatrale, A. E., Mantuano, P., Leo, M. G., Silvestris, N., Rolland, J. F., . . . Azzariti, A. (2013). Optimize radiochemotherapy in pancreatic cancer: PARP inhibitors a new therapeutic opportunity. *Mol Oncol, 7*(3), 308-322.

Quan, G., Choi, J.-Y., Lee, D.-S., & Lee, S.-C. (2005). TGF-β1 up-regulates transglutaminase two and fibronectin in dermal fibroblasts: a possible mechanism for the stabilization of tissue inflammation. *Archives of dermatological research, 297*(2), 84-90.

Radek, J. T., Jeong, J.-M., Murthy, S., Ingham, K. C., & Lorand, L. (1993). Affinity of human erythrocyte transglutaminase for a 42-kDa gelatin-binding fragment of human plasma fibronectin. *Proceedings of the National Academy of Sciences, 90*(8), 3152-3156.

Raimondi, S., Maisonneuve, P., & Lowenfels, A. B. (2009). Epidemiology of pancreatic cancer: an overview. *Nat Rev Gastroenterol Hepatol, 6*(12), 699-708.

Rhim, A. D., Oberstein, P. E., Thomas, D. H., Mirek, E. T., Palermo, C. F., Sastra, S. A., . . . Stanger, B. Z. (2014). Stromal elements act to restrain, rather than support, pancreatic ductal adenocarcinoma. *Cancer Cell, 25*(6), 735-747.

Rich, L., & Whittaker, P. (2005). Collagen and picrosirius red staining: a polarized light assessment of fibrillar hue and spatial distribution. *Braz J Morphol Sci, 22*(2), 97-104.

Rossin, F., D'Eletto, M., Falasca, L., Sepe, S., Cocco, S., Fimia, G., . . . Piacentini, M. (2014). Transglutaminase 2 ablation leads to mitophagy impairment associated with a metabolic shift towards aerobic glycolysis. *Cell Death & Differentiation*.

Ruiz, I., Del Valle, J., & Gomez, A. (2004). Gemcitabine and haemolytic-uraemic syndrome. *Ann Oncol, 15*(10), 1575-1576.

Santhanam, L., Berkowitz, D. E., & Belkin, A. M. (2011). Nitric oxide regulates non-classical secretion of tissue transglutaminase. *Commun Integr Biol, 4*(5), 584-586.

Satpathy, M., Cao, L., Pincheira, R., Emerson, R., Bigsby, R., Nakshatri, H., & Matei, D. (2007). Enhanced peritoneal ovarian tumor dissemination by tissue transglutaminase. *Cancer Res, 67*(15), 7194-7202.

Scarpellini, A., Germack, R., Lortat-Jacob, H., Muramatsu, T., Billett, E., Johnson, T., & Verderio, E. A. (2009). Heparan sulfate proteoglycans are receptors for the cell-surface trafficking and biological activity of transglutaminase-2. *J Biol Chem, 284*(27), 18411-18423.

Seufferlein, T., Bachet, J. B., Van Cutsem, E., Rougier, P., & Group, E. G. W. (2012). Pancreatic adenocarcinoma: ESMO-ESDO Clinical Practice Guidelines for diagnosis, treatment and follow-up. *Ann Oncol, 23 Suppl 7*, vii33-40.

Shannon HE, F. M., Xie J, Gu D, McCarthy BP, Riley AA, Sinn AL, Silver JM, Peterman K, Kelley MR, Hanenberg H, Korc M, Pollok KE, Territo PR. (2014). Longitudinal Bioluminescence Imaging of Primary versus Abdominal Metastatic Tumor Growth in Orthotopic Pancreatic Tumor Models in NOD/SCIDy(-/-) Mice. *Pancreas, in press*.

Shields, M. A., Dangi-Garimella, S., Krantz, S. B., Bentrem, D. J., & Munshi, H. G. (2011). Pancreatic cancer cells respond to type I collagen by inducing snail expression to promote membrane type 1 matrix metalloproteinase-dependent collagen invasion. *J Biol Chem, 286*(12), 10495-10504.

Shipley, L. A., Brown, T. J., Cornpropst, J. D., Hamilton, M., Daniels, W. D., & Culp, H. W. (1992). Metabolism and disposition of gemcitabine, and oncolytic deoxycytidine analog, in mice, rats, and dogs. *Drug metabolism and disposition, 20*(6), 849-855.

Shweke, N., Boulos, N., Jouanneau, C., Vandermeersch, S., Melino, G., Dussaule, J. C., . . . Boffa, J. J. (2008). Tissue transglutaminase contributes to interstitial renal fibrosis by favoring accumulation of fibrillar collagen through TGF-beta activation and cell infiltration. *Am J Pathol, 173*(3), 631-642.

Siegel, M., Strnad, P., Watts, R. E., Choi, K., Jabri, B., Omary, M. B., & Khosla, C. (2008). Extracellular transglutaminase 2 is catalytically inactive, but is transiently activated upon tissue injury. *PLoS One, 3*(3), e1861.

Siegel, R. L., Miller, K. D., & Jemal, A. (2015). Cancer statistics, 2015. *CA Cancer J Clin, 65*(1), 5-29.

Sollid, L. M., Molberg, Ø., McAdam, S., & Lundin, K. E. (1997). Autoantibodies in coeliac disease: tissue transglutaminase—guilt by association? *Gut, 41*(6), 851-852.

Sultana, A., Cox, T., Ghaneh, P., & Neoptolemos, J. P. (2012). Adjuvant therapy for pancreatic cancer. *Recent Results Cancer Res, 196*, 65-88.

Suto, N., Ikura, K., & Sasaki, R. (1993). Expression induced by interleukin-6 of tissue-type transglutaminase in human hepatoblastoma HepG2 cells. *Journal of Biological Chemistry, 268*(10), 7469-7473.

Tamura, M., Gu, J., Matsumoto, K., Aota, S.-i., Parsons, R., & Yamada, K. M. (1998). Inhibition of cell migration, spreading, and focal adhesions by tumor suppressor PTEN. *Science, 280*(5369), 1614-1617.

Thomazy, V., & Fesus, L. (1989). Differential expression of tissue transglutaminase in human cells. An immunohistochemical study. *Cell Tissue Res, 255*(1), 215-224.

Turner, P. M., & Lorand, L. (1989). Complexation of fibronectin with tissue transglutaminase. *Biochemistry, 28*(2), 628-635.

Verderio, E. A., Johnson, T., & Griffin, M. (2004). Tissue transglutaminase in normal and abnormal wound healing: review article. *Amino Acids, 26*(4), 387-404.

Verderio, E. A., Johnson, T. S., & Griffin, M. (2005). Transglutaminases in wound healing and inflammation. *Progress in experimental tumor research, 38*, 89-114.

Verma, A., Guha, S., Diagaradjane, P., Kunnumakkara, A. B., Sanguino, A. M., Lopez-Berestein, G., . . . Mehta, K. (2008). Therapeutic significance of elevated tissue transglutaminase expression in pancreatic cancer. *Clin Cancer Res, 14*(8), 2476-2483.

Verma, A., Guha, S., Wang, H., Fok, J. Y., Koul, D., Abbruzzese, J., & Mehta, K. (2008). Tissue transglutaminase regulates focal adhesion kinase/AKT activation by modulating PTEN expression in pancreatic cancer cells. *Clin Cancer Res, 14*(7), 1997-2005.

Verma, A., Wang, H., Manavathi, B., Fok, J. Y., Mann, A. P., Kumar, R., & Mehta, K. (2006). Increased expression of tissue transglutaminase in pancreatic ductal adenocarcinoma and its implications in drug resistance and metastasis. *Cancer Res, 66*(21), 10525-10533.

Vincent, A., Herman, J., Schulick, R., Hruban, R. H., & Goggins, M. (2011). Pancreatic cancer. *The Lancet, 378*(9791), 607-620.

Von Hoff, D. D., Ervin, T., Arena, F. P., Chiorean, E. G., Infante, J., Moore, M., . . . Renschler, M. F. (2013). Increased survival in pancreatic cancer with nab-paclitaxel plus gemcitabine. *N Engl J Med, 369*(18), 1691-1703.

Von Hoff, D. D., Ramanathan, R. K., Borad, M. J., Laheru, D. A., Smith, L. S., Wood, T. E., . . . Hidalgo, M. (2011). Gemcitabine plus nab-paclitaxel is an active regimen in patients with advanced pancreatic cancer: a phase I/II trial. *J Clin Oncol, 29*(34), 4548-4554.

Wang, W., Abbruzzese, J. L., Evans, D. B., Larry, L., Cleary, K. R., & Chiao, P. J. (1999). The nuclear factor-κB RelA transcription factor is constitutively activated in human pancreatic adenocarcinoma cells. *Clinical Cancer Research, 5*(1), 119-127.

Willett, C. G., Czito, B. G., Bendell, J. C., & Ryan, D. P. (2005). Locally advanced pancreatic cancer. *J Clin Oncol, 23*(20), 4538-4544.

Wilson, J. S., Pirola, R. C., & Apte, M. V. (2014). Stars and stripes in pancreatic cancer: role of stellate cells and stroma in cancer progression. *Front Physiol, 5*, 52.

Witkiewicz, A. K., McMillan, E. A., Balaji, U., Baek, G., Lin, W. C., Mansour, J., . . . Knudsen, E. S. (2015). Whole-exome sequencing of pancreatic cancer defines genetic diversity and therapeutic targets. *Nat Commun, 6*, 6744.

Wolpin, B. M., Chan, A. T., Hartge, P., Chanock, S. J., Kraft, P., Hunter, D. J., . . . Fuchs, C. S. (2009). ABO blood group and the risk of pancreatic cancer. *J Natl Cancer Inst, 101*(6), 424-431.

Yamane, A., Fukui, M., Sugimura, Y., Itoh, M., Alea, M. P., Thomas, V., . . . Hitomi, K. (2010). Identification of a preferred substrate peptide for transglutaminase 3 and detection of in situ activity in skin and hair follicles. *FEBS J, 277*(17), 3564-3574.

Ychou, M. (2003). An open phase I study assessing the feasibility of the triple combination: oxaliplatin plus irinotecan plus leucovorin/ 5-fluorouracil

every 2 weeks in patients with advanced solid tumors. *Annals of Oncology, 14*(3), 481-489.

Yuan, L., Choi, K., Khosla, C., Zheng, X., Higashikubo, R., Chicoine, M. R., & Rich, K. M. (2005). Tissue transglutaminase 2 inhibition promotes cell death and chemosensitivity in glioblastomas. *Mol Cancer Ther, 4*(9), 1293-1302.

Zeghari-Squalli, N., Raymond, E., Cvitkovic, E., & Goldwasser, F. (1999). Cellular pharmacology of the combination of the DNA topoisomerase I inhibitor SN-38 and the diaminocyclohexane platinum derivative oxaliplatin. *Clin Cancer Res, 5*(5), 1189-1196.

Zemskov, E. A., Janiak, A., Hang, J., Waghray, A., & Belkin, A. M. (2006). The role of tissue transglutaminase in cell-matrix interactions. *Front Biosci, 11*, 1057-1076.

Zemskov, E. A., Mikhailenko, I., Hsia, R.-C., Zaritskaya, L., & Belkin, A. M. (2011). Unconventional secretion of tissue transglutaminase involves phospholipid-dependent delivery into recycling endosomes. *PLoS One, 6*(4), e19414.

Zeng, Q., & Hong, W. (2008). The emerging role of the hippo pathway in cell contact inhibition, organ size control, and cancer development in mammals. *Cancer Cell, 13*(3), 188-192.

Zhang, W., Nandakumar, N., Shi, Y., Manzano, M., Smith, A., Graham, G., . . . Yi, C. (2014). Downstream of mutant KRAS, the transcription regulator YAP is essential for neoplastic progression to pancreatic ductal adenocarcinoma. *Sci Signal, 7*(324), ra42.

Zhao, B., Li, L., Lei, Q., & Guan, K. L. (2010). The Hippo-YAP pathway in organ size control and tumorigenesis: an updated version. *Genes Dev, 24*(9), 862-874.

Zhao, J., & Guan, J. L. (2009). Signal transduction by focal adhesion kinase in cancer. *Cancer Metastasis Rev, 28*(1-2), 35-49.

CURRICULUM VITAE

Jiyoon Lee

1. Education

- *Indiana University, Indianapolis, IN*
  Ph.D. in Biochemistry and Molecular Biology **2010 – 2015**

- *Sungkyunkwan University, Suwon, South Korea*
  B.S. in Genetic Engineering **2004 – 2008**

2. Research Experiences

- *Indiana University, Indianapolis, IN*
  Graduate Student **2010 – 2015**
  Department of Biochemistry and Molecular Biology
  Dissertation Title: **"Tumor-Stroma Interaction Mediated by Tissue Transglutaminase in Pancreatic Cancer"**
  Advisor: Daniela Matei, M.D.
  Committee: Maureen Harrington, Ph.D., Brittney-Shea Herbert, Ph.D., and Jingwu Xie, Ph.D.

- *Korea Research Institute of Bioscience and Biotechnology, Daejeon, South Korea*
  Intern Researcher **2009**
  Plant Systems Engineering Research Center
  Advisor: Jeong Mee Park, Ph.D.
  Involved in the studies of:
  - Molecular plant-microbe interactions
  - Plant gene expression and localization in animal cells

- *Sungkyunkwan University, Suwon, South Korea*
  Undergraduate Research Student **2007 – 2008**
  Department of Genetic Engineering
  Advisor: Moosik Kwon, Ph.D.
  Involved in the studies of:
  - Site-direct mutagenesis at specific sequence of mouse Prion genome
  - Plant tissue culture of transgenic tomatoes harboring Korean Mistletoe Lectin gene

3. Award and Fellowship

- **IU Simon Cancer Center Research Day Poster Presentation Award**, Indianapolis, IN — **2015**
- **Indiana University School of Medicine BioMedical Gateway Program Fellowship**, Indianapolis, IN — **2010 – 2011**

4. Publications

- **Jiyoon Lee***, Andrea Caperell-Grant, David Jones, and Daniela Matei. Effect of Tissue Transglutaminse-Mediated Modulation of Tumor Microenvironment on Response to Gemcitabine. *In Preparation*.
- **Jiyoon Lee***, Salvatore Condello, Bakhtiyor Yakubov, Robert Emerson, Andrea Caperell-Grant, Kiyotaka Hitomi, Jingwu Xie, and Daniela Matei. Tissue Transglutaminase Mediated Tumor-Stroma Interaction Promotes Pancreatic Cancer Progression. *Clinical Cancer Research.* (2015): clincanres-0226.
- Horacio Cardenas, Edyta Vieth, **Jiyoon Lee**, Mathew Segar, Yunlong Liu, Kenneth P Nephew, and Daniela Matei. TGF-β Induces Global Changes in DNA Methylation during the Epithelial-to-Mesenchymal Transition in Ovarian Cancer Cells. *Epigenetics*. 2014; 9(11):1461-72.

5. Abstracts and Poster Presentations

Conferences:

- **Jiyoon Lee*,** Bakhtiyor Yakubov, Bhadrani Chelladurai, Andrea Caperell-Grant, and Daniela Matei. (2014) Tissue Transglutaminase Modulates the Pancreatic Cancer Stroma Inducing Resistance to Gemcitabine. *Cold Spring Harbor Laboratory Meeting: Mechanisms and Models of Cancer*. Cold Spring Harbor, NY
- Horacio Cardenas, Edyta Vieth, **Jiyoon Lee**, Kenneth P. Nephew, and Daniela Matei. (2014) DNA Methylation Changes During Epithelial-to-Mesenchymal Transition in Ovarian Cancer Cells. *Indiana-Illinois End Epithelial Ovarian Cancer Coalition Workshop*. South Bend, IN
- **Jiyoon Lee***, Andrea Caperell-Grant, Bhadrani Chelladurai, and Daniela Matei. (2012) Tissue Transglutaminase in the Pancreatic Cancer Stroma. *Gordon Research Conferences: Transglutaminases in Human Disease Processes*. Davidson, NC

University Affiliated:

- **Jiyoon Lee*,** Salvatore Condello, Bakhtiyor Yakubov, Robert Emerson, Andrea Caperell-Grant, Kiyotaka Hitomi, Jingwu Xie, and Daniela Matei. (2015) Tissue Transglutaminase Mediated Tumor-Stroma Interaction Promotes Pancreatic Cancer Progression. *IU Simon Cancer Center Cancer Research Day*. Indianapolis, IN

- **Jiyoon Lee*,** Bakhtiyor Yakubov, Bhadrani Chelladurai, Andrea Caperell-Grant, and Daniela Matei. (2014) Tissue Transglutaminase Alters the Pancreatic Cancer Microenvironment. *Biochemistry and Molecular Biology Research Day*. Indianapolis, IN

- **Jiyoon Lee***, Bakhtiyor Yakubov, Bhadrani Chelladurai, Andrea Caperell-Grant, and Daniela Matei. (2014) Tissue Transglutaminase Alters the Pancreatic Cancer Microenvironment. *IU Simon Cancer Center Cancer Research Day*. Indianapolis, IN

- **Jiyoon Lee*** and Daniela Matei. (2013) Effects of Tissue Transglutaminase in the Pancreatic Cancer Stroma. *Department of Biochemistry and Molecular Biology Research in Progress*. Indianapolis, IN

- **Jiyoon Lee***, Andrea Caperell-Grant, and Daniela Matei. (2012) Role of Transglutaminase 2 in the Pancreatic Cancer Stroma. *Biochemistry and Molecular Biology Research Day*. Indianapolis, IN

6. Research Techniques

• **Cell Biology**	Cell culture and maintenance, Retroviral and lentiviral transduction, Transfection, Gene knockdown (siRNA/shRNA), Reporter (dual-luciferase) assay, Proliferation assays (BrdU, CCK-8, MTT)
• **Molecular Biology**	Bradford assay, SDS-PAGE, Western blotting, Co-IP, ELISA, Immunohistochemistry, Immunofluorescence, Cloning, Bacterial transformation (*E. coli*), plasmid/DNA/RNA isolation, cDNA synthesis, RT-PCR, qRT-PCR, EMSA, Collagen assays
• **Animal Work**	Development of orthotopic human pancreatic cancer xenograft mouse model, OCT cryomold preparation, Protein/RNA isolation from tumors
• **Imaging**	Confocal imaging (Zeiss LSM 510 META confocal Multiphoton microscope system) and Circular polarizing microscopy (inverted Nikon Diaphot 200 microscope)